Keck Adaptive Optics Note 838

Near-Infrared Tip-Tilt Sensor System Design Manual

Version 1.0
November 24, 2010

Authors:
Peter Wizinowich

Contributors:
Richard Dekany, Ean James, Sudha LaVen, Jim Lyke, Chris Neyman, Roger Smith, Thomas Stalcup, Marcos van Dam, Ed Wetherell

Document Revision History

Revision Number	Revision Date	Summary of Changes	Author
1.0	11/24/2010	SDR version	Peter Wizinowich

Table of Contents

Acronyms

AO	Adaptive Optics
API	Application Programming Interface
ARC	Astronomical Research Cameras (AKA Leach)
ATI	Advanced Technologies and Instrumentation
DAR	Differential Atmospheric Refraction
DTT	Downlink Tip-Tilt
EE	Ensquared Energy
EPICS	Experimental Physics and Industrial Control System
FWHM	Full Width at Half Maximum
GUI	Graphical User Interface
IFU	Integral Field Unit
KAON	Keck Adaptive Optics Note
KTL	Keck Task Library
LBWFS	Low Bandwidth WaveFront Sensor
LGS	Laser Guide Star
MAGIQ	Multifunction Acquisition, Guiding, and Image Quality
NGAO	Next Generation Adaptive Optics
NGS	Natural Guide Star
NGWFC	Next Generation Wave Front Controller
NIR	Near InfraRed
NSF	National Science Foundation
OBS	Optics Bench Subsystem
OSIRIS	Oh-Suppression near InfraRed Integral field Spectrograph
PSF	Point Spread Function
RMS	Root Mean Square
RTC	Real-Time Control
SC	Supervisory Controller
SDM	System Design Manual
SDR	System Design Requirements
SOW	Statement of Work
SR	Strehl Ratio
SR	System Requirement
STRAP	System for Tip-tilt Removal with Avalanche Photodiodes
TRICK	Tip-tilt Removal with Ir Compensation at Keck
TRS	Telemetry Recorder / Server
TT	Tip-Tilt
TTM	Tip-Tilt Mirror
TTS	Tip-Tilt Sensor
WCP	Wavefront Command Processor
WFP	WaveFront Processor
WFS	WaveFront Sensor
WIF	Wavefront controller InterFace
WMKO	W. M. Keck Observatory

Introduction

This system design manual (SDM) is written in support of the NSF ATI-funded near-infrared (NIR) tip-tilt sensor (TTS) project; the proposal is documented in KAON 777. The purpose of the SDM is to document the system level design for the NIR TTS system.

1. Overview

1.1 Design Concept

The NIR TTS system will provide high bandwidth (up to 1 kHz) tip-tilt (TT) information from one to three stars in a ~120" diameter field to the laser guide star (LGS) adaptive optics (AO) wavefront controller. The TTS system will be added to the existing LGS AO control system as shown schematically in Figure 1. The TT information could be used instead of or in addition to the TT information from the existing visible TT sensor (STRAP, Bonaccini et al., 1997) to drive the tip-tilt mirror (TTM).

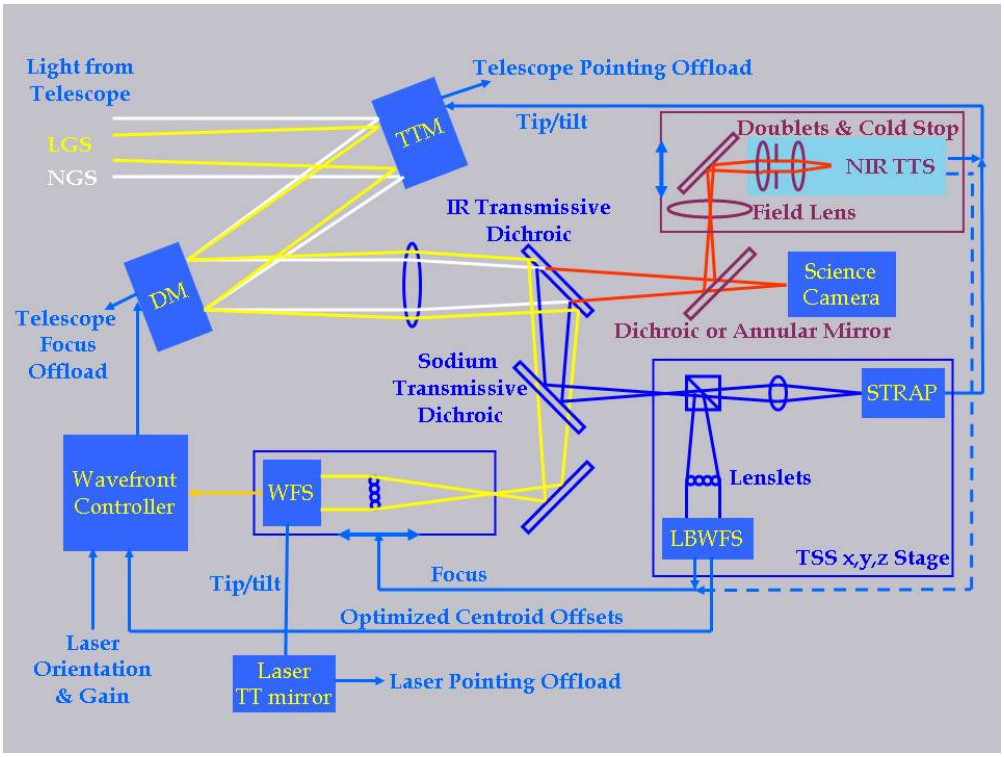

Figure 1: LGS AO control schematic with the new NIR TTS system added (upper right). *A fold located just in front of the science camera reflects light to the NIR TTS assembly mounted on a focus stage. The TTS output is processed to provide TT control of the Tip-Tilt Mirror (TTM) as an alternative to the existing visible TTS (STRAP) or in combination. Focus information, if available, could be used to control the wavefront sensor (WFS) focus.*

The TTS will be implemented with Keck I LGS AO. The Keck I system was chosen since it has a higher power, center launched laser and hence higher Strehl performance. The major elements of the TTS include the following:

- Dichroic beamsplitters to send the appropriate wavelength light to the TTS while transmitting the science light to the Keck I science instrument, OSIRIS.
- Relay optics to relay the required field to the TTS camera with the right magnification. These optics include a field lens (outside the camera dewar), a dewar window, some reimaging optics, a pupil stop and a filter.
- A NIR camera dewar which will house an H2RG detector and some optics.

- Camera control and readout electronics.
- Real-time controller modifications to accept and process the NIR camera data.
- Real-time telemetry modifications to accept, store, and access the new real-time control system data.
- Motion control (total of 3 degrees of freedom) for the dichroic exchanger to move between 3 (or 4) positions, a focus stage for the relay optics and camera assembly, and a stage to change between two filters.
- Device control to control the camera.
- Operations software modifications to calibrate and operate the system for science.

These elements have been divided into the five major subsystems shown in Figure 2. The Operations Software, Controls and Real-Time Control are modifications to existing AO systems. The Camera System is a new system. The opto-mechanical system and the near-IR camera portion of the Camera System represent additions to the existing AO bench.

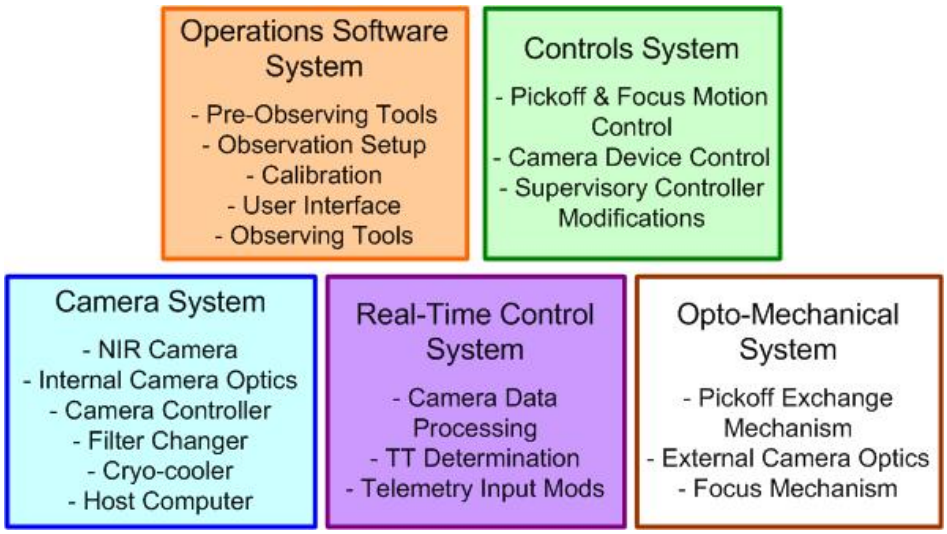

Figure 2: NIR TTS major subsystems

1.2 Potential Performance Benefits

The NSF ATI proposal for the NIR TTS identified three limitations of Keck LGS AO that this proposal was intended to alleviate:

- Improve the sky coverage for intrinsically rare science objects.
- Allow LGS AO science in heavily dust obscured regions such as star forming regions.
- Improve the astrometric precision and spatial resolution currently limited by residual tip-tilt errors.

The NIR TTS will allow the performance to be improved in several ways:

- Using AO-corrected tip-tilt stars improves the level of tip-tilt correction.
- Using AO-corrected tip-tilt stars allows fainter stars to be used thereby increasing sky coverage.
- Using NIR tip-tilt stars allows objects that were previously dust obscured to be observed with LGS AO.
- Using NIR tip-tilt stars will allow some red science objects to be used for tip-tilt sensing (previously off-axis tip-tilt stars bright enough in the visible were required) thereby reducing tip-tilt anisoplanatism.
- Using multiple NIR tip-tilt stars may reduce the tip-tilt anisoplanatism error.
- Using simultaneous NIR and visible tip-tilt stars could improve tip-tilt correction for some science targets.

If the NIR sensor also provided focus information then performance would be further improved:

- Using a higher bandwidth focus measurement would reduce the error due to sodium layer altitude changes. Currently focus corrections are provided by the low bandwidth wavefront sensor (LBWFS) which must integrate for periods of at least a few seconds.
- Using a higher bandwidth focus measurement would require less time to start science observations for observations with faint tip-tilt stars. The current LBWFS used to sense focus can take several minutes to converge on focus for faint guide stars.

Our baseline design does not provide focus information from the NIR sensor. However, we will design the system so that this is a future option.

1.3 System Requirements and Design Choices

The system requirements document (KAON 823) includes a list of the areas that directly impact the science and the system requirements. We use these science area categories here to provide a design overview in relationship to the requirements. For each category we indicate whether the system level design meets the requirement or allows the requirement to be achieved:

- Sky coverage - requirements met by design.
    - The NIR TTS optics have been designed to pass a 120" diameter field of view
    - The NIR TTS detector provides a 100"x100" field on the sky. The corners are vignetted by the 120" diameter field of view of the optics.
    - The NIR TTS can be used for acquisition.
- Tip-tilt residuals – requirements achievable by design.
    - Differential atmospheric refraction correction is provided between the science and TT sensing wavelengths by changing the requested star(s) centroid positions on the TTS.
- Science and tip-tilt sensing wavelengths - requirements met by design.
    - Two pickoff options are offered. A dichroic that reflects K to the NIR TTS while transmitting shorter wavelengths. Another dichroic that reflects H while transmitting K. A 3rd position will either remove the pickoff (initial implementation) or allow a future pickoff option (nominally an annular mirror).
    - A filter in the TTS camera dewar allows either H or Ks-band light to be used.
- Throughput and emissivity – requirements met by design.
    - The dichroics have good reflection and transmission performance.
    - The NIR TTS optics are optimized for H and K'-band.
    - The H2RG has high sensitivity at both H and K'-band.
    - A cold pupil stop and cold baffles are located in the TTS camera dewar.
- Science field of view – requirements met by design.
    - The entire science field of view is transmitted by the dichroics.
    - A future annular mirror option only transmits the IFU field.
- Observing modes – requirements met by design.
    - The TTS camera and re-imaging optics are mounted on a focus stage to stay parfocal to the OSIRIS focal plane.
    - Dithering, nodding and offsetting are all supported. The tip-tilt stars can be located anywhere on the detector (assuming good pixels); they do not have to be centered at the intersection of four pixels.
    - Non-sidereal tracking is only a goal, however the current design would support this mode.
    - Non-point sources can be used with reduced performance. The largest allowable region for centroiding is 0.8"x0.8" versus the goal of 1" diameter objects.
- Positioning accuracy and repeatability – requirements achievable by design.
- Observing efficiency – requirements achievable by design.
    - Observing efficiency budget to be designed during the preliminary design.
- Higher bandwidth focus measurements
    - This is a goal only. The real-time control system will provide focus. A choice was made not to incorporate astigmatism into the current optical design. The system is designed to support experiments to measure the benefits of focus sensing.

- Performance monitoring – requirements achievable by design.
    - Tools will be designed during the preliminary design.
- Observation planning – requirements achievable by design.
    - Tools will be designed during the preliminary design.

A system requirements compliance matrix is provided in section 12.

2. Design Considerations

This section begins with some design constraints imposed by the existing OSIRIS science instrument (section 2.1), AO bench (2.2) and the NIR TTS detector (2.3), which has already been procured. In section 2.4 the impact of differential atmospheric refraction is considered, which will move the tip-tilt star away from the center of a quad cell. The impact and performance of not operating in quad cell mode is then evaluated in section 2.5. Measuring focus requires the tip-tilt star to be at the center of a quad cell as reviewed in section 2.6. A single star could be maintained at the center of a quad cell with a tip-tilt mirror as discussed in 2.7; we have decided to proceed without this additional complexity given that it would only work for 1 tip-tilt star.

2.1 OSIRIS Science Instrument

Since the NIR TTS will be used with OSIRIS it is important to understand some features of this instrument. Much of the following data is from the OSIRIS Users' Manual version 2.2 (dated April 1, 2008).

OSIRIS provides four spatial scales to choose from (0.020, 0.035, 0.050 and 0.100 arcsec per lenslet). The pupil mask size for each of these plate scales is shown in Figure 3. The 0.020 arcsec scale is optimized for image quality and has a slightly oversized pupil that is circumscribed around the 10.94 m outer edges of the Keck primary mirror. It therefore has an elevated thermal background (K=11.2 mag/sq arcsec). The 0.035 and 0.050 arcsec scales are optimized for maximum sensitivity at thermal wavelengths (K=11.8 mag/sq arcsec). They both have circular pupils equivalent to a 10 m telescope. The 0.1 arcsec scale has an oversized pupil allowing a great deal of excess background (K=10.6 mag/sq arcsec). For this reason a duplicate K-band filter is installed with a smaller, 9 m diameter effective pupil.

The filters, scales and fields of view for the spectrograph are provided in Table 1.

The imager uses a Rockwell Scientific Hawaii-1 detector with 1024x1024 pixels and a plate scale of 0.020 arcsec/pixel. For most cases the imager will be sky background limited since the cold pupil is oversized (since the pupil is poorly formed). The imager zero point (defined as Mag = -2.5 log(flux in DN/sec) + Mag (zero point)) is 27.8, 28.1 and 27.6 mag at J, H and K, respectively. The imager background is 16.2, 14.6 and 10.6 mag/sq arcsec at J, H and K, respectively. The spectrograph zero points are 23.5, 24.3 and 23.7 mag at J, H and K, respectively.

Jim Lyke reports that we do not currently adjust the AO focus for OSIRIS between filters. Between pixel scales there is a ± 2 mm difference between the two most extreme scales.

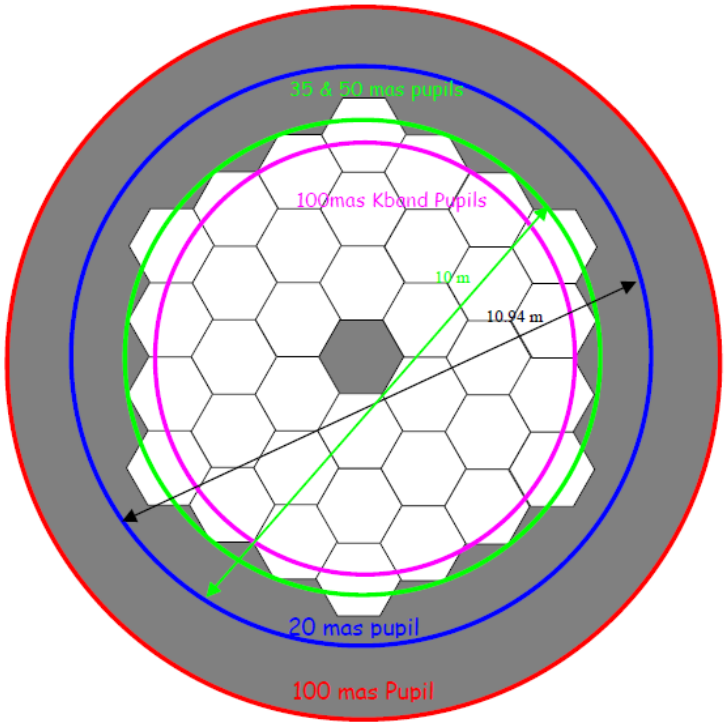

Figure 3: Scale drawing of the pupils for each of the four plate scales.

Filter	Shortest Wavelength Extracted(nm)	Longest Wavelength Extracted(nm)	Number of Spectral Channels	Number of Complete Spectra	Approx. Lenslet Geometry	FOV for 0.020"	FOV for 0.035"	FOV for 0.050"	FOV for 0.100"
Zbb	999*	1176*	1476	1019	16x64	0.32x1.28	0.56x2.24	0.8 x 3.2	1.6 x 6.4
Jbb	1180	1416*	1574	1019	16x64	0.32x1.28	0.56x2.24	0.8 x 3.2	1.6 x 6.4
Hbb	1473	1803	1651	1019	16x64	0.32x1.28	0.56x2.24	0.8 x 3.2	1.6 x 6.4
Kbb*	1965	2381	1665	1019	16x64	0.32x1.28	0.56x2.24	0.8 x 3.2	1.6 x 6.4
Zn4	1103	1158	459	2038	32x64	0.64x1.28	1.12x2.24	1.6 x 3.2	3.2 x 6.4
Jn1	1174	1232	388	2038	32x64	0.64x1.28	1.12x2.24	1.6 x 3.2	3.2 x 6.4
Jn2	1228	1289	408	2678	42x64	0.84x1.28	1.47x2.24	2.1 x 3.2	4.2 x 6.4
Jn3	1275	1339	428	3063	48x64	0.96x1.28	1.68x2.24	2.4 x 3.2	4.8 x 6.4
Jn4	1323	1389	441	2678	42x64	0.84x1.28	1.47x2.24	2.1 x 3.2	4.2 x 6.4
Hn1	1466	1541	376	2292	36x64	0.72x1.28	1.26x2.24	1.8 x 3.2	3.6 x 6.4
Hn2	1532	1610	391	2868	45x64	0.90x1.28	1.58x2.24	2.25x3.2	4.5 x 6.4
Hn3	1594	1676	411	3063	48x64	0.96x1.28	1.68x2.24	2.4 x 3.2	4.8 x 6.4
Hn4	1652	1737	426	2671	42x64	0.84x1.28	1.47x2.24	2.1 x 3.2	4.2 x 6.4
Hn5	1721	1808	436	2038	32x64	0.64x1.28	1.12x2.24	1.6 x 3.2	3.2 x 6.4
Kn1	1955	2055	401	2292	36x64	0.72x1.28	1.26x2.24	1.8 x 3.2	3.6 x 6.4
Kn2	2036	2141	421	2868	45x64	0.90x1.28	1.58x2.24	2.25x3.2	4.5 x 6.4
Kn3*	2121	2229	433	3063	48x64	0.96x1.28	1.68x2.24	2.4 x 3.2	4.8 x 6.4
Kn4*	2208	2320	449	2671	42x64	0.84x1.28	1.47x2.24	2.1 x 3.2	4.2 x 6.4
Kn5	2292	2408	465	2038	32x64	0.64x1.28	1.12x2.24	1.6 x 3.2	3.2 x 6.4

Table 1: OSIRIS spectrograph filters, scales and fields of view

The relative locations of the imager and spectrograph are shown in Figure 4. On Keck II the AO optical axis is located partway between the spectrograph and imager fields. OSIRIS will be moved to Keck I in August 2011. Prior to that time we will need to decide on the optimal location of the AO optical axis to be used in aligning OSIRIS; a recommendation will be made as part of the NIR TTS preliminary design.

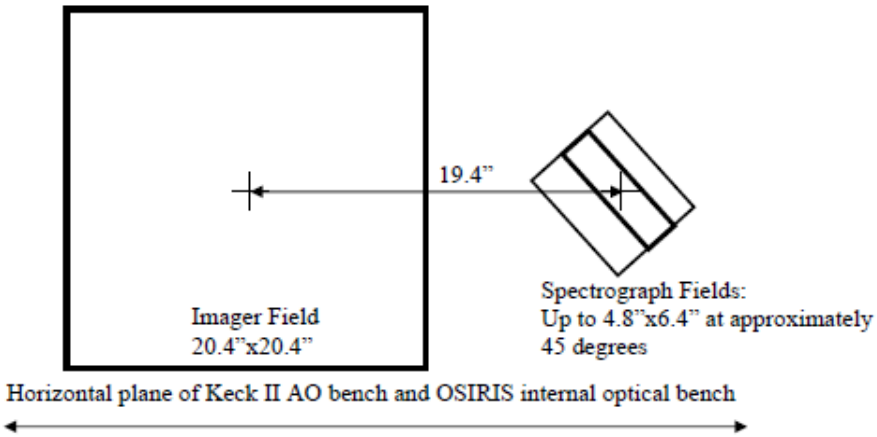

Figure 4: Relative locations of the imager and spectrograph focal planes. The perspective of this image is from OSIRIS looking toward the AO system. On Keck II the AO rotator axis is located partway between the spectrograph and imager fields.

Figure 5 (provided by Jason Chin) shows the layout of OSIRIS with respect to the AO bench. Based on this drawing the OSIRIS focal plane is estimated to be 393 mm from the edge of the AO bench. Note that center line of OSIRIS is offset by 53 mm with respect to the AO optical axis.

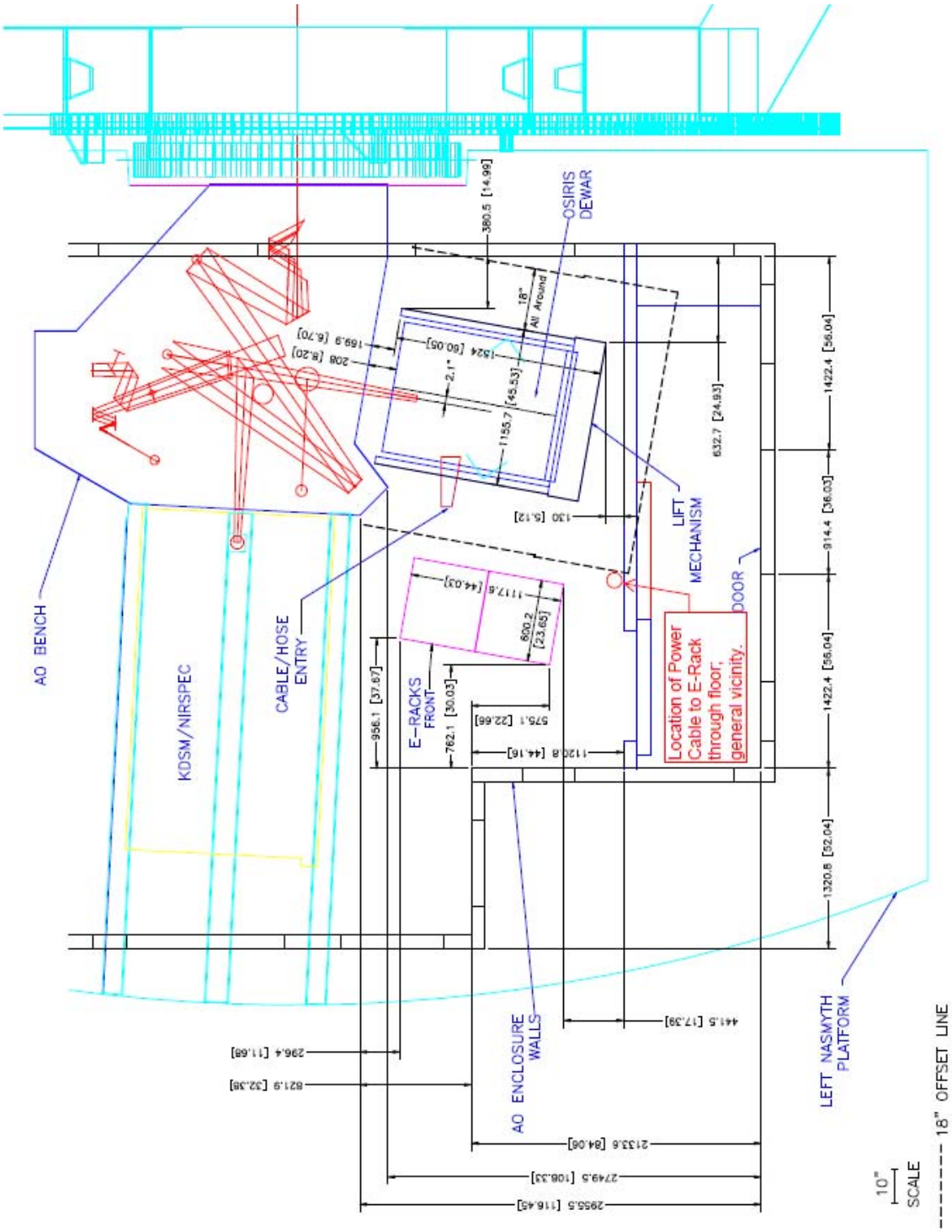

Figure 5: OSIRIS layout in Keck 1 AO (Rev A 2009-03-05)

2.2 AO Bench

A schematic of the AO bench is shown in Figure 6. The portion of the bench where the NIR TTS will need to be located is shown in Figure 7. The pupil simulator, item 23 in Figure 6 could be repackaged if necessary to provide additional space for the NIR TTS.

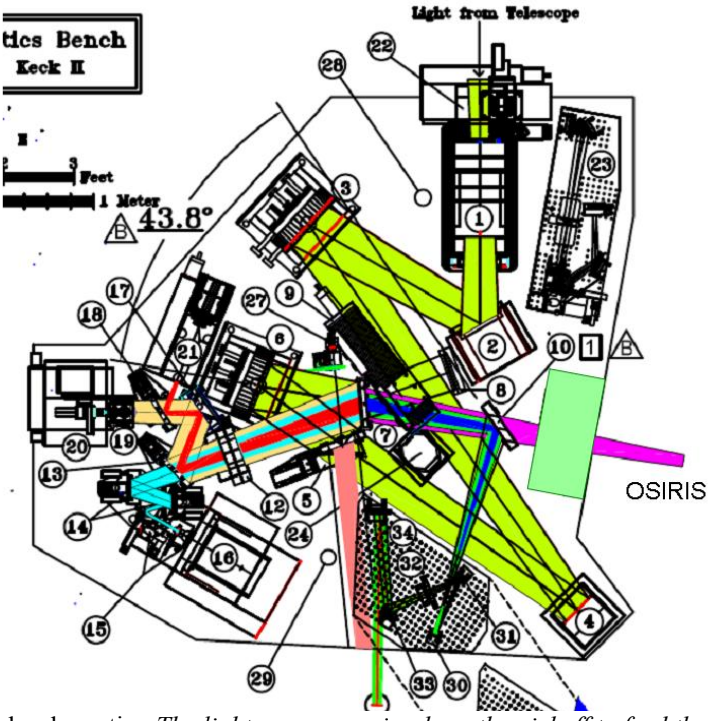

Figure 6: AO bench schematic. *The light green area is where the pickoff to feed the NIR TTS will be located. Item 2 is the fast tip-tilt mirror, item 7 is the IR transmissive dichroic, item 10 is the interferometer fold mirror and item 23 is the pupil simulator.*

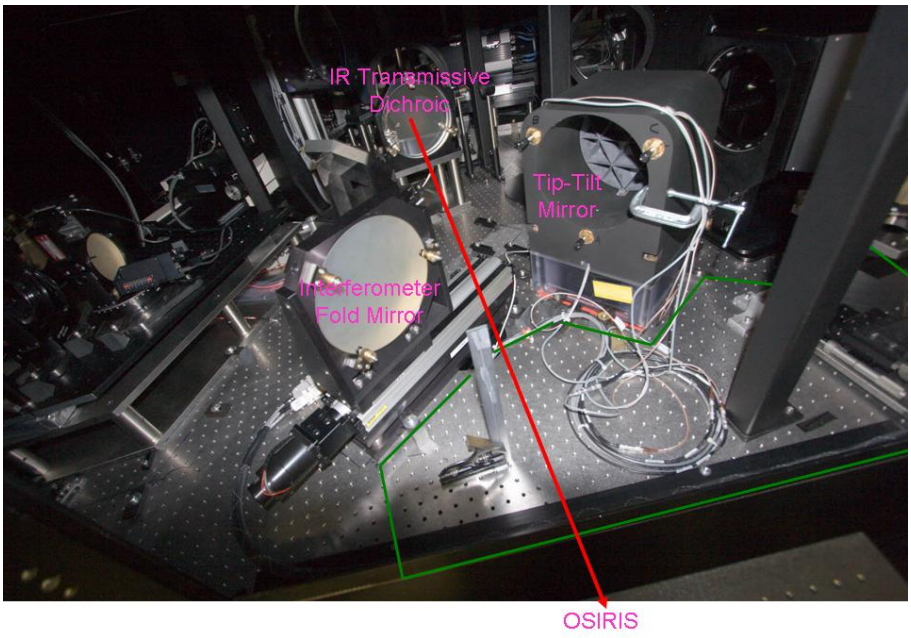

Figure 7: The Keck I AO bench. The red line shows the light path to OSIRIS. The green bordered area is roughly where the NIR TTS and its pickoff will need to be located.

2.3 Tip-Tilt Sensor Detector

The H2RG detector has been procured and is in-house. The pixel quantum efficiency plot produced by Teledyne at 2.0 μm is shown in Figure 8 for the received detector. The median QE is ~ 84% at this wavelength with 95% of the pixels having a QE > 58% at this wavelength; 97.7% of the pixels are operable

with the inoperable pixels mostly concentrated in two areas at the bottom of the chip. According to Teledyne the feature at the bottom of the chip is due to some chemical re-flow on the edge during substrate removal; this feature is not expected to propagate. At 1.23 μm the median QE is 65% with 95% of the pixels having a QE > 38%; 95.3% of the pixels are operable.

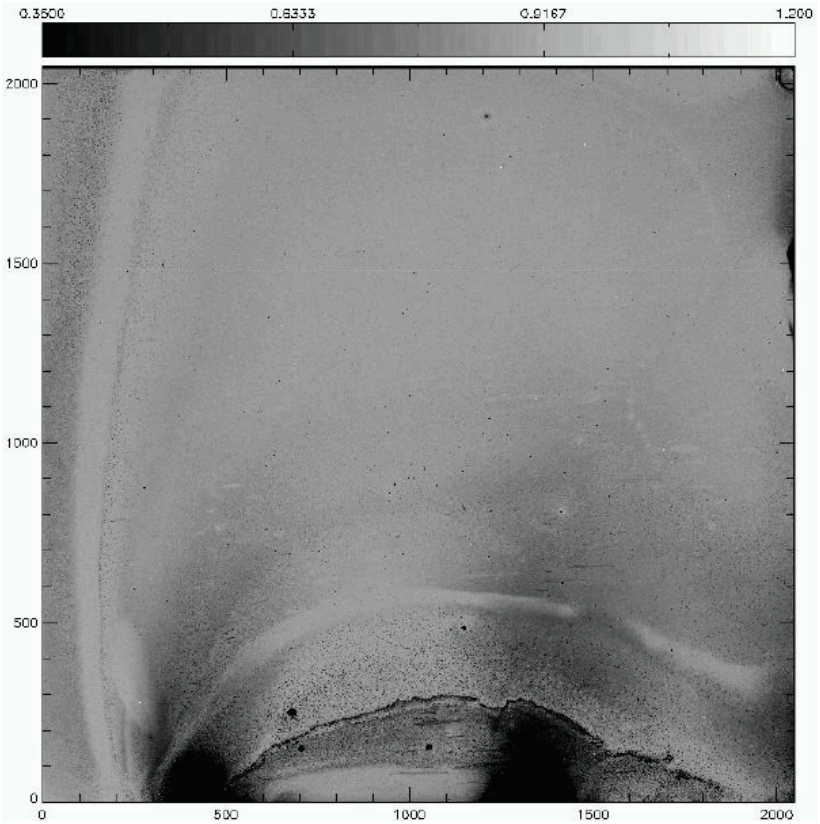

Figure 8: Pixel quantum efficiency at 2.0 μm

2.4 Differential Atmospheric Refraction

Differential atmospheric refraction (DAR) will cause the science image to move with respect to the tip-tilt star image if these two observations are made at different wavelengths and/or with stars of different colors.

The relevant system requirement is "The NIR TTS system shall support differential atmospheric refraction corrections between the TTS and the science instrument for a ≤ 20 minute (TBC) science exposure for zenith angles ≤ 60°."

As an example, the DAR term between a science observation in J-band (center wavelength of 1.25 μm) and K-band tip-tilt sensing (center wavelength of 2.2 μm) is 86 mas * tan z, where z is the zenith angle (as derived in atmdisp$.xls from KAON 134). Over the course of a 20 minute integration the zenith angle can change from 45° to 50° resulting in a DAR change of 16 mas. This is large compared to the stability requirement of 5 mas over a 1 hour exposure. A strategy is therefore needed to maintain the science object position to better than 5 mas while the tip-tilt star image moves on the NIR TTS.

The DAR mechanism used in the existing AO system is for the wavefront sensor or STRAP to use centroid offsets during a science exposure. The sensor is then physically moved between science exposures to zero the centroid offsets. Physically moving the NIR TTS would require a 2-axis translation stage or a tip-tilt mirror in the path to this sensor (this would not work for more than one star). An atmospheric dispersion corrector could be another possible alternative however we have not chosen this option due to its additional complexity and cost. Assuming neither of these options it will be necessary to allow the tip-tilt star to be located at an arbitrary location with respect to the intersection of 4 pixels or at least to work within a significant fraction of a pixel from this intersection.

2.5 Tip-Tilt Measurement Analysis and Simulations

The impacts of pixel scale and star positioning on tip-tilt measurement accuracy have been evaluated. The results are summarized and discussed in this section.

Differential atmospheric refraction and the need to accurately position the science object on the science instrument, plus the goal of non-sidereal tracking, make it difficult to position a single TT star at the intersection of 4 pixels. Maintaining the star at a 4 pixel intersection could be accomplished with a tracking device such as a tip-tilt mirror in the TTS path. However, once you have three TT stars then it becomes impractical to have all 3 stars at the intersections of 4 pixels. We have therefore taken the route of determining how best to work with stars that are at arbitrary locations on the TTS. A fallback, which doesn't appear necessary, would be to only work with one star and to have a tip-tilt mirror in the TTS path. You could also constrain your TT star selection to be near pixel intersections, to maximize performance, but again this does not seem to be necessary.

Two analyses were performed. In the first approach, discussed in the next section, a simple excel spreadsheet was used to understand the impact of pixel scale and decentration from the 4 pixel intersection. This was useful for developing a physical understanding. A more sophisticated analysis, summarized in section 2.5.2, was performed by Marcos van Dam to quantify the performance impact.

The conclusions from these analyses are:

(1) Use 50 mas pixels.
(2) Implement a correlation algorithm (better performance than centroiding).
(3) Implement a 4x4 centroiding algorithm (simpler + may work better for far off-axis stars).
(4) Implement some level of seeing disk background subtraction. Alternatively implement an approach to measuring gain or Strehl.
(5) The region of interest (ROI) will need to change to be best centered on each star.
(6) Multiple stars do improve the performance.

2.5.1 Pixel Scale and Positioning Error – Simple Analysis

Figure 9 is a schematic representation of three star images on the NIR TTS detector. The image of star A is ideally located at the intersection of four pixels to allow for optimal tip-tilt correction (since it is null seeking). The performance might be expected to degrade as the star position moved off the intersection to position B or worse of all to position C.

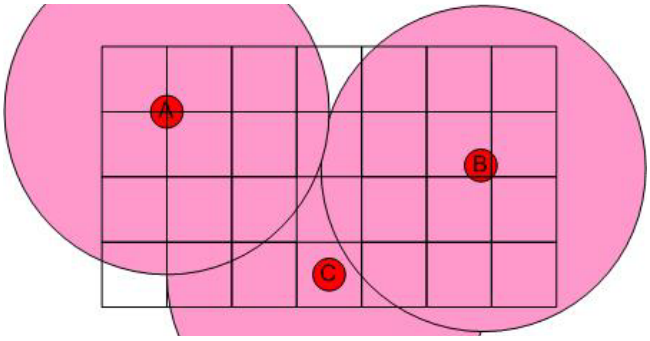

Figure 9: Positioning stars on the NIR TTS detector.
The grid represents the boundaries of individual pixels. The red and pink circles represent the approximate full-width-at-half-maximum diffraction-limited core and seeing limited halo, respectively, of star images. This is roughly to scale assuming 100 mas pixels, a 50 mas core and 0.5 arcsec seeing.

A simple quantitative analysis was performed with an MS Excel tool. The seeing limited halo and the diffraction-limited core were both assumed to be Gaussian with a full-width-at-half maximum (FWHM) of λ/D and λ/r_0, respectively; λ is the NIR TTS operating wavelength, D is the telescope diameter and r_0 is the spatial scale of the turbulence (Fried's parameter). Figure 10 is a cut through a star image, with a Strehl of 0.41 at 2.2 μm, on the NIR TTS that is offset from the intersection of 4 pixels by 0.03". The measured tilt

for this and other offsets of the image from the center of 4 pixels is shown in Figure 11. The measured tilt is seen to be a linear function of the actual tilt only for a small range of decenter from the pixel intersection, less than ~ 20 mas. The measured tilt is also a strong function of the Strehl of the image. This is due to the contribution of the seeing limited disk. If the seeing limited disk were perfectly subtracted then all of the curves in Figure 11 would overlap the SR = 1 curve (albeit with lower SNR for lower SR). In the absence of good seeing disk subtraction it will be important to know the Strehl of the image if the image is not kept centered near the intersection of 4 pixels. Even when it is kept centered without good seeing disk subtraction it will be important to know the Strehl in order to set the optimal gain. A potential method to measure the seeing disk background is briefly discussed in section 8.5.6; seeing disk subtraction will require more attention during the preliminary design (this is not critical to the use of the correlation approach discussed in the next section).

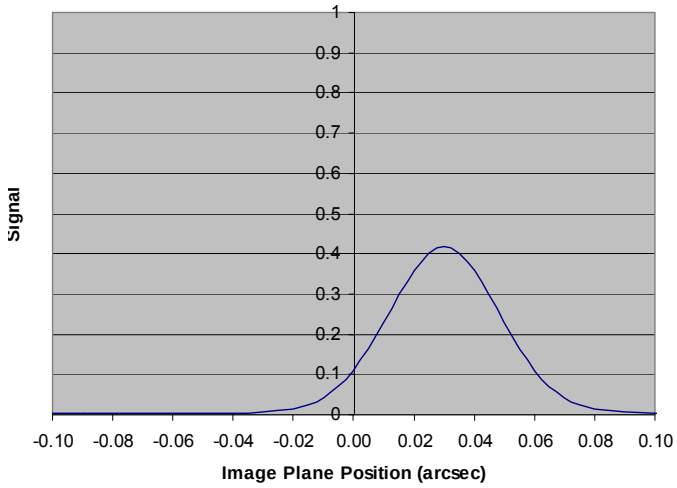

Figure 10: A cut through a NIR TTS image with an offset of 30 mas.
λ = 2.2 μm, rms wavefront error = 329 nm, $r_0(\lambda=0.5\mu)$ = 0.16 m, off-axis distance = 0", isokinetic angle = 44", zenith angle = 30° and pixel size = 0.10".

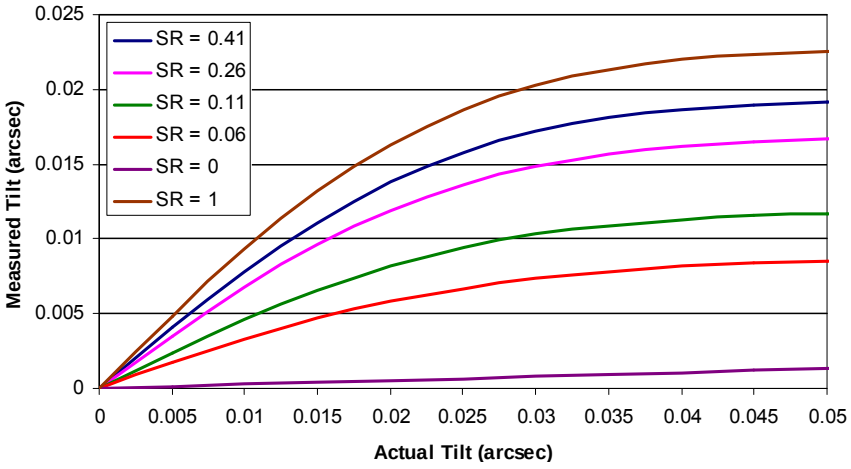

Figure 11: Tilt measured by the NIR TTS for 100 mas pixels and 2x2 pixel centroiding.
The measured tilt is a function of Strehl ratio and is only linear for a small range of decenters from the intersection of 4 pixels. For the parameters used to produce Figure 6, the SR of 0.41 corresponds to an off-axis distance of 0" which falls to SR = 0.26, 0.11 and 0.06 for off-axis distances of 30", 50" and 60", respectively.

We can make the system more linear by using smaller pixels and more pixels to determine a centroid; unfortunately at the expense of reduced field of view for acquisition and increased readout and dark noise.

This is seen in Figure 12 where the pixel size has been reduced to 50 mas and 4x4 pixels were used for centroiding. The performance is now essentially linear for all image decenters. Knowing the Strehl is still critical to setting the proper gain if the seeing disk cannot be adequately subtracted. Note that Figure 12 only extends to 25 mas or ½ of a pixel since it is assumed that the ROI will be shifted by 1 pixel for larger offsets.

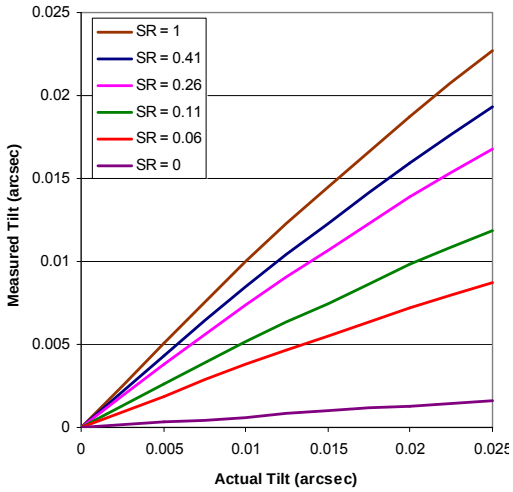

Figure 12: Tilt measured by the NIR TTS for 50 mas pixels and 4x4 pixel centroiding.
Note that once the actual tilt exceeds 25 mas that you would switch to a different 4x4 pixel area for centroiding.

An analysis needs to be performed during the preliminary design of how well the seeing disk needs to be subtracted in order to be able to use the SR = 1 curve in Figure 12. We will also need to determine how well we can determine the seeing disk (see section 8.5.4).

2.5.2 Pixel Scale and Positioning Error – Simulation Results

The results of Marcos van Dam's analysis of the TTS performance are documented in KAON 826 which is summarized here. Three cases were evaluated: 100 mas and 50 mas pixels using a centroiding algorithm and 50 mas pixels using a correlation algorithm. All were done with 4x4 pixels. The difference between the actual tilt and the measured (or specified) tilt is shown in Figure 13 for K = 14^{th} and 16^{th} magnitude stars. Similar to the results in Figure 11 and Figure 12 the measured tilt drops as the Strehl is reduced (e.g. the star gets fainter). The correlation algorithm, with 50 mas pixels, produces the most accurate and linear tilt measurement and the result is quite insensitive to the stellar magnitude (at least for stars ≤ 16^{th} magnitude). The Strehl stability versus offset for the correlation algorithm can also be seen in Figure 14. The Strehl for the centroid algorithm, also shown in Figure 14, can be seen to fall versus offset as fainter stars are used.

KAON 826 also examines the case of multiple (3) guide stars in an equilateral triangle at a specified radius; the Strehl for the 30" and 60" radius cases are also plotted in Figure 14.

A matched filter could potentially be considered as an alternative to a correlation algorithm, but we have not explored this option.

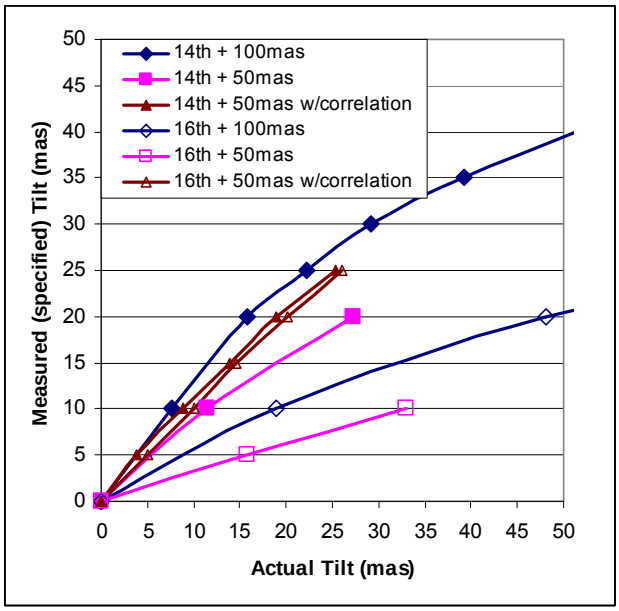

Figure 13: Simulation results for measured versus actual tilt

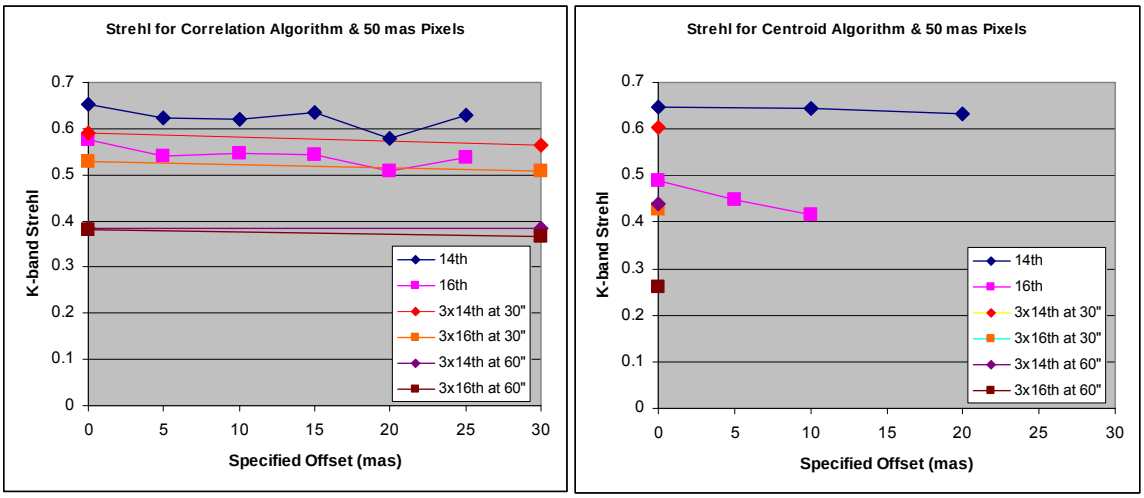

Figure 14: K-band Strehl for the correlation (left) and centroid (right) algorithms versus specified offset for the case of 50 mas pixels

2.6 Measuring Focus

In principle, the NIR TTS could measure focus aberrations if astigmatism was added to the NIR TTS optical path. The advantage of this technique is that it offers a higher bandwidth measurement of the true focus than the LBWFS, and hence higher bandwidth measurements of changes in the sodium layer altitude when used in conjunction with the LGS WFS focus measurements. This could significantly improve the observing efficiency since currently significant time is lost waiting for the low bandwidth wavefront sensor (LBWFS) to settle after each dither or offset. The required amount of astigmatism is a function of how accurately the focus needs to be measured. A measurement with 50 to 100 nm rms focus error would likely be sufficient. The downside of adding astigmatism is that it will broaden the TT star image and therefore impact the centroiding accuracy.

The results of Marcos van Dam's analysis of measuring focus with the NIR TTS are documented in KAON 827 which is summarized here. The concept is to add astigmatism to the NIR TTS optical path as a means of measuring defocus using a quad cell as illustrated in Figure 15.

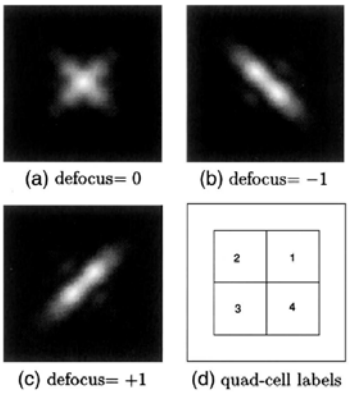

Figure 15: Focal plane images obtained when the beam has 45° astigmatism
(from Patterson & Dainty, Optics Letters 25, 1687 (2000))

It was found that the focus can easily be sensed by the tip-tilt sensor without causing a reduction in Strehl due to aberrations in the tip-tilt sensing spot. In the case of using a bright guide star, the accuracy of the signal is limited by what appears to be contamination from very high-order spherically symmetric aberrations. These aberrations, particularly spherical aberration, should be measured with the LBWFS and corrected. However, the impact of these aberrations on the focus measurement error can be kept below 20 nm if the sensor runs at 1 Hz. If the tip-tilt sensor is operating under noisy conditions, the individual focus measurements are extremely noisy, but a time average of the measurements can still be used to yield a focus estimate. The gain of the signal is significantly reduced, so needs to be calculated from the control loop, in the same way that the centroid gain of an NGS AO system changes. Operating the tip-tilt sensor off-axis also causes a reduction in the sensitivity of the focus measurement.

The above focus analysis assumed that the star image was centered on a quad cell. Van Dam separately noted that measuring focus with the star offset from the quad cell would only be possible if you had a good way to calibrate the zero point and concluded that it would not really be possible to have accurate focus calibrations especially since the offset would be dynamically changing. A potential solution would be to keep one star nulled on a quad cell with a TTM in the path to the NIR TTS. You would then need to combine this TTM position information with the centroid residual to determine the science path TT error.

2.7 Tip-Tilt Mirror

A tip-tilt mirror (TTM) in the path to the NIR TTS could be used to reposition the tip-tilt star(s) without impacting the science field. If it had sufficient range it could also allow for a larger field in which to find a tip-tilt star. It could be used to deal with DAR either as a tracking device or as a positioning device between science exposures. It could allow for focus measurements on a single star as discussed in section 2.6. If necessary, a TTM could be used to dither to measure the centroid gain.

In the absence of a TTM you either need to be able to do tip-tilt sensing at an arbitrary location (including the middle of a pixel) or to be restricted to only be able to position the science object to locations sufficiently close to the intersection of 4 pixels.

The cons of implementing a TTM include cost, and additional development and operations complexity. Unless the TTM has a very modest stroke the TTM would need to be located at a pupil plane which requires an intermediate pupil plane, which would be strongly preferred to be outside of the dewar.

Our current baseline is not to include a TTM in the path to the NIR TTS given that good TT performance can be achieved without it and because of the cons listed above. We may choose to include a TTM as a future upgrade if appropriate. The fold mirror just prior to the camera could potentially be replaced with a 2-axis high precision tracking TTM. Only modest ≤ 0.025 mas on-the-sky motions in each axis of this TTM would be required to center a TT star at the intersection of 4 pixels, which should have little impact on the pupil.

3. Opto-Mechanical Design

This section covers the optical design for the entire NIR TTS, including the optical pickoff and the reimaging optics between the optical pickoff and the NIR TTS detector, and the mechanical design for hardware outside of the NIR TTS camera. We begin with the mechanical design concept to provide the reader with an initial overall perspective on the opto-mechanical system (section 3.1), even though later sections will need to be read to understand the components. We then discuss the plate scale (3.2), the optical pickoff (3.3) and the optical design for the re-imaging optics (3.4) before finishing with the optical alignment concept (3.4.2).

3.1 Mechanical Design Concept

The mechanical design concept is shown in Figure 16. This figure shows both the optical pickoff exchange mechanism and the NIR TTS camera with reimaging optics mounted on a focus stage. Two views of the NIR TTS mechanics on the AO bench are provided in Figure 17 and Figure 18. The latter image also provides a top view of OSIRIS. The front face of the dichroics is located 300 mm from the OSIRIS focal plane and at a 30° incidence angle in these figures.

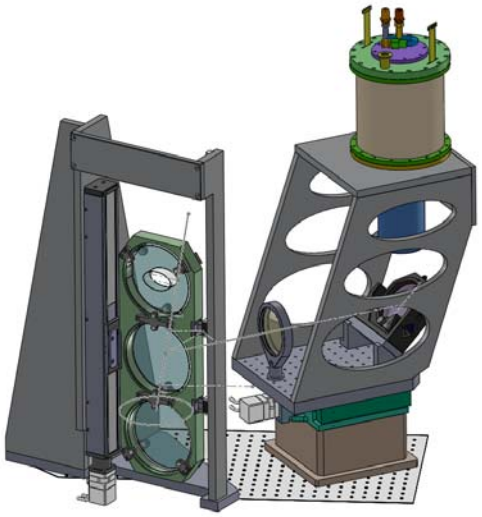

Figure 16: Mechanical concept. The optical pickoff exchange mechanism (left) and the NIR TTS camera with reimaging optics on a focus stage (right).

An exchange mechanism will be used to switch between optical pickoff options. A vertical translation stage approach has been selected. As discussed in section 3.3.2 only a 3 position device, including open, is needed if the optical pickoff mechanism must be located on the AO bench (i.e. > 400 mm from the focal plane). A three or four position device to accommodate three optics (H reflective dichroic, K reflective dichroic, annular mirror) is desirable if the optical pickoff mechanism can be located between the AO bench and OSIRIS (i.e., ≤ 300 mm from the focal plane); this is the option shown in Figure 16. The advantage of having the optical pickoff closer to the focal plane is that it allows the annular mirror option and it also means that the NIR TTS can be closer to the optical pickoff mechanism therefore requiring less real-estate on the AO bench. Its disadvantage is the need for an enclosure extending off the AO bench.

The optical pickoff exchange mechanism does not interfere with the AO bench or its cover; the top position for the optical pickoffs is close to the ceiling and the bottom position extends below the AO bench. The optical pickoffs shown in Figure 16 are 150 mm diameter and 20 mm thick (they could be reduced by ~ 25 mm in diameter if they are located at the 300 mm from the OSIRIS focal plane location shown in Figure 18). The translation stage is a Parker Daedal 402600XR1. The vertical bar to the right of the optical pickoff holders provides a guide roller track to ensure positioning repeatability and to reduce susceptibility to vibrations. The co-alignment and repeatability of the fold optics must be good enough to ensure that a re-acquisition is not required when switching between fold optics.

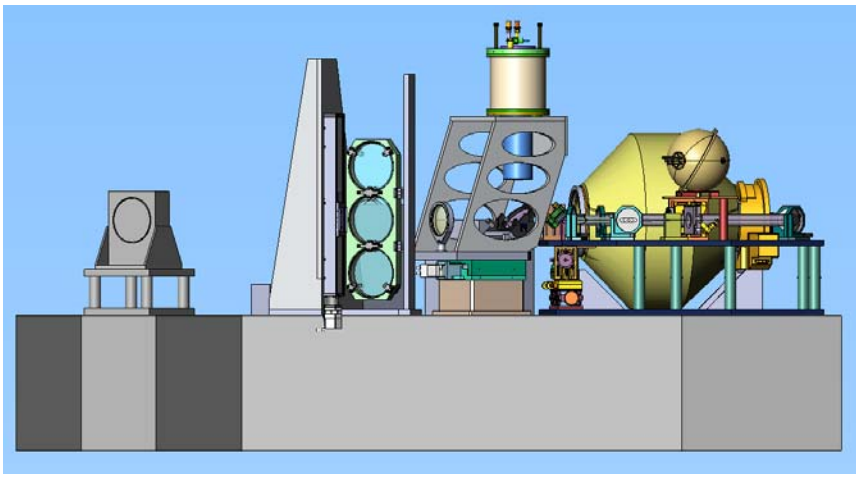

Figure 17: Side view of the NIR TTS mechanics on the AO bench

The focus of the AO system is adjusted to maintain focus on the science instrument. Given the ± 2 mm focus difference between the spectrometer pixel scales it will be necessary to have a focus adjustment for the NIR TTS of ≥ 4 mm. The field lens and the camera dewar, which includes the reimaging optics, are therefore mounted on a short throw focus stage (a Parker Daedal 808CTE-04).

The structure supporting the NIR TTS dewar is angled so as not to hit the existing pupil simulator. The connections at the back of the camera dewar currently extend ~ 50 mm into the AO bench ceiling. During the preliminary design we will investigate a modified approach to avoid this conflict and/or the option of cutting a hole in the ceiling. The currently favored approach is to cut a hole in the ceiling and move the camera up slightly so that the compressed gas lines for the cryocooler that mate to the top of the dewar do not enter the AO enclosure; the top of the dewar would be approximately flush with the top of the AO enclosure ceiling.

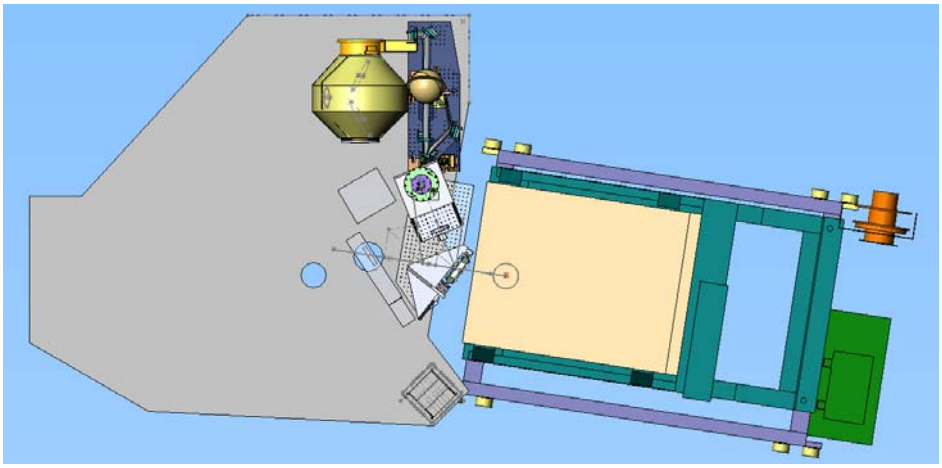

Figure 18: Top view of NIR TTS mechanics on AO bench. OSIRIS is shown at right. The blue mechanism at top is the pupil simulator. The gold mechanism at top is the rotator.

3.2 Plate Scale

Choosing the optimal plate scale is a balance between field of view and centroiding performance. For reference, note that the diffraction-limited core diameter at Ks (2.15 μm wavelength) is 44 mas and the optimal field of view is 120" diameter.

A plate scale of ~0.05"/pixel or less would be desirable from the analysis in section 2.5. This plate scale would give a field of 102"x102", and a diagonal of 145", on the procured H2RG detector. This case and

the case of a 0.06"/pixel plate scale are shown against the detector in Figure 19. Given the quality of the detector we do not need to consider plate scales larger than 60 mas/pixel. A somewhat smaller plate scale would improve the centroiding. We have selected 50 mas/pixel as the plate scale; this choice will be re-assessed during the preliminary design. This plate scale meets the requirement of a minimum field of view of 100" diameter.

A plate scale of 0.05"/pixel, or 0.360 mm/" given the 18 μm pixels, requires a demagnification of 0.727/0.36 = 2.0 corresponding to a final f/# of 6.8 (versus the f/13.66 AO focal ratio).

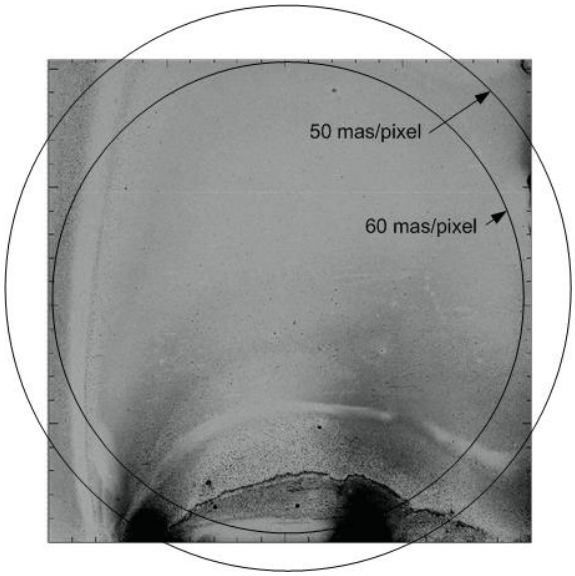

Figure 19: 120" diameter field of view, for 2 different plate scales, superposed on the H2RG detector *The field of view has been displaced slightly upward with respect to the detector.*

3.3 Optical Pickoff

3.3.1 Fields of View

The position and size of the three detectors are shown with respect to each other in the focal plane in Figure 20. The OSIRIS imager and integral field unit (IFU) size and position are from Figure 4. It is possible to decenter the OSIRIS imager and IFU together with respect to the optical axis (defined by the AO rotator axis) during the initial alignment of OSIRIS to the Keck I AO system. The NIR TTS is shown with a small decenter down to be consistent with Figure 19.

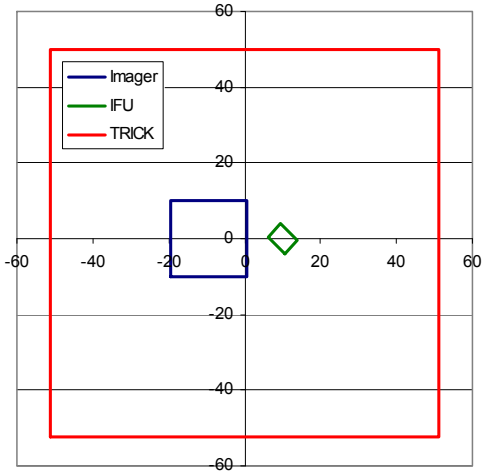

Figure 20: The OSIRIS imager and integral field unit (IFU), and the NIR TTS detector (TRICK), in the focal plane (units are arcsec). *(0,0) represents the AO optical axis. The largest IFU field is shown.*

3.3.2 Size

A fold mirror and/or dichroic will be used to reflect the required light to the NIR TTS and pass the science field to the science camera, OSIRIS. If we assume that the fold is on the AO bench then it must be located > 393 mm from the focal plane (from section 2.1). If we allow it to extend into the space between OSIRIS and the AO bench then the fold must still be located > 185 mm from the focal plane.

The NIR fold should be located as close to the OSIRIS image plane as possible in order to minimize vignetting and the required size of the fold. The required major axis diameter of the fold or dichroic

$$d = (fov * ps + t / f\#) / \cos\theta ,$$

depends on the field of view (fov) of the TTS sensor, the plate scale (ps = 0.727 mm/arcscec) at the focal plane, the distance (t) of this fold from the focal plane, the focal ratio (f# = 13.66) of the beam and the angle of incidence (θ) on the fold mirror. Assuming fov = 120", t = 300 mm and θ = 45° then D = 154 mm. If the distance of the fold from the focal plane were increased to t = 500 mm then the fold diameter is increased to d = 175 mm.

A very similar equation can be used to calculate the major axis diameter of the hole in a fold mirror required to transmit the fov to the science instrument. In order to transmit the maximum IFU size of 4.8"x6.4" the mirror would need a hole of 41 mm in height and 58 mm in width if t = 500 mm and θ = 45°. For the smallest IFU size of 0.32"x1.28" the hole could only be reduced to 38 mm x 53 mm.

The hole in a fold mirror would vignette a field of diameter

$$fov = (d * \cos\theta + t / f\#) / ps.$$

The vignetted field of view would be 62" for the smallest IFU size and 67" for the largest IFU size, assuming t = 300 mm. The vignetted field would be 102" for the smallest IFU size and 107" for the largest IFU size, assuming t = 500 mm. This implies that an annular mirror concept is only valid for t ≤ 300 mm.

The field at the dichroic, for t = 500 mm and 300 mm, is represented in Figure 21 by circles showing the size of the expanding f/13.66 beam for multiple image points at the dichroic. The circle size is 36.6 mm for t = 500 mm and this reduces linearly with the distance to the focal plane, t. This figure provides a check on the required outer diameter of the dichroic. The height of the dichroic need only be ~110 mm for t = 500 mm. Assuming a dichroic at 30° incidence angle the dichroic could be 127 mm if it were a circular optic.

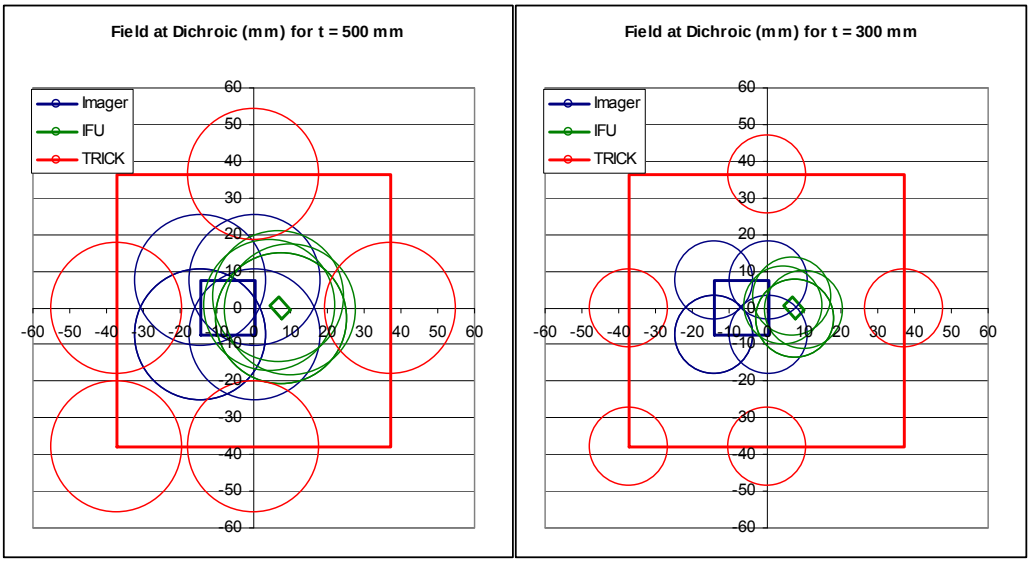

Figure 21: The OSIRIS and NIR TTS fields of view projected onto the dichroic.
The distance of the dichroic from the focal plane is 500 mm (left) and 300 mm (right). The circles represent the size of the expanding f/13.66 beam on the dichroic for points in the focal plane at the corners of the imager and IFU fields and at the sides of the imager field. Units are mm.

3.3.3 Optical Pickoff Options

The fold options that have been considered are listed in Table 2. Case 1 is with no fold in the beam. Case 2 is an annular mirror, the IFU field is transmitted through the hole in the mirror, and the mirror reflects an annular field to the TTS. Case 3 is a K-band reflective dichroic that transmits the shorter wavelength bands to OSIRIS. Case 4 is a H-band reflective dichroic that transmits K-band to OSIRIS. Case 5 and 6 are for IFU science only and consists of an annular mirror with an H-band reflective dichroic at its center. This allows you to do H-band TT sensing with stars in the IFU field or K-band TT sensing with stars in the outer reflected annulus. We did consider a partially K-band reflective dichroic but for emissivity and throughput reasons we discarded this option.

The K-band dichroic (case 3) would always be the best choice for J & H-band science. The H-band dichroic (case 4) is the only option listed for K-band imaging science. The annular mirror (case 2) would be a better option for K-band IFU science if there were tip-tilt stars in the outer annulus (where they are most likely to be). The annular mirror with an H-band dichroic (case 5 and 6) at its center offers a compromise between cases 2 and 4, and therefore the option of only requiring two dichroics, at the expense of lower throughput to the IFU and no K-band imaging, respectively.

Case	Science λ	IFU	Imager	NGS location	Tip-tilt λ	NIR fold
1	JHK	Yes	Yes	0-60" off-axis	Vis	n/a
2	JHK	Yes	No	35-60" off-axis	K (or H)	annular mirror
3	JH	Yes	Yes	0-60" off-axis	K	K-dichroic
4	K	Yes	Yes	0-60" off-axis	H	H-dichroic
5	K	Yes	No	<35" off-axis	H	H annular mirr
6	K	Yes	No	35-60" off-axis	K (or H)	H annular mirr

Table 2: Configuration options for tip-tilt sensing

To provide broad user applicability at least a 3 position exchange mechanism should be provided. We could start with the K-band and H-band dichroics in this mechanism and later add the annular mirror in the open position assuming the performance predictions have been achieved. Imaging science with STRAP would be impacted because either the H-band or K-band dichroic would need to be in the science path however, there would be no impact on IFU science with STRAP since the annular mirror could be used.

3.3.4 Dichroic Optical Impact on Science Path

A tilted plane parallel plate inserted into the science path will introduce a variety of aberrations including lateral chromatic, longitudinal chromatic, astigmatism, coma and spherical. The AO deformable mirror could be used to remove the non-chromatic aberrations in the science path, which will put these aberrations instead in the NIR TTS optical path and also in the wavefront sensor path.

The third-order wavefront aberrations for a tilted plate are

$$\Delta W_{spherical} = -[t/(f/\#)^4][(n^2-1)/(128n^3)] = -1 \text{ nm}$$

$$\Delta W_{coma} = -[(t\sin\alpha)/(f/\#)^3][(n^2-1)/(16n^3)] = -50 \text{ nm}$$

$$\Delta W_{astig} = -[(t\sin^2\alpha)/(f/\#)^2][(n^2-1)/(8n^3)] = -749 \text{ nm} ,$$

where we have used the current design parameters of thickness t = 15 mm, angle of incidence α = 30°, f/# = 15 and fused silica index n = 1.44. During the preliminary design we will look at reducing the angle of incidence given its quadratic impact on astigmatism.

The lateral and longitudinal displacement as a function of wavelength are given by

$$\Delta y(\lambda) = t\{\sin\alpha - \cos\alpha \tan[\sin^{-1}(\sin\alpha/n(\lambda))]\} .$$

$$\Delta z(\lambda) = [(n-1)/n]t \ .$$

Across the J-band the index of fused silica varies from 1.4498 to 1.4452 resulting in a lateral chromatic aberration of 17.3 μm and a longitudinal chromatic aberration image blur of 1.1 μm.

The impact of these aberrations was evaluated in Zemax by adding this new dichroic, located 300 mm from the focal plane, to the existing Zemax model of the telescope and AO system. The resulting RMS wavefront error versus field position is shown in Figure 22.

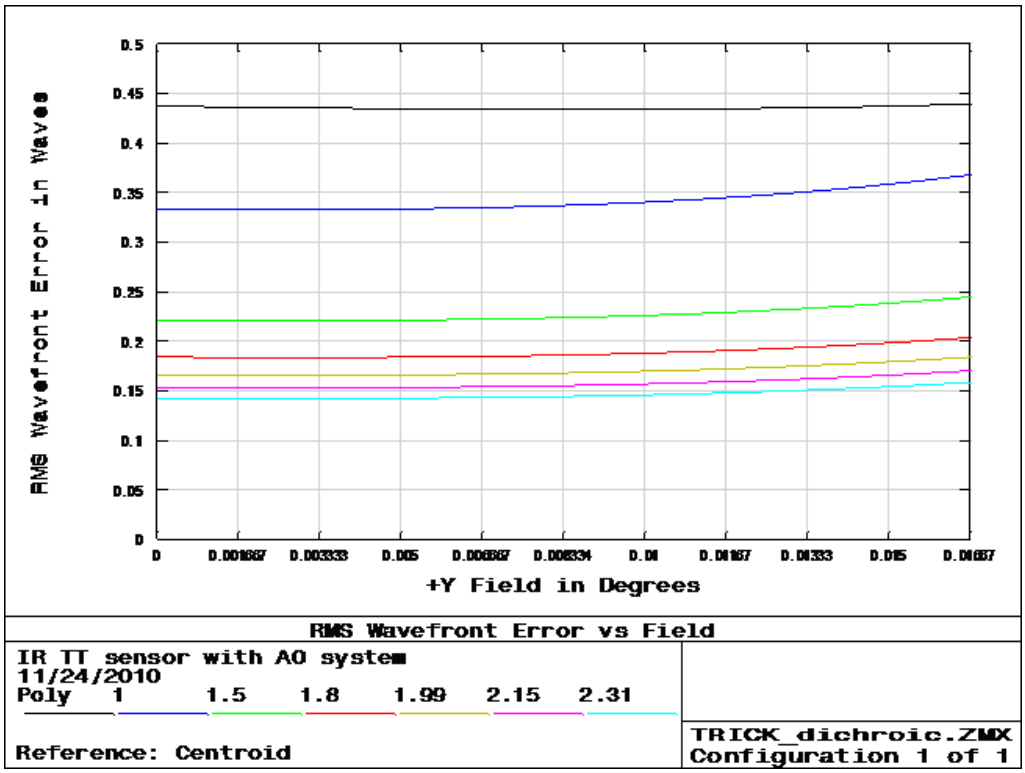

Figure 22: RMS wavefront error for a 15 mm thick fused silica dichroic at 30° angle of incidence

Non-chromatic aberrations to the science instrument can be measured with image sharpening and corrected with the deformable mirror by using centroid offsets on the wavefront sensor. However, this would result in putting these aberrations into the NIR TTS path. A similar plane parallel plate, tilted by the same amount in the orthogonal direction, in the science or NIR TTS path could be used to remove the astigmatism in that path at the expense of doubling the lateral and longitudinal color and coma.

The compensation approach we have settled on for the system design is to add a Zernike surface and wedge to the 2nd surface of the dichroic. The Zernike surface compensates for astigmatism and the wedge corrects for lateral chromatic. The resultant greatly improved wavefront error is shown in Figure 23 and the resultant spot diagrams in Figure 24. This solution results in the best compensation of the science, NIR TTS and wavefront sensor paths. It is in fact an improvement over the current situation since the correction added to the 2nd surface of this dichroic is also used to compensate for astigmatism from the existing dichroic. The existing IR transmissive dichroic does have a wedge so we have existing experience with procuring such dichroics, however the additional very low power cylinder is a new requirement.

Note that leaving a small amount of non-common path astigmatism between the science and NIR TTS paths would facilitate focus sensing with the NIR TTS.

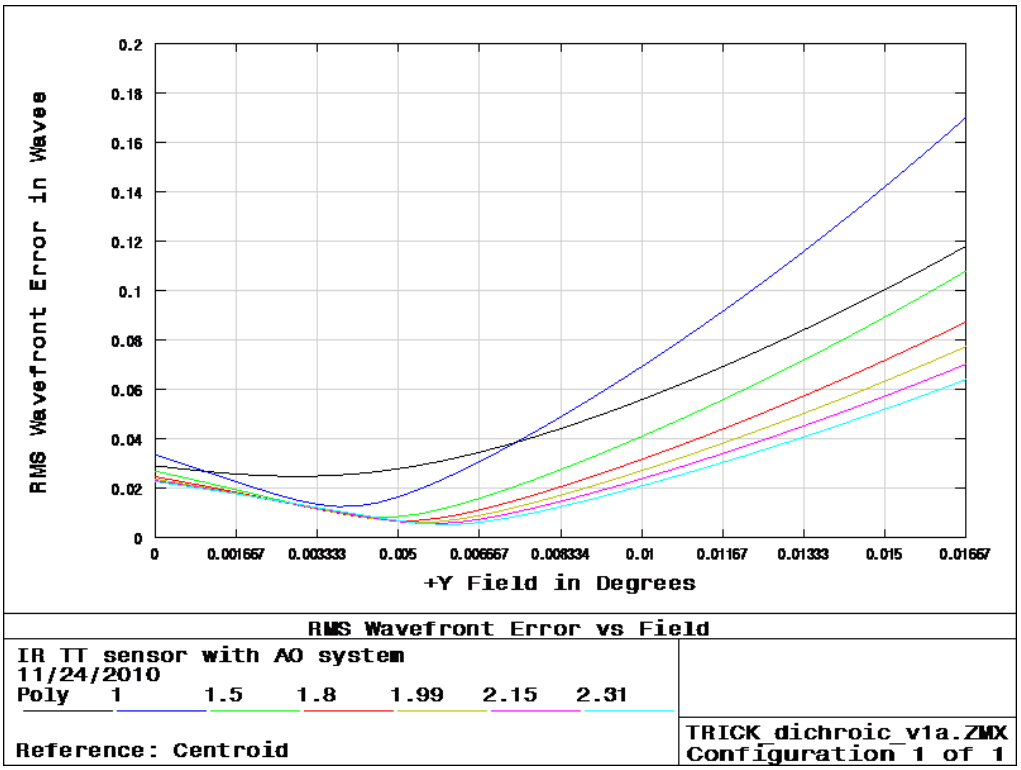

Figure 23: RMS wavefront error for a 15 mm thick fused silica dichroic at 30° angle of incidence, with a 0.55° wedge and a 19.343 m radius cylinder

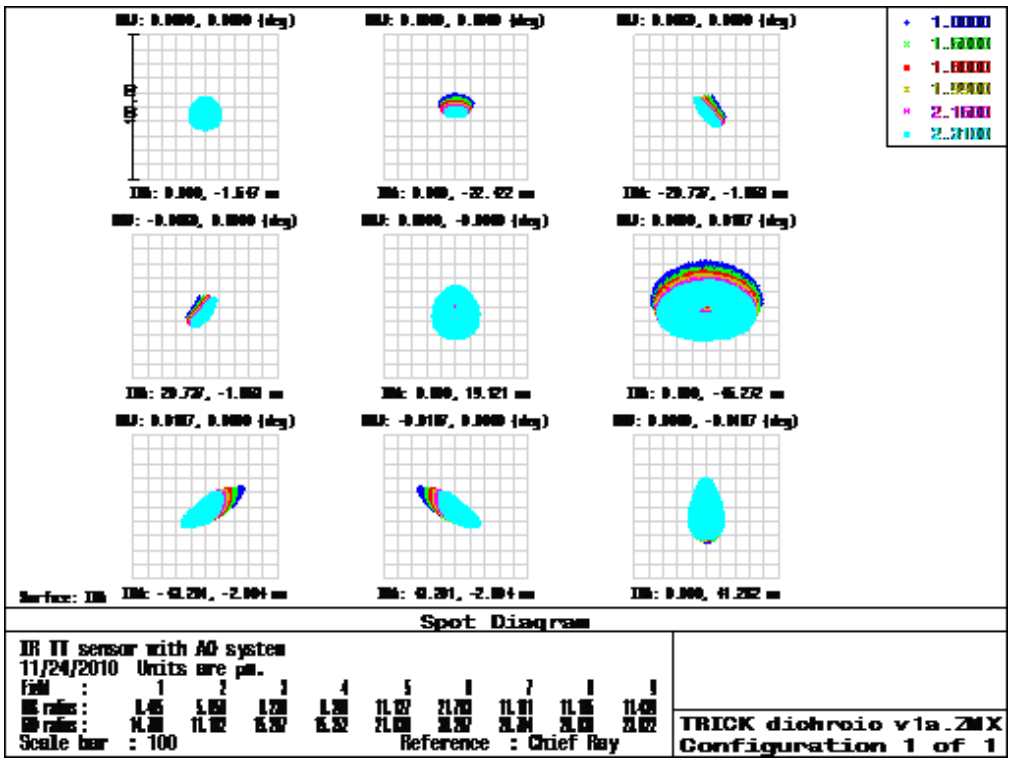

Figure 24: Spot diagrams for the case shown in Figure 23

3.3.5 Dichroic Requirements

The dichroic specifications are summarized in Table 3. The current Keck AO IR transmissive / visible reflecting dichroics were obtained, using a similar specification table, from Custom Scientific. Previous versions were obtained from Barr Associates. We will pursue quotes from both of these vendors.

Table 3: Dichroic specifications

Category	Specification	
Name	**H-band reflective**	**K-band reflective**
Quantity	1	1
Diameter	140 ± 0.5 mm	
Thickness	15 ± 0.5 mm	
Clear aperture (CA)	≥ 135 mm of central diameter	
Wedge angle	TBD to minimize lateral dispersion	
Cylinder radius	TBD to minimize astigmatism	
Edges	chamfered edges, bevel = 2 mm at 45° on both surfaces	
Substrate material	Infrasil (vendor supplied)	
Environmental conditions	temperature: -5 to +25°C; pressure: 450 to 760 mm-Hg; relative humidity: 0 to 100%	
Reflectance (1st surface)	≥ 96% average, ≥ 93% min. for 1.45 ≤ λ ≤ 1.8 μm	≥ 97% average, ≥ 95% min. for 1.95 ≤ λ ≤ 2.4 μm
Anti-reflectance (2nd surface)	≤ 0.5% for 0.975 ≤ λ ≤ 2.4 μm	
Transmittance (through optic)	≥ 96% average, ≥ 93% min. for 0.975 ≤ λ ≤ 1.40 μm & ≥ 97.5% average, ≥ 95% min. for 1.95 ≤ λ ≤ 2.4 mm	≥ 96% average, ≥ 93% min. for 0.975 ≤ λ ≤ 1.81 μm
Polarization	the optics shall be non-polarizing (i.e. ≤ 0.1% polarizing)	
Angle of incidence	37° ± 0.1° (TBC)	
Wavefront rms (focus removed)	≤ 20 nm rms in reflection & transmission	
Wavefront rms (with focus)	≤ 450 nm rms in reflection & transmission	
Smoothness	≤ 10 nm rms for any 2 points separated by ≤ 25 mm	
Surface quality	60/40 scratch/dig for both surfaces (MIL-F-48616, section 4.6.7.2)	
Adhesion durability	Tape test per MIL-F-48616, section 4.6.8.1	
Abrasion durability	Cheesecloth test per MIL-F-48616, section 4.6.8.3	
Cleanability	Solvents test per MIL-F-48616, section 4.6.9.2	
Performance tests required	Spectrophotometer curves over the CA at the nominal incidence angle. Interferometric scans in reflection & transmission over the CA. Adhesion, abrasion & solubility test results from a witness sample from the same coating run. Certification that each requirement has been met.	

3.3.6 Emissivity

The K-band reflective dichroic will add background in K-band to the NIR TTS to the extent that it is not 100% K-band reflective. This dichroic will not add significant background to the JH science being done with OSIRIS.

The H-band reflective dichroic will add background to K-band science with OSIRIS to the extent that it is not 100% K-band transmissive. This dichroic will not add significant background to the H-band tip-tilt sensing.

The annular mirror, used for K-band IFU science, would add significant thermal background to the central part of the NIR TTS field and the outer part of the OSIRIS field. If the annular mirror was at a focal plane then the pupil stop in OSIRIS would prevent the thermal background from this mirror from reaching the IFU. Similarly, the pupil stop in the TTS would prevent thermal background from the hole in the mirror from reaching the outer radius of the TTS field; the part of the field used for TT sensing with the annular mirror. The extent to which this background will contaminate the field depends on how far the annular mirror is from the focal plane. For the 300 to 500 mm distance at which the dichroic is expected to be from

the focal plane the additional thermal background should have no impact on the IFU and little impact on the minimum radius at which TT stars can be used. This statement will be checked with the optical model.

In order to remove this background either a narcissus mirror could be installed on the opposite side of the dichroic from the NIR TTS so that the NIR TTS would be looking at its cold reflection in the narcissus mirror or something cold could be placed at this location. Our baseline plan is to procure high reflectivity/transmission dichroics in order to minimize the increase in background. A narcissus mirror or cold surface could be a future upgrade if necessary. This topic will be further assessed during the preliminary design.

3.4 Re-imaging Optics

Reimaging optics will be required to achieve the desired 0.05"/pixel plate scale. A pupil location is required for a cold pupil stop to reduce thermal background. Two filter options will be used: a Ks (1.99 to 2.30 μm) filter (chosen to block the steepest part of the thermal background) and an H filter. Consideration will be given to placing the pupil stop on the filters to allow selection of pupil size; for example to use a circumscribed pupil (for maximum resolution and throughput) in H-band while selecting a smaller (inscribed) pupil for best thermal background rejection in K-band.

A reflective optical design was briefly considered due to the broad range of operating wavelengths, but was quickly discarded due to the small space envelope available and the need for an accessible real pupil image. The refractive optical design that has been developed is described in the following section.

3.4.1 Optical Design

The current design based on refractive optics has all spherical surfaces and is shown in Figure 25.

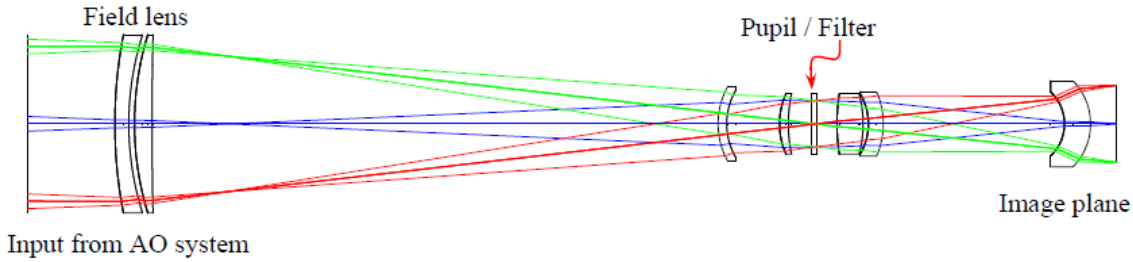

Figure 25: Reimaging optics layout

The first element group is a field lens to create a real pupil image. Due to the large wavelength range it is a doublet to control chromatic aberration of the pupil image. It was moved before the image plane to both shorten the overall camera length and to reduce the problem of reimaging dust and defects present on its surface. A fold mirror, not shown in this diagram, is incorporated to fit the system in the available space on the AO bench. In order to keep the dewar at a reasonable size, the field lens and fold mirror will be warm while the remaining optics are located inside the dewar. It is currently under consideration whether to make the first lens the dewar window or if it is better to use an additional flat window.

The next portion of the camera optics was initially modeled as a pair of doublets surrounding the pupil image similar to a double Gauss lens. As the system was optimized these were driven to the current configuration. A flat piece of glass is included at the pupil location to represent the H or K-band filter. A mask will likely be deposited directly on the filter to function as the cold stop.

The final element is a thick meniscus with a small net power which functions as a field flattener and provides some aberration compensation.

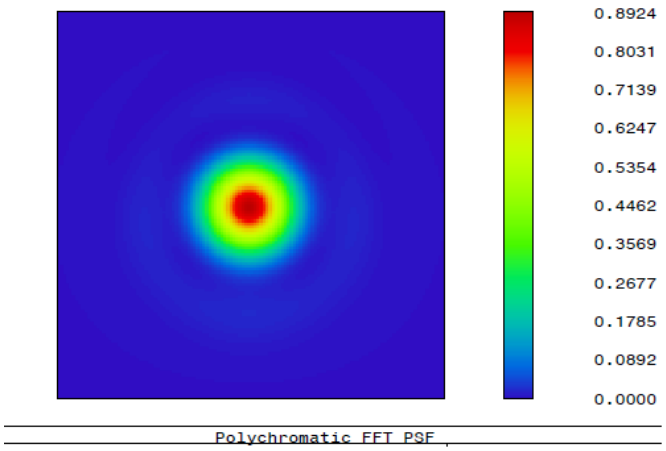

Figure 26: H-band PSF at 60" off-axis. The Strehl is 89%.

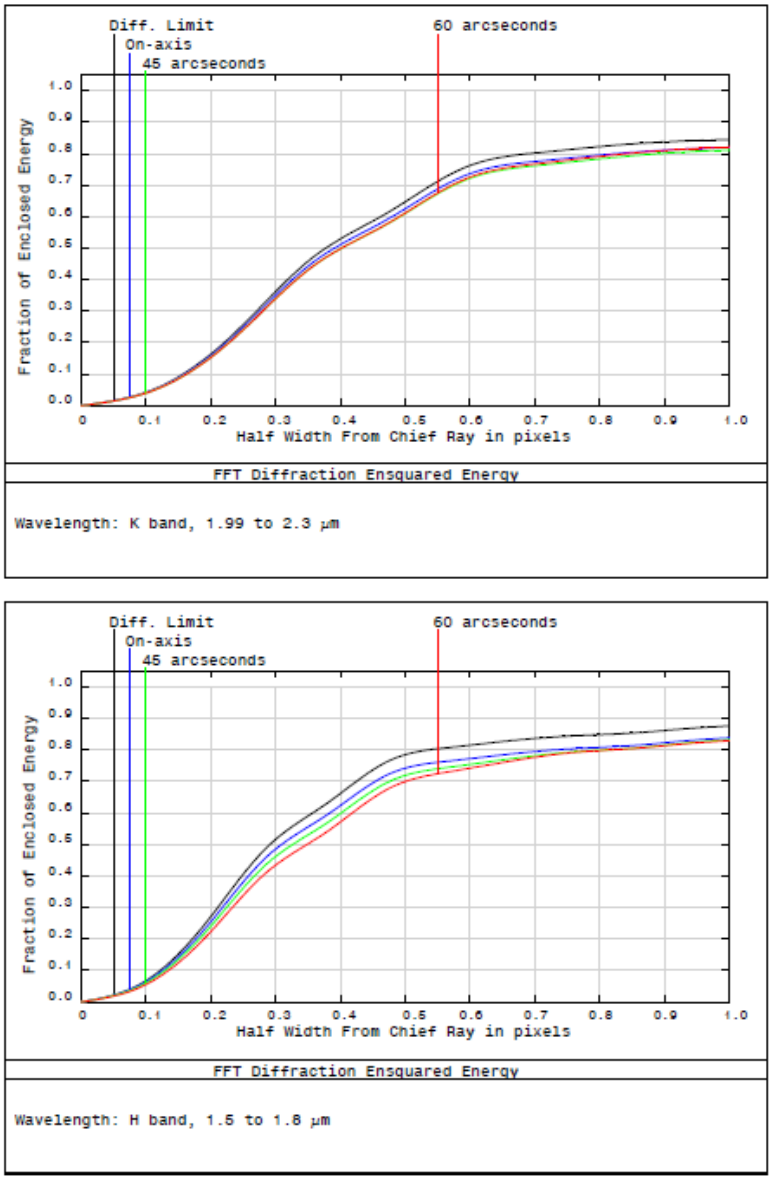

Figure 27: Ensquared energy for K-band (top) and H-band (bottom). The plate scale is 50 mas/pixel.

The performance of the current design is quite good, with the lowest Strehl over the entire 120" diameter field of 93% for K band and 89% for H band. On-axis Strehl is 97% for K and 94% for H. Figure 26 shows the worst PSF for the system. The PSF models for the other points and wavebands are very similar.

The ensquared energy for both H and K bands at three different field points are shown in Figure 27. The horizontal axis is given in terms of pixels from the chief ray position.

The system prescription is shown below in Table 4.

Table 4: Reimaging optics system prescription (all units are mm)

#	Type	Radius	Thickness	Glass	Semi-Diameter
5	STANDARD	255.36	8.017	SILICON	50.0
6	STANDARD	162.44	3.262		50.0
7	STANDARD	167.38	10.009	ZNSE	50.0
8	STANDARD	1735.89	325.424		50.0
9	STANDARD	42.06	5.001	SILICON	21.0
10	STANDARD	37.14	30.336		19.0
11	STANDARD	40.59	5.044	BAF2	17.0
12	STANDARD	78.47	13.000		17.0
13	STANDARD	--	3.000	CAF2	17.0
14	STANDARD	--	12.000		17.0
15	STANDARD	111.48	14.954	BAF2	17.0
16	STANDARD	-65.39	3.095		17.0
17	STANDARD	-32.25	8.571	F_SILICA	17.0
18	STANDARD	-43.52	104.085		18.0
19	STANDARD	-24.26	15.001	ZNSE	18.0
20	STANDARD	-33.94	14.590		24.0
21	STANDARD	--	0.000		21.7

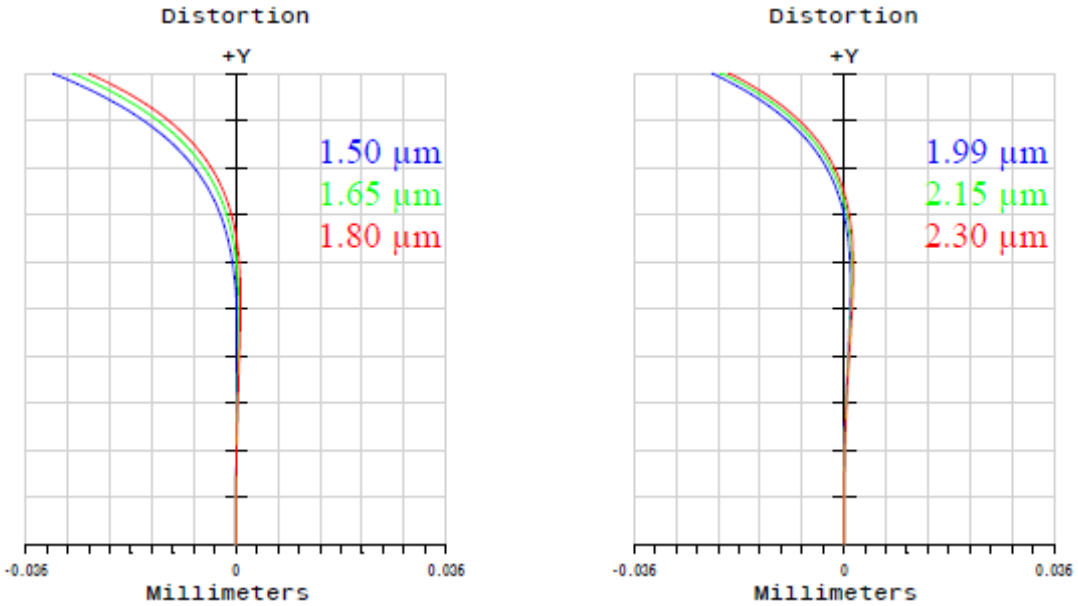

Figure 28: Field distortion for H (left) and K-band (right). The maximum field is 60". The horizontal scale is 3.6 µm or 10 mas per small tick mark.

The field distortion for this system is shown in Figure 28. It is somewhat wavelength dependent, with the H-band field showing slightly more distortion than for K-band. For H-band the distortion is less than 10 mas up to a field angle of 48", while for K-band it is less than 10 mas up to a field angle of 52".

The pupil image quality is very good in this camera. The current camera model uses a paraxial model of the telescope which eliminates any effects from the AO system. In this model, the pupil image for the circumscribed Keck pupil is 25.96 mm diameter. To determine the quality of this pupil image, the model was changed to place the object at the telescope exit pupil and the image quality at the nominal pupil plane in the camera was examined. Figure 29 shows the spot diagrams obtained in this manner for points corresponding to the center, edge, and ¾ diameter areas of the pupil.

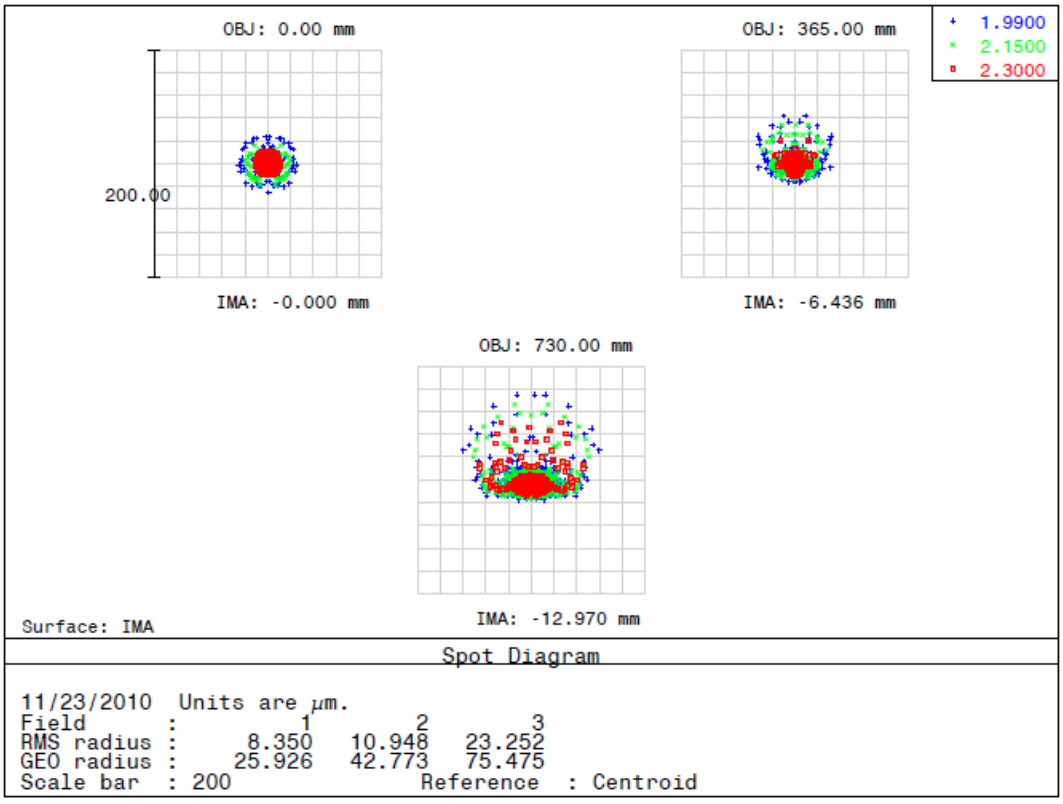

Figure 29: K-band pupil image spot diagrams. H-band differs by only a few μm in radius.

Since there are many other aspects of the system that depend on the optical design, it will be brought to maturity early in the preliminary design phase. There are several planned improvements to the current optical design:

- A design with fewer lenses will be attempted to reduce the overall complexity.
- The use of five different types of glass will require several batches to apply the anti-reflection coatings. This would increase cost so a design with fewer types of glass will be investigated.
- The cost/benefit trade for including aspheric surfaces will be investigated.
- Design elements such as changing the field lens to a cemented doublet will be considered to help with the alignment and overall system manufacturability.

During the preliminary design we will also combine this independent reimaging optics design with the existing telescope and AO system Zemax model, including the impacts of a pickoff dichroic.

Note that for AO-correction of the TT star we would want to include a MEMS deformable mirror at a pupil location; however we have declined to pursue this option for the NIR TTS. Similarly if we wanted to

include a TTM in the path the best location would be at a pupil; however, again we have declined to pursue this option. There is a mirror between the field lens and the next optic that might have little impact on pupil motion if it were used for small TT adjustments.

3.4.2 Cold Baffling

In addition to the cold pupil stop, a light-tight cold baffle must surround at least part of the light path to block the considerable thermal radiation emitted by surrounding surfaces. In K-band reimaging systems the cold baffle normally extends as far forward as the field lens which usually serves as the dewar window; but we will study whether a shorter cold baffle will suffice such that the fold mirror can remain outside the dewar where it is readily adjusted or replaced by a tip-tilt mirror.

Figure 16 shows the cold baffle only extending to cover the first lens after the field lens. This is quite close to the cold pupil stop. The baffle can be extended by moving the fold mirror closer to the field lens.

3.5 Optical Alignment

Access will be limited to the Keck I AO bench with OSIRIS in the beam. Much of the optical alignment will therefore be done prior to installation on the AO bench. Only alignment to the AO rotator axis should be required once the system is installed on the AO bench. The AO rotator axis can be defined by placing the pupil simulator on the rotator axis. The image position on the rotator axis can be defined by placing the AO input fiber on the rotator axis.

For access reasons it will probably be necessary to install the NIR TTS assembly on the AO bench prior to installing the dichroic fold mechanism. Both should be initially aligned to the positions and orientations in the mechanical model.

3.5.1 Optical Pickoff Alignment

The vertical translation stage is aligned off the telescope to insure that the stage moves vertically, the reflective optical surfaces are perpendicular to vertical and each optic is centered at a height of 305 mm from the AO bench mounting surface when it is in its in-beam position.

The vertical translation stage will initially be populated with mirrors in each of the dichroic positions. A paper target should be able to be supported at the mirror face. The defining points for the reflective surface face toward the AO input so that once these are aligned the mirrors can be replaced with dichroic fold optics without affecting the alignment.

The fold optics should be centered on the optical axis of the AO rotator. A visual horizontal centering should be sufficient, preferably by moving the optic in the plane of its surface. A laser source can be input to a multimode fiber either at the AO input or in the pupil simulator. The laser source should provide sufficient light even through the IR transmissive dichroic to center the dichroic fold optics. A mask can be put in front of the deformable mirror if necessary to stop down the beam.

After centering the beam the paper targets can be removed. The defining points for each mirror could be adjusted if necessary to insure that the reflected beam remains parallel to the AO bench (at a height of 305 mm). The entire assembly can be rotated about a vertical axis, and/or translated along the optical axis, until the reflected beam is centered on the NIR TTS field lens and dewar entrance window.

The mirrors can be replaced with the dichroics once the alignment is at a satisfactory point. It will be important that a re-acquisition will not be required when switching between dichroics. A small known offset may be acceptable but it must be repeatable.

3.5.2 NIR TTS Assembly Alignment

The NIR TTS assembly consists of the field lens, a fold mirror, and camera dewar mounted on a focus translation stage.

The optical system from the field lens to the detector will be pre-aligned off the telescope such that the optics and detector are centered on an optical axis parallel to the focus translation stages axis and at a height of 305 mm above the AO bench mounting surface.

The reimaging optics (other than the field lens), the pupil stop and filters will be mounted in a snout extending from the dewar. The alignment procedure and how to test the image quality will be determined once the mechanical system design is further developed.

The field lens positioning is not critical. It should be sufficient to center the field lens at the required position mechanically. Its tilt could be checked by placing a laser beam at a height of 305 mm, aligning the focus translation stage to be parallel to this, and making sure that the field lens reflects the laser beam back on itself. This procedure could also be used to ensure that the dewar entrance window surface is centered and orthogonal to the focus direction (prior to installing the field lens).

After installation on the AO bench the remaining step is to align the NIR TTS assembly to the AO rotator axis. The field lens should be centered on the rotator axis and the fiber image should be in focus at the required position with respect to the field lens. Images of the fiber can then be taken with the camera. The backend of the assembly will be moved to center the image on the camera while maintaining the rotator axis centered on the field lens.

The pupil alignment can be checked during the day with the AO fiber source and a mask, with 4 symmetric off-axis holes near the edge of the pupil, placed in front of the deformable mirror. The fiber can be moved out of focus so that the 4 images are separated on the NIR TTS. The relative flux of the 4 images on the NIR TTS is a measure of the pupil alignment or misalignment. This approach is used to check and adjust the NIRSPEC pupil mask alignment when NIRSPEC is installed with the AO system.

4. NIR TTS Camera

We will use the already procured Teledyne H2RG serial number GBA222 detector (18 μm/pixel). This detector uses the latest 2.5 μm cut-off HgCdTe recipe exhibiting low noise; 10.5 e- for correlated double sampling readout. Experiments with a very similar device (H2RG GBA220) indicate that multiple sampling will deliver substantial noise reduction. TT stars can be used anywhere on the detector with object selection performed by identifying one or more simultaneous regions of interest (ROI). Sequential windowed non-destructive readout will be employed with sample averaging to reduce readout noise with each ROI being sampled at the appropriate rate for the TT in that ROI, while also delivering the necessary frame rate.

4.1 Dewar

The camera dewar design is based on the TTS dewar design developed for the NGAO preliminary design. This design is documented in KAON 730 and a cutaway view of the dewar is shown in Figure 30. We will use this project as an opportunity to complete the NGAO TTS dewar design and to prototype it.

A snout will be added to this dewar design for the reimaging optics, a pupil mask and a filter mechanism. These optics need not be at the detector temperature but nonetheless require deep cooling to <~160K to reduce black body emission from the lens barrel and baffles from generating significant background flux. We are planning to use the same flexure type lens mounts and window support as used in another Keck instrument, MOSFIRE (McLean et al., 2008), to mount the optics.

The cryocooler is a CryoTiger mixed gas Joule-Thompson cooler. The vendor will guarantee performance for lengths up to 250 ft (76 m), but compressor lines much longer have been used by other observatories, with no significant impact to performance. The increase in load relative to the NGAO design still leaves adequate cooling margin. The increase will be <2W due to the increased window size, <0.4W for heavier or additional mechanical support of cold components, and only ~0.1W for the increased radiation shield area due to the low emissivity of the shield itself and the polished dewar interior.

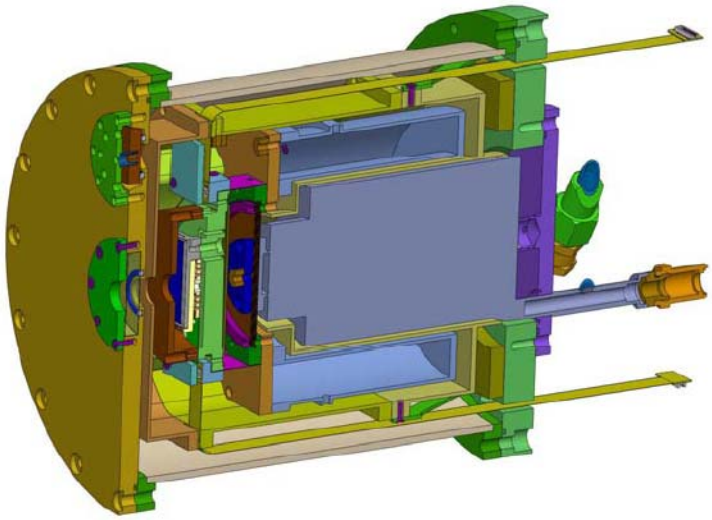

Figure 30: NGAO TTS cryostat. *The outer flanges are 8 inches in diameter and the chamber itself is 7 inches in diameter. All electronics are mounted externally. The green flanges on the front of the dewar are the entrance window (center) and pressure release valve cover.*

Vacuum will be sustained in the presence of residual outgassing and O-ring diffusion by either an ion pump or a very large charcoal getter supplemented by an easily exchanged zeolite dessicant (at room temperature) which will probably not have to be changed once the instrument is delivered. The NGAO design supports either choice. The observatory has expressed a preference for the ion pump. (Roger Smith notes experiences with ion pumps producing electrical noise and knows of a recent case where an ion pump failure caused damage to a focal plane mosaic under development at another institution.)

We have reviewed the NGAO TTS dewar mechanical design and have concluded that it will meet the needs of the NIR TTS. There are a few areas however that will require further evaluation:

- The back surface of the dewar is currently the mounting surface. We need to evaluate the impact of the long moment arm if the re-imaging optics are cantilevered far from this surface. The concern here is not flexure since the dewar is down looking and gravitationally stable, but a low resonant frequency could make the camera susceptible to ambient vibration.
- The thermal load calculations will need to be updated to incorporate the additional mass of the reimaging optics and the larger entrance window for the larger field of view. While we will check the extent to which cool down time is increased the principal risk is that the increase in cold head temperature under the increased load will be unacceptable. Initial assessment suggest this will not be a problem but the analysis may lead to a change in the gas mixture selection to provide more margin or faster cooling, trading against dark current which can be predicted now that the detector has been procured.
- We will reconsider the getters and ion pump for maintaining vacuum during the preliminary design.

A conceptual drawing of the NGAO TTS dewar mounted on the AO bench with the additional reimaging optics and a filter wheel in an extended dewar is shown in Figure 31.

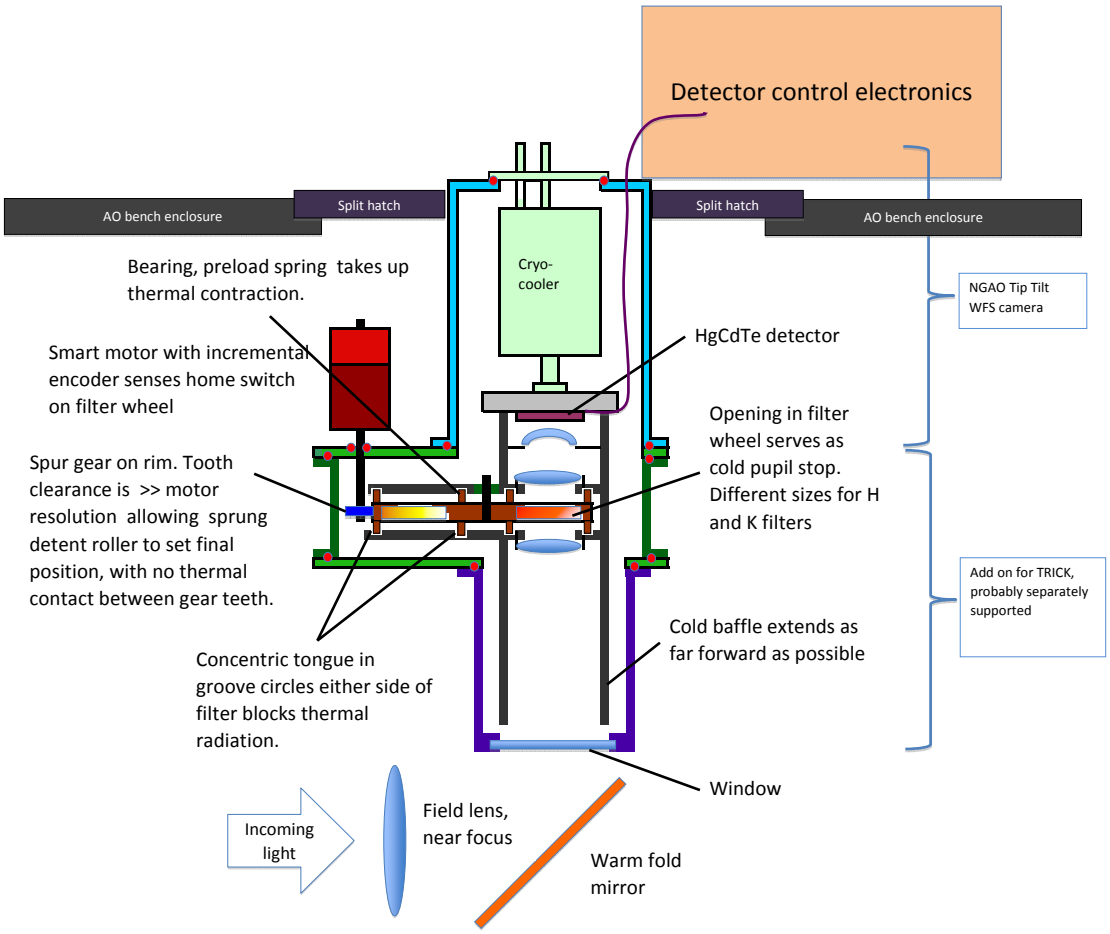

Figure 31: Conceptual drawing of NIR TTS camera system

4.2 Filter and Filter Changer

Two filters, H and Ks, will be housed near or at a pupil within the camera dewar. We have reviewed the filter choices with reference to the NIRC2 filters (http://www.keck.hawaii.edu/realpublic/inst/nirc2/filters.html). Ks or Kp would be preferred for the K-band filter due to their shorter cutoff and hence lower background contribution. We have opted to go with the 2MASS H and Ks filters (http://www.ipac.caltech.edu/2mass/releases/allsky/doc/sec3_1b1.html#s6) since this will enable a good match with the 2MASS catalog which we will be using to identify TT stars.

A third position of the filter mechanism is required to block the beam so that dark current can be measured, as well as for diagnostic purposes such as verifying read noise performance. Additional positions could prove useful for example to test focus sensing by introducing some astigmatism. A not uncommon approach is to rim-drive the filter wheel via a spur gear with a large tooth clearance allowing it to be drawn into a final precise position by a detent without being over-constrained. A stepper motor is used to park the drive gear such that the teeth do not make contact once in final position, thus providing both a thermal break and allowing for positioning repeatability. The spring loaded detent mechanism serves the secondary but important function of providing a thermal contact to the moving wheel. A cryogenic switch on the detent senses when it is engaged.

The filter positioning accuracy is modest; 1 mm positioning accuracy should be easily sufficient. However, considerably better accuracy than this is easily achieved, and will be required if the cold pupil stop is located on the filter. Placing the pupil stop on the filter has the attraction that the size of the stop can be optimized for each passband. In H band a stop which circumscribes the primary could be used to maximize throughput and resolution while in Ks band it would be preferable to inscribe the pupil stop in the primary

to minimize thermal background. If an extra filter position was available a larger Ks band stop could also be supported for those cases where guide stars are bright enough to exceed background.

Note that filters are required in addition to the pickoff dichroics since cold filters are needed to reject the thermal background; the dichroics are also unlikely to be able to be built to match the filter profiles.

4.3 Readout Electronics

Two options were considered for the readout electronics: the SIDECAR ASIC used for MOSFIRE and the Astronomical Research Cameras (ARC) SDSU-III readout electronics used for OSIRIS. The SDSU-III readout electronics (from KAON 730), shown in Figure 32, was selected for a combination of reasons including superior noise performance, controller cost, ease of implementation, cost of interfacing, and schedule and budget risk. The primary factor was the hands-on experience of the Caltech team that will develop the camera with the ARC readout electronics and the demonstrated performance by this team with these electronics.

Multichannel readout (16 or 32 channels) will be supported for rapid full field imaging during acquisition, while only single channel readout in window mode will be used for TT sensing.

The host computer will adopt the OSIRIS/NIRES style detector server. This approach will be compatible with the existing client-server architecture including the Keck Task Library (KTL) and the Experimental Physics and Industrial Control System (EPICS).

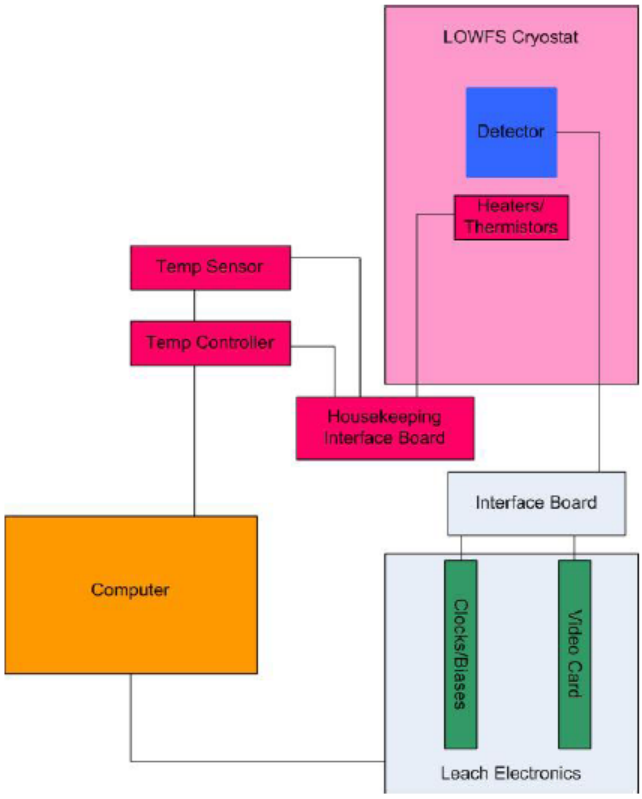

Figure 32: Electronics diagram for the NIR TTS. *All electronics for the array are external to the cryostat. The flex cable from the array is extended through the back cover to interface boards external to the cryostat. These interface boards then lead to the Leach readout electronics (the clocks biases card and the video card). House keeping signals (heaters and thermistors) come from a different flex cable.*

4.4 Detector Readout Modes and Noise Performance

The detector is read out non-destructively in window mode, through a single channel. The window coordinates are updated prior to each window scan by issuing command over a high speed serial line to the H2RG multiplexer taking ~5 µs, allowing the readout of multiple windows at any location during any given exposure. This flexibility can be utilized to accommodate some combination of multiple guide stars (when available with sufficient brightness).

Conventional readout algorithms employing multiple sampling to beat down the read noise suffer a >50% duty cycle penalty at high frame rates. We overcome this limitation by using a readout mode already tested at the California Institute of Technology (CIT) in which the detector is only reset when the integrated signal level approaches saturation as shown in Figure 33, typically every 100 to 1000 exposures for guide stars faint enough to be impacted by read noise. The "exposures" are then synthesized by using the group of samples representing the end of one exposure as the "zero level" for the next exposure to obtain duty cycles of > 99%. When reset becomes necessary there will be a gap in the data stream that will be small compared to the update rate.

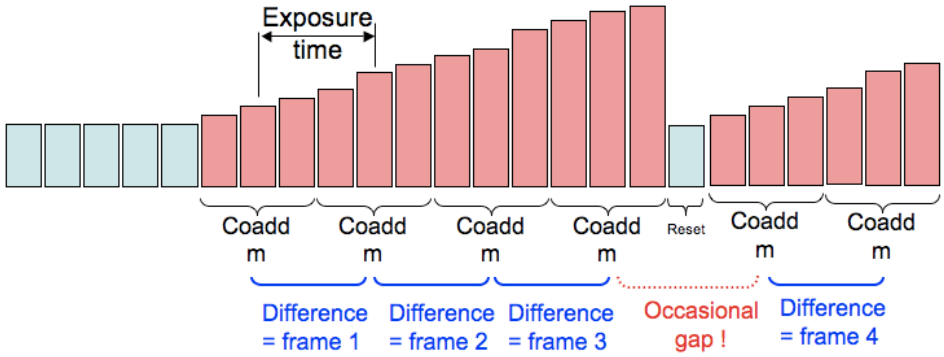

Figure 33: In "Differential Multi-Accumulate" readout mode the detector is reset only when necessary to avoid saturation to obtain ~100% duty cycle. Reset occurs every 100 to 1000 frame scans. Non destructive reads are averaged and exposures are synthesized by differencing averaged frames.

For an N pixel square window, the frame scan time, $t_s = 5.16N^2 + 10.32N + 5.28$ µs = 143 µs for a 4x4 pixel window, or 47 µs for a 2x2 window. A representative low noise 2.5 µm cut-off H2RG tested at CIT, exhibited the following noise components added in quadrature: 11 e- of white noise, which scales as the square root number of samples per exposure, 0.06 e- of dark noise which scales inversely with the square root number of samples per exposure and a 2.4 e- floor due to 1/f noise. The total noise as a function of exposure rate and number of pixels per frame is shown in Figure 34.

Full field readout can be used for confirmation of guide star positions, reading out through multiple channels to keep read time down to ~1 second. A 1.3" region centered on the TT star can be read out at 1 kHz, but elevated read noise (12 e-), to provide initial guiding until the TT loop is closed. As the spot position is stabilized by the TT feedback, the window size will be reduced to 2x2 or 4x4 pixels.

Any change in the pixel readout cadence imprints a pattern on the data via the self heating pattern in the sensor and through electrical crosstalk from digital to analog circuits within the detector controller. The pixel readout rate will therefore always be fixed (nominally at 6 micro-seconds per pixel). We will test whether self heating has any impact on the tip-tilt performance when transitioning between acquisition and tracking, and when switching between ROIs.

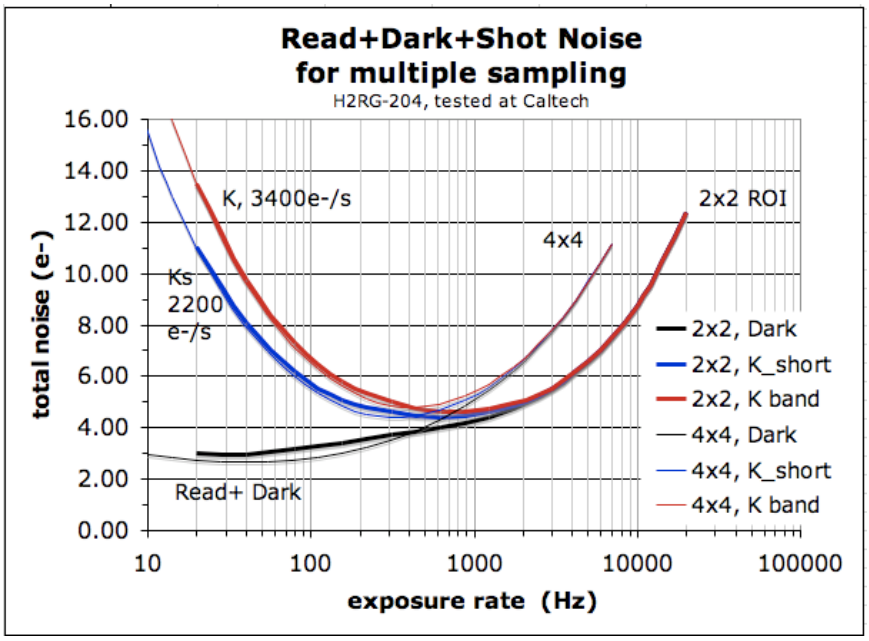

Figure 34: Laboratory noise measurements after coadding non-destructive reads for a low noise 2.5 µm cutoff H2RG in the dark and with projected background (sky, telescope and AO) noise added.

4.5 Camera Hardware Locations

The camera itself will mount on the NIR TTS focus stage via a TBD interface plate. The readout electronics must be within ~1.5 m (TBC) of the camera. These electronics will therefore reside in a glycol cooled, thermally insulated enclosure on top of the AO bench cover. The camera host computer will reside in an electronics rack in the AO electronics room (another option which could be considered would be to locate the host computer in the computer room next to the control room).

The location of the cryocooler compressor, Lakeshore Temperature controller and ion pump controller is TBD. Ideally the cryocooler compressor would be located in the Keck I mechanical room and the two controllers would be located in the AO electronics room. If the cryo lines cannot be this long then the compressor will need to be located on the Nasmyth platform in a vibration isolated manner.

If an ion pump is to be used it will be located on the rear hatch of the dewar beside the compressed gas lines so that all connections to the dewar are on the exposed top surface which is expected to protrude through the ceiling of the AO enclosure.

5. Real-Time Controller

The existing real-time control system (Johansson et al., SPIE Proc. 7015-121, 2008) must be upgraded to interface to the TTS readout electronics and to use the information provided by the TTS. We intend to contract with Microgate, the fabricator of this control system, to provide a hardware interface for the TT data and additional processing power for the tip-tilt computations (see KAON 824 for the statement of work; note that Microgate was selected due to their expertise with the existing systems and our past very positive experience with this vendor). The resultant system should be able to utilize data from both the existing visible TT sensor and the NIR TTS, including up to one visible TT star and three NIR TT stars. We have an operational spare real-time control system in a lab at WMKO headquarters that will be used to fully test the system prior to telescope integration.

5.1 Top Level Schematics

The main components of the real-time controller are shown in Figure 35. The down-link tip-tilt (DTT) mirror is controlled by the DTT controller which uses either the wavefront sensor (WFS) camera or the STRAP tip-tilt sensor for its tip-tilt information. Both STRAP and the DTT controller are part of the

Microgate controller as seen in Figure 36. The WFS camera interfaces to the Microgate controller over an AIA port.

From the RTC perspective the only parts of Figure 35 that are potentially affected by integration of the NIR TTS will be the WIF, WFP and TRS. No changes are required to the wavefront sensor camera or STRAP. No changes are required to the DM, DTT or UTT controllers.

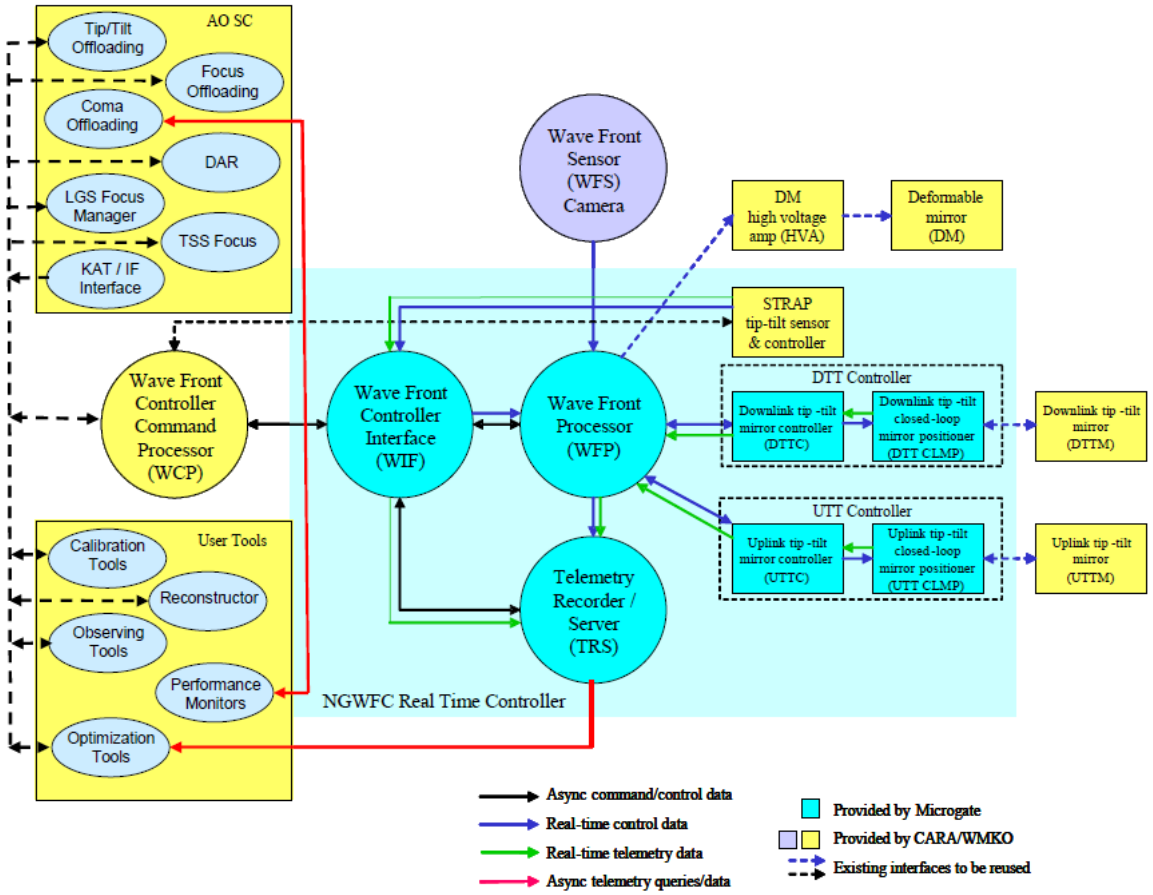

Figure 35: The main components of the real-time controller

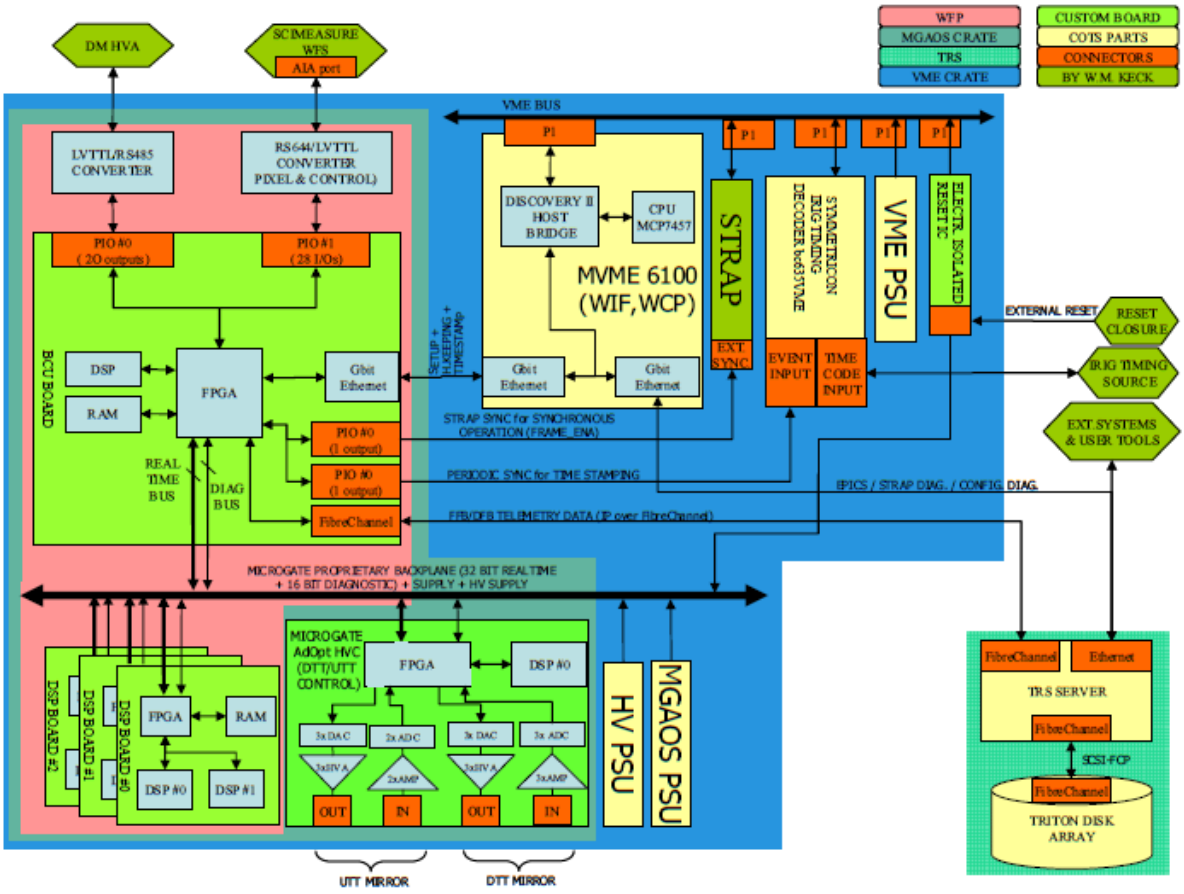

Figure 36: A block diagram of the Microgate real-time controller system

The mechanical layout of the front panel of the VME crate in which the Microgate AO system (MGAOS) real-time controller resides is shown in Figure 37 (from the Microgate Detailed Design Review document). There are spare slots in the VME portion and also within the MGAOS system (which has its own non VME bus internally). Either the existing BCU board would need to be modified to accept an interface from the NIR TTS readout electronics or a new BCU board would need to be added to accommodate this interface.

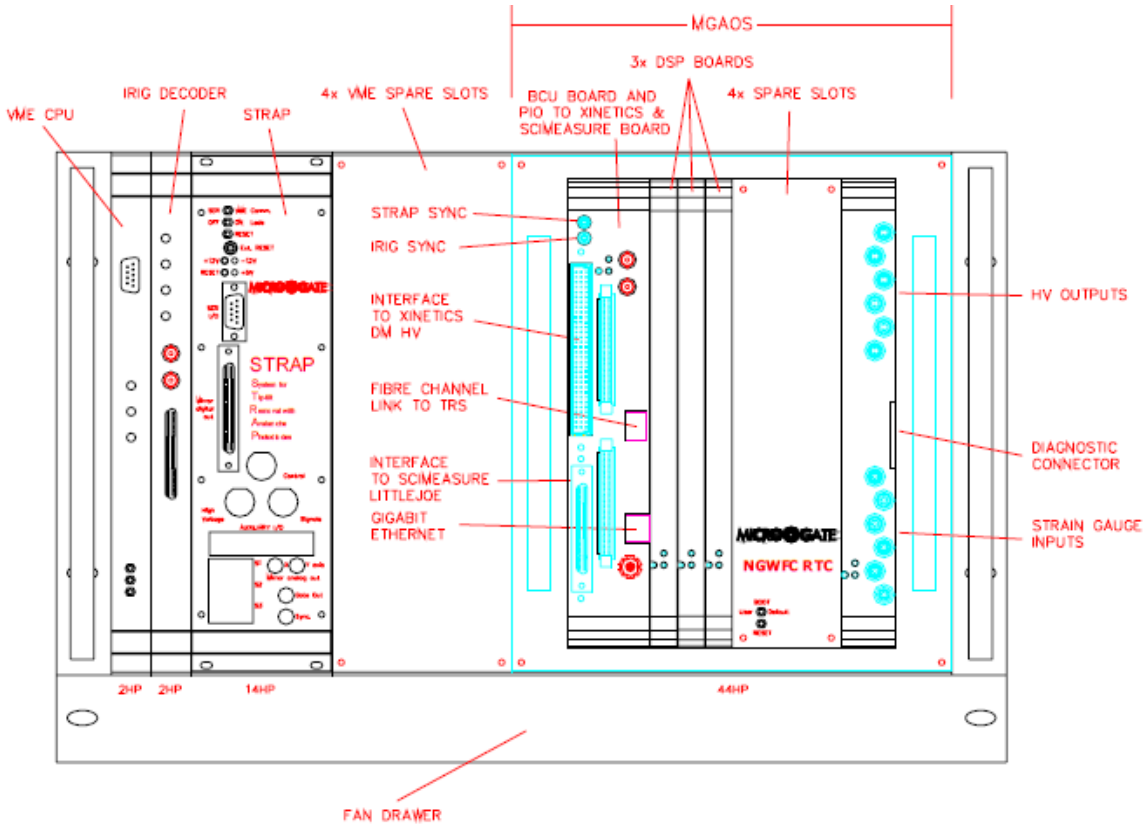

Figure 37: VME and Microgate real-time controller crate mechanical layout

5.2 Camera to Real-Time Controller Interface

Figure 38 provides a schematic of the major elements of the NIR TTS system. This camera is also referred to by the acronym TRICK for Tilt Removal with Ir Compensation at Keck. The TRICK camera controller (AKA Leach) will interface to the NGWFC RTC through a new interface to the WIF. The raw camera pixel data will be provided to the Microgate controller via a unidirectional fiber optic interface from the ARC timing board, providing a continuous data stream along with configuration information. No path exists on this fiberlink to send command or status information from the Microgate system back to the Leach controller.

Data packets from the camera to RTC should map to a single ROI. Since ROIs can be quite small the header which identifies the origin of the data needs to be very short, to minimize overheads. It is proposed that data be transmitted in packets whose format and purpose are identified by a single 16 bit header word.

If possible, special characters will be used to identify the packet header word. This would be based on the special characters (K28.x) made available by the 8-10 bit encoding technique used by the Hotlink transceivers. This requires further investigation to ensure that the ARC controller supports these special characters. The special characters will identify the header word, leaving the entire 16 bit (65536 codes) word value for packet type definition.

An ARC timing board was procured in November 2010 with a modification to provide two fiber transmitters to allow communication to both the host computer and the real-time controller. This board will be tested to ensure that the two fiber interface approach functions properly and also to test whether special characters can be used to identify the packet header word (the preferred format discussed in the Microgate SOW).

If the special characters prove to be inaccessible there is a fallback. Pixel data are unsigned 16 bit with an offset to ensure that noise does not cause underflow in the absence of signal. It is therefore the case that data values sufficiently below the offset are never seen and could be used for packet labels in place of the "special characters".

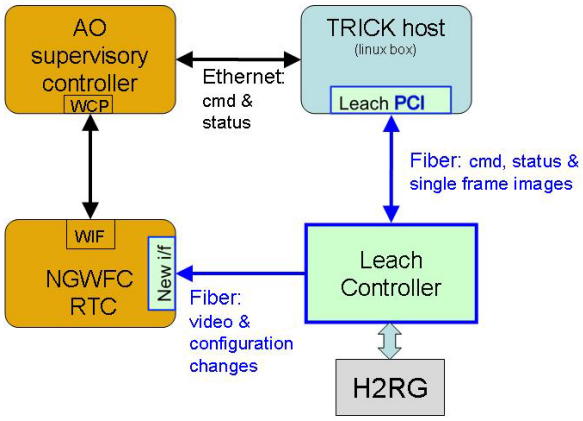

Figure 38: Top-level interface schematic

Data and configuration changes are provided over a fiber optic link from the NIR TTS camera readout electronics to the Microgate RTC. Commands to the Microgate RTC are provided over the existing interface between the AO system and the Microgate RTC.

5.3 Real-Time Controller Software

The Microgate controller will need to perform the following data processing steps in real-time on the data received from the camera:

- coadd multiple samples for each pixel for noise reduction.
- subtract the preceding co-added packet to obtain the difference (or "frame" value shown in Figure 33) for that pixel.
- subtract sky frames and
- scale by a flat field.

The equation describing this process is

$$i_c[k,t] = i_f[k](i[k,t]-i[k,t-1] - i_b[k])$$

where i[k,t] is the coadd of m frames of incident flux at pixel k, i[k,t-1] is the coadd of the previous m frames at pixel k, $i_b[k]$ is the background level at pixel k, $i_f[k]$ is the normalized flat-field gain response for pixel k, and $i_c[k]$ is the resulting compensated pixel. A pixel gain map file will be provided to the Microgate controller by the AO control system whenever the controller is restarted. The processed pixel values will need to be thresholded.

The real-time controller (RTC) will be capable of performing either a 4x4 pixel centroid or a correlation algorithm on the data from each ROI. The centroiding process is the same as that described in KAON 517.

The correlation algorithm is that presented by Poyneer (Appl. Opt. 42, 5807 (2003)). The correlation, C, between the reference image, r[i,j], and the subimage from each ROI, s[i,j], is calculated either directly or using FFTs (whichever way is faster). The reference image will be determined offline and will be provided to the Microgate controller. The direct implementation is

$$C[m,n]=\sum_i \sum_j r[i-m, j-n]s[i,j]$$

And the Fourier transform implementation is

$$C[m,n]=F^{-1}\left[F^*\{r\}\cdot F\{s\}\right]$$

Given the discrete maximum, (Δ_x,Δ_y), the sub-pixel shift is found using parabolic interpolation in one direction at a time:

$$\hat{x}=\Delta_x+\frac{0.5(C_{-1}+C_1)}{C_{-1}+C_1-2C_0} \quad \text{and} \quad \hat{y}=\Delta_y+\frac{0.5(C_{-1}+C_1)}{C_{-1}+C_1-2C_0}$$

Note that the star images used for the tip-tilt measurement will not normally be located at the intersection of 4 pixels. In addition, the star image will move on the detector during the course of a science exposure due to such effects as differential atmospheric refraction. The position of the centroid offset position to which the tip-tilt mirror should drive the star image and the location of the ROI will therefore need to be periodically updated. These updated positions will be provided to the wavefront controller.

The TT RTC control loop is illustrated schematically in Figure 39. The STRAP controller processing is unchanged. The NIR TTS camera (TRICK) controller processing is similar with two exceptions: the initial processing to coadd samples and then to subtract the previous packet, and the choice of using a centroid or correlation algorithm. The TT errors calculated for each ROI and the STRAP TT error are then averaged together after applying multiplicative scaling factors. The scaling factors are a function of the SNR for each TT star and their positions with respect to the science object.

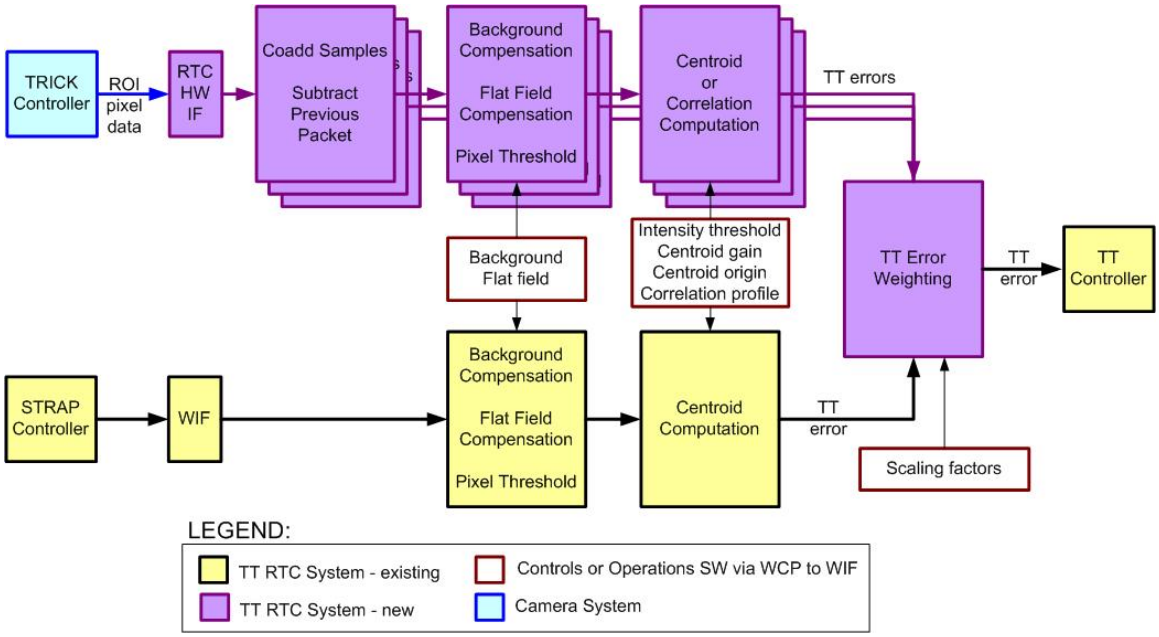

Figure 39: TT RTC Control Loop

The controller must also be capable of calculating focus from an astigmatic image. This focus value is only planned to be used for calibration (see section 2.6) and for experimental purposes (e.g. astigmatism could be introduced by the deformable mirror in order to test the on-sky utility of that approach to focus measurement).

5.4 Estimating Tip-Tilt from Multiple Stars

The purpose of this section is to review approaches to estimating tip-tilt from multiple TT stars.

Given a set of guide stars with known locations we can make measurements of the variation in position caused by atmosphere turbulence. In principle this information can be used to infer the instantaneous position of an object located in different average position on the sky. Let us call this vector deviation in direction $\boldsymbol{\Theta}_{sc}$ representing the instantaneous motion for the science direction,

$$\Theta_{sc} = \begin{bmatrix} \theta_{SCx} \\ \theta_{SCy} \end{bmatrix}. \qquad (1)$$

The subscripts x and y denote motion along two arbitrary orthogonal axes. The deviation in position for each measured guide star, Θ_i, is given by a measurement vector

$$\Theta_i = \begin{bmatrix} \theta_{ix} \\ \theta_{iy} \end{bmatrix}. \qquad (2)$$

The measurement of all n (typically 2-3) guide stars can be combined into a single measurement vector Θ_{gs} of greater dimension, given by

$$\Theta_{gs} = \begin{bmatrix} \theta_1 \\ \vdots \\ \theta_n \end{bmatrix}. \qquad (3)$$

The general minimum variance estimator is given on page 87 of Luenberger (1969). Applying this general estimator to the this problem for tip tilt in the science direction, the result is

$$\widehat{\Theta}_{SC} = \left\langle \Theta_{SC} \Theta_{gs}^T \right\rangle \left\langle \Theta_{gs} \Theta_{gs}^T \right\rangle^{-1} \Theta_{gs}. \qquad (4)$$

The notation $\langle\ \rangle$ is used to denote expectation values, superscript T is the vector transpose operation and superscript minus 1 is the matrix inverse, which is assumed to exist. An equivalent method was suggested by Don Gavel for tip tilt and low order mode estimation for the Keck NGAO project (see KAON 695 equation 46; a slightly different notation is used).

The expectation values needed to evaluate equation 4 are the covariance matrices between tip and tilt in the various directions. These can be evaluated by measurements, simulations or from theoretical considerations (the final results are given as integrals over the turbulence profile). The first covariance matrix involves the covariance between the measurements and the observation (science object) directions; this matrix can be calculated from theory or estimated from the data possibly aided by the measured turbulence profile. The second covariance matrix involves only directly measured quantities. As such it could be taken directly from measurements made at the start of an observation and updated from telemetry as the observation proceeds, to compensate for changing conditions.

An alternative to the above formalism is the modal estimation technique used by Marcos Van Dam in KAON 826. This technique uses 3 NGS tip tilt measurements, identical to the vector in equation (3) above. These measurements are then used to estimate 5 atmospheric modes. These modes are global tip and tilt in the science direction and 3 tilt anisoplanatism modes. These last 3 modes can be visualized as focus (1 mode) and astigmatism (2 modes) located above the telescope at an altitude consistent with the anticipated atmospheric turbulence profile. These three modes are used to fit the differential motion of the three NGS. This provides a better solution than just fitting global tip and tilt alone. The values of the 3 tilt anisoplanatism modes are not used in the control of the AO system.

5.5 Tip-Tilt Mirror Controller

The existing control algorithms are discussed in KAON 517. The tip-tilt mirror controller dataflow diagram is shown in Figure 40.

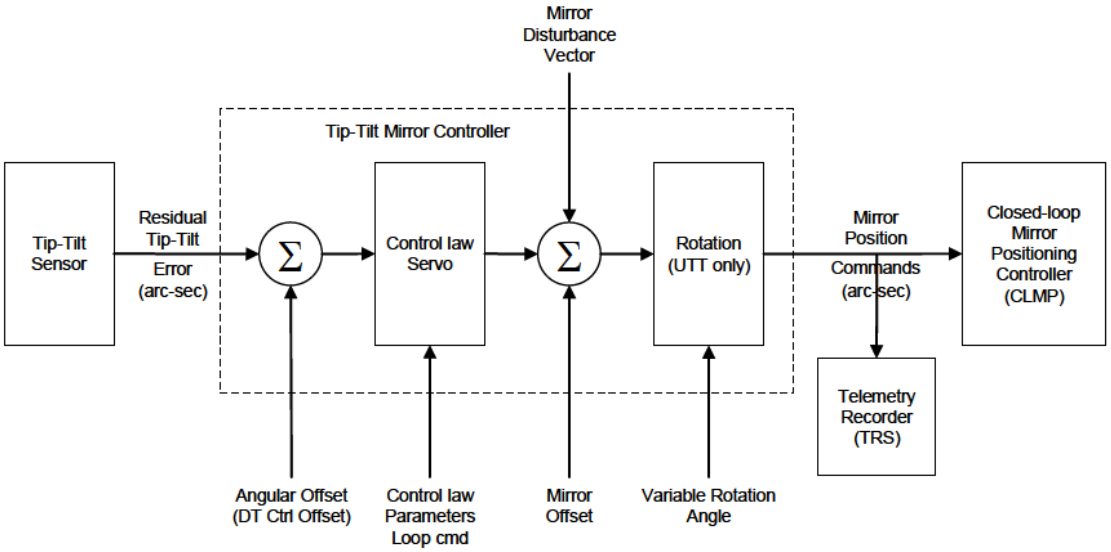

Figure 40: A dataflow diagram of the tip-tilt mirror controller

The residual tip-tilt error is received from the appropriate tip-tilt sensor via the WFP as an input *xy* pair, (C_{ix}, C_{iy}), already scaled appropriately to be in units of arcsec. When STRAP is selected as the tip-tilt sensor, the real-time APD quad-cell flux values are used in a centroid computation, without flat field compensation, and the resulting centroids are multiplied by the STRAP system matrix to convert from quad-cell units to arcsec and to convert for any rotational difference between the STRAP sensor and the (*x, y*) coordinate system of the tip-tilt controller:

$$\begin{bmatrix} C_{ix} \\ C_{iy} \end{bmatrix} = \begin{bmatrix} a_{11} & a_{21} \\ a_{12} & a_{22} \end{bmatrix} \begin{bmatrix} C_{Sx} \\ C_{Sy} \end{bmatrix}$$

where (C_{Sx}, C_{Sy}) are the STRAP centroids. The STRAP system matrix values are determined offline using an IDL calibration tool.

We need to modify the WFP to process the raw NIR TTS data into a residual tip-tilt error in arcsec (i.e., the left hand input shown in Figure 40). The Microgate telemetry recorder/server (TRS) will need to be modified to write NIR TTS data to disk.

6. Control Loops Overview

Prior to discussing the controls and operations software it is useful to provide an overall schematic of the control loops between the multiple subsystems. Such an overview is provided in Figure 41. The components of each of the five major systems are indicated using the color scheme shown in the legend of Figure 41, as are the relevant existing hardware components and the light path between these components.

Observations of a new target are begun by taking a TRICK acquisition image via MAGIQ. This image will be used to repoint the telescope, to select the ROIs and to provide the total seeing-limited flux for each TT star. The operator selects which ROIs are to be used, whether or not STRAP will also be used and what algorithm (centroid or correlation) will be used by the RTC. The camera reset time is set by the magnitude of the brightest star.

When the TT loop is closed the data from each ROI and from STRAP are sent to the RTC in order to determine the TT to be sent to the TTM. The existing offload control loop offloads the TTM to telescope pointing (and in the future we might add rotator control based on any rotation seen in the 3 TT star images).

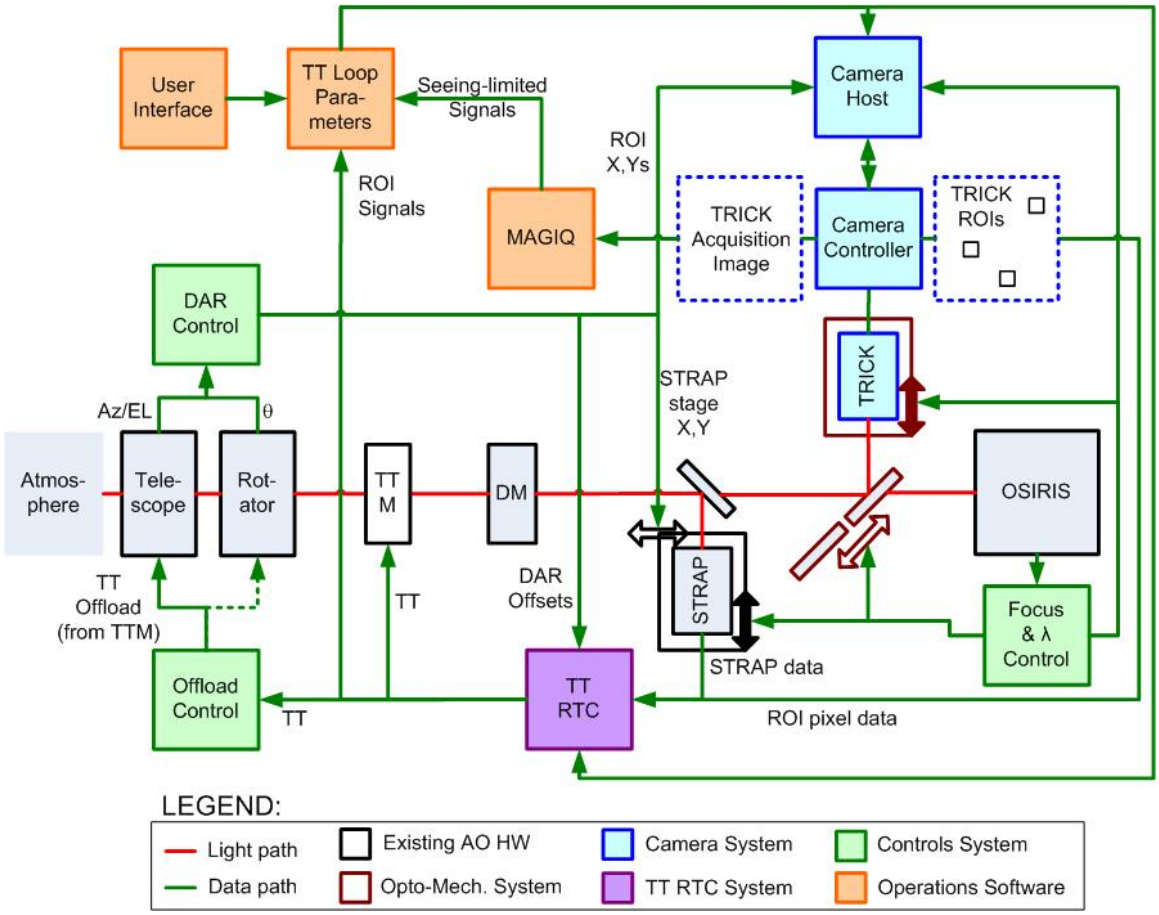

Figure 41: Control Loops Overview

The DAR loop is acting continuously to provide centroid origin offsets to the RTC and to reposition the STRAP x,y stage and ROI positions as appropriate. The focus control loop adjusts the position of the STRAP and camera focus stages as a function of OSIRIS plate scale and TRICK camera wavelength. The wavelength control loop selects the appropriate dichroic and TRICK camera filter as a function of the OSIRIS science filter.

Dithering is not shown explicitly in Figure 41 but in this case the TT loop is automatically opened, the ROIs and STRAP x,y position are changed, and the TT loop is re-closed. The high order DM control loop is kept closed during this operation.

7. Controls

The controls system includes modifications to the existing AO optics bench subsystem (OBS) and supervisory controller (SC; see the SC box on the left side of Figure 35). The motion and device control listed below fall into the OBS category while the other software changes fall into the SC category.

7.1 Motion Control

Three degrees of motion control are planned. A stage to move the desired optical pickoff into or out of the beam, a focus stage to match the TTS focus to that of OSIRIS and a stage to switch between the H and K-band filters in the camera dewar.

It will be sufficient to position the optical pickoff and filter to the ~ 1 mm level since they are moving parallel to their optical surfaces. Note that 1 mm is small compared to the ~ 22 mm point source beam size on the optical pickoff and the pupil size on the filter.

The focus stage should be capable of being positioned accurately enough not to significantly enlarge the diffraction-limited core (34 mas or 25 μm at the AO focus). From the geometric perspective if we only allowed a 5 μm blur due to defocus then this would correspond to a defocus of 13.66 x 5 μm = 68 μm, where 13.66 is the f/# input to the TTS. A positioning accuracy of ± 0.05 mm is therefore sufficient for the focus stage.

The pickoff and focus motion control will be accommodated within the existing PMAC servo control system used for the AO system. There are two PMAC channels currently available within the Keck I AO system for this application.

The filter motion control, likely a stepper motor with limit switches and a stepper controller, will be provided by the camera subsystem. Control and status of this filter wheel will be provided through keywords.

7.2 Device Control

Software will be provided to remotely control the TTS camera (e.g., to control power on/off, startup, shutdown, integration time, region of interest control, number of samples, start of integration, etc.).

Software will be provided to remotely control the new functionality incorporated in the real-time controller.

7.3 Differential Atmospheric Refraction Compensation

The DAR offset controller is responsible for calculating and compensating for the affects of DAR in order to keep the science object fixed on the science instrument. DAR is a relative calculation based on the difference in wavelengths between the science instrument and the sensor measuring TT. The effective wavelengths of the science instrument and TTS are functions of the color of the science object and TT objects, respectively. The amount of DAR changes with telescope elevation and its orientation is in the direction of the vertical angle on the AO bench.

The existing DAR tracking code will be updated to include the NIR TTS. The OSIRIS side of DAR is already in place. The TTS side of the code is already in place for NGS AO mode when the NGS WFS is used for TT tracking and for LGS mode when STRAP is used for TT tracking. The code should be in updated to use the NIR TTS for either LGS or NGS AO. The center wavelength of the NIR TTS will be an input to DAR; this will change between usage of the H-band and K-band reflective dichroics.

DAR tracking will be performed as following during observing:

1. DAR tracking is on automatically turned on whenever the TT loop is closed and will provide changing centroid offsets to the wavefront controller for each ROI.
2. If the image moves more than ½ pixel from the center of a ROI then it is time to change the ROI that is being used. This will normally only be done between science exposures (e.g. during nods, dithers, repositions, filter or plate scale changes). During a long science exposure it may be desirable to update the ROI. This must be done in a TBD coordinated fashion between the camera and the wavefront controller. Note that self heating of pixels may be an issue when changing ROIs which may require waiting a short time before taking a science exposure after a new ROI is selected.

Note that if the NIR TTS was used for acquisition instead of ACAM for STRAP then the DAR offset between the NIR TTS and STRAP would also need to be known.

7.4 Focus Compensation Control

In the current system the focus position of the NGS WFS or LBWFS/STRAP are automatically adjusted when the science instrument configuration (e.g. plate scales, filters, IFU or imager) is changed. The same correction will need to be applied to the NIR TTS focus stage when the NIR TTS is being used.

7.5 Non-Sidereal Tracking

A requirements goal is to support non-sidereal tracking. This mode is already supported by STRAP so it is not a high priority. This mode will be feasible with the NIR TTS since the centroid offset can be constantly

updated and the ROI can be changed between exposures. The goal of maintaining the science object position to 10 mas for a 50 arcsec per hour non-sidereal object would require changing the centroid offset by 5 mas every 0.36 seconds and changing the ROI by 1 pixel (50 mas) every 3.6 seconds. Currently we plan to consider this mode during the design phase but will not implement it at least initially.

7.6 Rotator Control

Three stars on the NIR TTS would provide enough information to tell you whether the AO rotator was tracking properly. We are not currently planning to use this information to correct the rotator position or tracking rate. However if the rotator did not track adequately then we would find that the off-axis TT stars were giving a radial dependent TT error in the direction of the rotation error. If we discover this to be the case then we will need to add a future upgrade to provide a feedback control loop to the rotator to hold the TT star positions.

8. Operations Software

The Keck I LGS AO operations software (the items shown in the User Tools box in Figure 35 plus some pre-observing tools) will need to be modified and added to in order to integrate the TTS system.

8.1 Pre-Observing Software

8.1.1 Acquisition Planning Tool

Pre-observing software will be provided to the astronomer to pre-select targets for TTS operation. The TT star locations will be included in the observer's target list along with their H and Ks-magnitudes. The observer can use up to three TT stars for the NIR TTS and one star for the visible STRAP sensor and LBWFS; a LBWFS star is always required for LGS AO observing and this is necessarily the same star that would be used for STRAP. If 3 near-IR stars are desired then at least 4 stars should be included in the star list since one or more of these could be galaxies. As a goal some guidance should be provided as to the optimal configuration of TT stars.

The acquisition planning tool will be a web-based utility that displays survey images and catalog positions of possible guide stars. Observers can determine whether a guide star is within reach of the system and add it to their starlist. Once complete, the observer may submit their starlist via this tool in the proper format. The existing AO Guide Star Tool, shown in Figure 42, will be modified to accommodate the selection of three NIR tip-tilt stars.

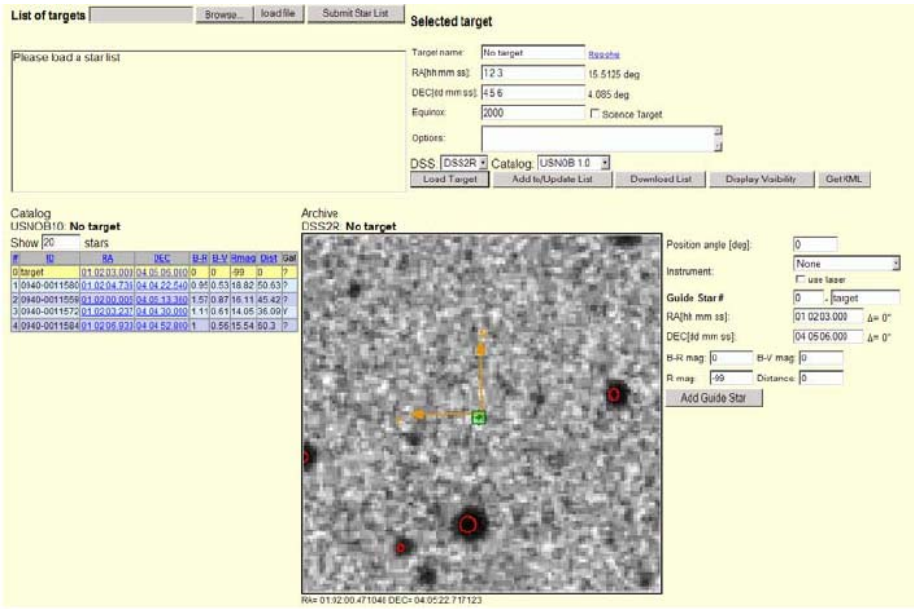

Figure 42: AO Guide Star Tool Web Page

TT stars should not be selected too close to the edge of the field so as not to preclude dithering; an appropriate size box for the observer's desired dither size will be superposed on the selected stars to help this assessment. The annular mirror will only be included in the acquisition planning tool as a goal.

The acquisition planning tool will initially have access to the images (e.g. DSS) and catalogs (e.g. USNOB 1.0, Vizier GSC2.2 and 2.3, and 2MASSPSC) currently available via the AO Guide Star Tool (e.g. DSS). As a goal, the acquisition planning tool will have access to 2MASS images as well. Brief descriptions of these catalogs can be found in section 3 of KAON 567. Images from other surveys and other catalogs should be able to be added in the future. It should also be possible to load user supplied images or catalog information.

8.1.2 Performance Estimation Tool

A requirements goal is to provide a performance estimation tool.

At minimum the observer should have access to web-based documentation that provides performance examples (Strehl and ensquared energy) for a range of observing conditions. This would include on-sky performance characterization data from the commissioning period that would be periodically updated as additional data was acquired. It could also include simulation results that are anchored to these on-sky results but that extend the performance predictions to a wider range of conditions.

The ideal case would be to provide a performance simulator to produce Strehl and ensquared energy estimates, and possibly a point spread function image. The user-provided inputs to this tool would include the starlist from the acquisition planning tool, the seeing conditions (these would have default median conditions or for at telescope planning adjustments could allow real-time inputs from the Mauna Kea MASS/DIMM), the telescope elevation (or observation date/time which would calculate this), the NIR TTS camera setup (choice of pickoff and filter) and the science instrument setup (including camera, filter and spectral order).

Two approaches have been considered for a performance prediction tool: a scaling law tool and Monte Carlo simulations. The scaling law approach would interpolate or extrapolate the measured results (or initially simulated results) to match the actual observing setup and atmospheric conditions. Better predictions of an AO system could potentially be obtained by Monte Carlos simulations. These simulations could potentially be provided as part of a web service (see for example http://eraserhead.caltech.edu/web_services/web_services.html).

At present, we assume that the Scaling Law Method is the basis for the future prediction tool design. Further, we assume that the main interface to the performance tool will be the upgraded version of the AO guide star tool discussed in section 8.1.1. The processing steps on the graphical user interface (GUI) would be arranged as follows:

i. User selects targets from database query or from Keck Star List file.

ii. User selects NGS targets from one of several online catalogs, or manually enters additional targets if necessary. These are added to the Star List file.

iii. User confirms guide star by consulting images from Digitized Sky Survey.

iv. User configures date and checks elevation (airmass) and telescope limits (K1 for TRICK).

v. User configures science instrument (FOV, wavelength, spectral order, etc.) and tracking mode (STRAP, TRICK, both, etc.). (Pull down list or separate popup window).

vi. User selects AO atmospheric conditions. User can choose from median, (also, 75%, 25%) profiles for Cn2 and wind speed. User can also select from MASS/DIMM archive files. GUI should show summary statistics (r0, Greenwood frequency) as well as profile. (Likely a separate popup window.)

vii. User selects AO evaluation. GUI lets observer compare performance with different guide star configurations. Compare performance with different IR tracking modes, number of TT stars and compensation, tip/tilt only or tip/tilt and focus. GUI would return Strehl, ensquared energy and possibly an option to download a PSF model. (This is likely done from a separate popup window).

viii. User can modify the Star List with NGS targets based on results from above steps.

ix. User can save the modified Star List and AO performance prediction results. The user should be able to in someway set a 1st and 2nd priority flag for the TT star configurations.

These steps would be selected from the main GUI and, other than loading a target location and querying the NGS catalog, could be done in an order different than presented above.

The prediction tool will need to be interfaced to the following software (details are still to be determined):

i. Keck Star List: Format (http://www2.keck.hawaii.edu/optics/lgsao/lgsstarlists.html) for these target lists will need to be modified in some fashion to indicate NIR targets (1, 2, 3), pickoff selection, and tracking mode.

ii. AO Guidestar Tool: This will need to be interfaced to Mauna Kea MASS/DIMM profile information and the AO scaling law performance prediction software.

8.2 Observation Setup

The observation setup will be done via the AO acquisition tool. This is where the various observing modes (NGS, NGS with STRAP, LGS) are currently selected. Additional LGS modes will need to be made available to support NIR TTS usage.

The observer or operator will need to be able to select between multiple tip-tilt sensor options in order to setup the AO bench. The impact of each of these options, listed below, on the NIR TTS setup is discussed in the sub-bullets:

- WFS (for NGS AO observing only)
  - The NIR TTS pickoff mechanism should be in the open position.
- STRAP
  - The NIR TTS pickoff mechanism should be in the open position.
- NIR TTS in H-band
  - The NIR TTS pickoff mechanism should be in the H-band reflective dichroic position.
  - The NIR TTS focus stage should be at the H-band focus position corresponding to the current instrument configuration.
  - The NIR TTS filter positioner should be in the H filter position.
- NIR TTS in Ks-band
  - K-band reflective dichroic position.
  - Ks-band focus position corresponding to the current instrument configuration.
  - Ks-band filter.
- NIR TTS with annular mirror (if this option exists)
  - Annular mirror position.
  - Ks-band focus position corresponding to the current instrument configuration plus Ks-band filter or H-band focus position plus H-band filter.
- NIR TTS and STRAP
  - Both sensors are configured appropriately.

For the NIR TTS the following parameters need to be selected and communicated to the real-time control system:

- Choice of TTS (NIR TTS or NIR TTS + STRAP)
- Number, location and size of ROIs. This could initially come from the target list coordinates of the TT stars. The ROI locations will be regularly updated due to DAR; the actual locations could come from the camera controller.

- Number of samples to be taken between resets – could come from camera
- The pixel read rate (this will always be the same but may need to be set)
- Algorithm to be used (centroid or correlation)
- Background to be subtracted from each ROI
- Flat field for each ROI for scaling
- Weight to be applied to each ROI for determining the TT to be applied to the TTM
- What telemetry is to be recorded by the telemetry recorder system
- Initial centroid offset to be used (this will be regularly updated)

For the NIR TTS the following parameters need to be selected and communicated to the NIR TTS camera controller when it is in TT tracking mode (a separate mode exists for acquisition):

- Number, location and size of ROIs
- Number of samples to be taken between resets
- The pixel read rate (this will always be the same but may need to be set)

8.3 Calibrations

8.3.1 Camera Calibrations

The following camera calibrations will be required:

1. Flat fields in the H and K-band configurations for photometric and gain calibration purposes. Dome flats can be taken before or after observing. Dome flats are successfully used for NIRC2 and OSIRIS. These could be taken in parallel with the OSIRIS dome flats. Dome flats for NIRC2 are extremely stable and are available as a library. We could have a similar library of flats for the NIR TTS.
2. A bad pixel map for ROI selection purposes. This can be obtained from the dome flats.
3. Dark frames for characterization purposes. The filter mechanism will provide a blocked position.
4. An on-sky photometric calibration in both H and K-band. This would be obtained by observing photometric standards. It would be advantageous to have the NIR TTS filters match those used for the 2MASS catalog if that will be our primary source for identifying TT stars. Once calibrated the camera could be used to update the magnitudes of stars being used for TT sensing and these could be written to the science image FITS header or recorded by the observer for future observations.

8.3.2 Focus Calibration

The NIR TTS needs to be kept conjugate to the science instrument. During the day a fiber at the input to the AO system is used to position the NGS WFS, LBWFS and STRAP at a focus conjugate to the science instrument. Offsets for different science instrument plate scales or filters are also calibrated.

In order to position the NIR TTS conjugate to the science camera focus we will implement a procedure similar to the following:

1. Position the AO input fiber at the science instrument focus.
2. Add 45° astigmatism to the deformable mirror.
3. Close the TT loop with the NIR TTS and zero centroid offset so as to drive the fiber image to the center of a ROI.
4. Position the NIR TTS focus stage to zero the focus value provided by the real-time TT control system.

A simple IDL-type calibration tool will be developed to support the NIR TTS focusing.

8.3.3 Distortion Mapping

The extent to which absolute positions are known on the NIR TTS will impact how well the science object can be positioned on the science instrument. A field distortion measurement will need to be made at least once, or after any major changes to the system.

An initial distortion map can be made by moving the AO input fiber around the field and recording the corresponding position on the NIR TTS; given that the fiber positioning will have its own errors the corresponding position on OSIRIS could also be measured for fiber positions that also land on the OSIRIS detectors. The fiber approach is likely sufficient to meet the nodding and positioning requirement of ≤ 120 mas (3-sigma) for moves ≤ 60 arcsec and ≤ 70 mas for moves ≤ 5 arcsec.

A more accurate distortion map could be obtained on the sky by observing a cluster with known astrometry. Such a field has been used for distortion mapping on NIRC2.

8.4 User Interfaces

Engineering GUIs will be required to control the camera and motion control devices.

The existing AO user interface will need to be edited to include the appropriate NIR TTS control, feedback and data.

The TT plot provided to the user will need to use the TT residuals from the appropriate sensor; this may be transparent since this is computed by the real-time controller. A plot of TTS intensity, magnitude or Strehl ratio would be useful. STRAP provides a plot in magnitudes that is a useful cloud detector.

There must be a way to display the full frame NIR TTS image and to identify star locations on this image as part of the acquisition process. This last function will be provided by MAGIQ. It would be useful for the tool to provide measured magnitudes and FWHM.

8.5 Observing Tools and Sequences

8.5.1 Acquisition

Acquisition will be performed by a full frame readout mode of the TTS detector. The locations of up to three stars will be selected for ROI readout.

Pre-observing software will be provided for the astronomer to pre-select targets for TTS operation. Taking an acquisition frame will be the final step in determining the appropriateness of a target for TT sensing and its precise position for the ROI.

The acquisition steps include the following:

1. Next target selected and telescope slew begins.
2. NIR TTS software calculates desired TT star locations on the NIR TTS and NIR TTS setting.
    - The TT star locations should be identified in the observer's target list along with their H and K magnitudes.
    - The observer selects the science instrument configuration: science wavelength, science mode (IFU or imaging) and plate scale for IFU science.
    - The observer or operator selects the NIR TTS wavelength (H or K).
    - The desired TT star locations on the NIR TTS are calculated, including the effects of differential atmospheric refraction. This calculation is performed continuously to account for DAR and for changes in the system configuration.
    - The frame reset time is calculated based on the magnitude of the brightest TT star.
3. Observing assistant identifies and centers the brightest TT star on ACAM once the slew has been completed and closes loops.

- We may move to using the NIR TTS for this acquisition longer term if it improves observing efficiency. The TT stars could automatically be identified by searching around the expected target coordinates.
- Guiding with ACAM (i.e. MAGIQ) is left on.
- If STRAP is also to be used then its TT loop could be closed at this point and the ACAM guiding could be turned off.
- Laser propagated.
- DM loop closed.

4. NIR TTS software centers the field on the NIR TTS and closes the tip-tilt loop.
    - A telescope offset is made to nominally center the science object.
    - An image is taken on the NIR TTS.
    - The centroids for each TT star are determined.
    - A difference is taken with the desired positions. If the difference is below a threshold then the TT loop is closed with the largest region of interest required. Otherwise a telescope offset is made to move the TT stars to the desired positions and the TT loop is closed.
    - Guiding with ACAM should be stopped just before closing the NIR TTS TT loop.
    - The region of interest is automatically reduced to the desired region of interest as the centroid errors are reduced below a threshold.
5. Science image taken, if sufficiently short, to verify centering. An offset can be made if needed.

We intend to modify the existing WMKO MAGIQ acquisition software for NIR TTS acquisition. For MAGIQ use the camera interface must provide: full frame images for field identification and sub frame images for centroiding needed for pointing adjustments and offsetting. Images are best delivered in binary format directly via an application programming interface (API). FITS images could be used instead however this would add 1 to 2 seconds of overhead per frame. Camera exposure time and binning control should be available so they can be integrated into the MAGIQ GUI. A camera definition file will be needed to be used by MAGIQ. MAGIQ is also capable of saving a FITS image.

8.5.2 Tip-Tilt Loop Parameter Optimization

A high level tool is needed to provide the tip-tilt loop parameters needed by the RTC. These include weighting factors to be used for each sensor and ROI, as well as the tip-tilt loop gain and bandwidth. These parameters will be dependent on such factors as the tip-tilt star positions and magnitude, and the seeing conditions.

In order to have the best performance the NIR TTS system will need some level of automation for setting the various parameters for the operation of the tip/tilt loop. The necessary modifications would need to be made to the current AO acquisition tools and the control loop gain optimization tools. Information about the current AO acquisition tool (aoacq.pro) is found at http://www2.keck.hawaii.edu/optics/ao/ngwfc/aoacq.html. Information about the control loop optimization tool (bw_widget.pro) is found at http://www2.keck.hawaii.edu/optics/ao/optimizer/index.html.

The acquisition tool currently sets the exposure time of the various sensors based on the natural guide stars catalog magnitude. Next, based on the available detector counts it adjusts the exposure time to be as short as possible but with sufficient SNR; this allows the system to adapt to changes in elevation and atmospheric transparency for example. The AO acquisition tool would be extended to work with the NIR TTS. The control parameters (integrator leak factor and control loop gain) are set by the acquisition tool based on a detector exposure time and a lookup table of previously determined control loop gain settings found to be optimal for that exposure time during “typical” conditions. These values can be refined by using the optimization tool (bw_widget.pro). This tool analyzes the AO telemetry to determine the control loop gain that would result in the smallest reported residual error in the AO diagnostics. The user has the option of changing the gain to this value. The user can run this feature of the optimization tool iteratively to refine the AO loop performance. A similar procedure would be run using suitable noise statistics from 1-3 NIR TT stars. This option will need to be added to the current optimization tool and it will need to use information from 1-3 stars to optimize the overall TT loop performance.

Exposure time is an interesting question given that up to 3 TT stars of different magnitudes will be used on the same detector. The NIR TTS detector non-destructive read sampling rate will be constant and the "exposure time" will be set by the time when the array needs to be reset to avoid saturation as discussed in section 4.4. The reset rate will be set by the brightest star being used. Given the detector well depth of ~100,000 electrons there is still sufficient well depth between the brightest and faintest stars that could usefully be used together.

The other control loop parameter of importance for NIR TTS optimization is the so called "centroid gain" this is the conversion factor from centroid to input tilt. The current design proposes to use a seeing disk background measurement (section 8.5.4) to reduce the sensitivity to the centroid gain and a calculated NGS star Strehl (section 8.5.5) to estimate the centroid gain factor. Alternatives to this technique include the following two methods.

The first is dithering the TTM by a known amount at a known frequency. Using synchronous detection techniques it is possible to recover the error signal at the dither frequency. If the current "centroid gain" is correct then the dither amplitude from the tilt measurement should equal the input dither amplitude. This method requires accurate calibration of the TTM amplitude and good knowledge of system loop transfer functions, and must avoid vibration contributions.

The second method is used in the current AO system. It uses the prior knowledge that noise in the TT diagnostics is white and therefore the signal's power spectral density should be flat from about 100 Hz to 500 Hz. Assuming that the control loop transfer function is known then the loop gain and centroid gain are merged into one factor. By estimating the centroid gain that satisfies the flatness of the high frequency spectrum one can determine the centroid gain.

A decision has not yet been made about the ultimate optimization algorithms. Laboratory and on-sky testing could be used to determine the best methods and these could be developed into the final operational software.

8.5.3 Nodding, Dithering or Repositioning

Nodding (moves > 5") or dithering (moves ≤ 5" and > 20 mas):

1. Open TT loop.
2. Offset telescope by desired amount.
3. Calculate new TT star position(s) on the NIR TTS.
4. Close TT loop on the calculated TT star positions after the telescope offset is complete.
    - Note that TT offloading and DAR tracking should start as soon as the TT loop is closed.

Repositioning (moves ≤ 20 mas):

1. Calculate new TT star position(s) on the NIR TTS and implement these new positions.

8.5.4 Seeing Disk Background Measurement

The following steps define a potential process for seeing disk background measurement:

1. With the LGS and TT loops closed take an 8x8 pixel image around each TT star.
2. Use the pixels outside the central 4x4 pixel to measure the seeing disk.
3. Extrapolate the seeing disk measurement into a seeing disk flux for each pixel in the central 4x4 pixels.

The nested windows arrangement proposed for the TMT could be used to make this measurement. The outer window will be sampled less often and would therefore be noisier.

Proper subtraction of the seeing disk is one means of making the TT sensor gain insensitive to the Strehl ratio. This measured background could be subtracted as part of the RTC system data processing.

8.5.5 Strehl Ratio Determination

If the Strehl ratio is known in each ROI then the optimal TT gain can be determined. A method for determining the Strehl is to first measure the total signal for each TT star in the acquisition image. To first order the Strehl ratio is then simply the signal in the 2x2 pixel region around the star (especially if the seeing disk has already been subtracted) divided by the total signal measured in the acquisition image. This Strehl ratio would feed back into the TT loop parameter optimization in section 8.5.2 and would also be a useful diagnostic to publish for the observer or operator.

8.5.6 Sky Background Measurement

The sky background can easily be measured by offsetting to blank sky, however this may be insufficient if the sky background is changing rapidly. An alternative or additional approach would be to continually read a single or a few pixels somewhere on the detector to provide an on-the-fly sky background measurement; at minimum this would inform the observer when a new sky background was required.

This measured background could be subtracted as part of the RTC system data processing.

8.5.7 Science Image FITS Header

Some additional items will need to be available for the FITS header associated with each science image. These parameters will need to be available as keywords so that they can be written to the FITS header. At minimum these keywords would include which TTS was in use (WFS, STRAP or the NIR TTS), how many TT objects were used and the TT gain. A fuller list will be developed for the preliminary design.

8.5.8 Telemetry Recorder System

A command to the real-time control system will determine what real-time data will be recorded by the telemetry recording system. It will also be desirable to record some control system parameters along with the telemetry. These items are TBD.

9. Predicted Performance

9.1 Throughput and Emissivity

A spreadsheet tool has been developed to calculate the throughput and emissivity to the NIR TTS detector (this is based on a tool developed for NGAO, KAON 723). This spreadsheet will be updated as the throughput is better understood for each of the components. The calculation includes sky, telescope, AO system and NIR TTS throughput and includes a degradation term for aging of the optics. Each component is also assigned a temperature that is used for the emissivity calculation.

The percent throughput is shown in Table 5. At the center of the Ks band the throughput of the AO system to the dichroic pickoff feeding the NIR TTS is calculated to be 69%, including the impact of dust and aging (71% in H-band). The throughput of the NIR TTS optics including the K-band reflective dichroic is 75%. The overall throughput is 47%.

The emissivity in units of photons/(m^2-sec-nm-$arcsec^2$) is given in Table 6. The background contribution of the AO and NIR TTS optics is 1.7 times that of the sky + telescope at 2.1 μm. The final percentages in Table 6 are for the degraded case.

Table 5: Percent Throughput

Optic	Coating	Temp C	One-year Degradation	Wavelength Kp 1.9	2	2.1	2.2	2.3
Kmirror, surf 1	CoatingData!Keck_Al	2.0	2.0%	97.3%	97.3%	97.3%	97.3%	97.3%
Kmirror, surf 2	CoatingData!FSS99_106_45	2.0	1.0%	98.0%	97.8%	97.6%	97.4%	97.3%
Kmirror, surf 3	CoatingData!Keck_Al	2.0	1.0%	97.3%	97.3%	97.3%	97.3%	97.3%
TT mirror	CoatingData!FSS99_106_45	2.0	2.0%	98.0%	97.8%	97.6%	97.4%	97.3%
OAP1	CoatingData!FSS99_106_45	2.0	2.0%	98.0%	97.8%	97.6%	97.4%	97.3%
DM1	CoatingData!FSS99_500_0	2.0	2.0%	97.6%	97.6%	97.6%	97.6%	97.6%
OAP2	CoatingData!FSS99_106_45	2.0	2.0%	98.0%	97.8%	97.6%	97.4%	97.3%
IR/Vis Dichroic IR Path	CoatingData!None	2.0	1.0%	95.0%	95.0%	95.0%	95.0%	95.0%
IR/Vis Dichroic IR Path	CoatingData!None	2.0	1.0%	99.5%	99.5%	99.5%	99.5%	99.5%
TRICK Dichroic, surf 1	CoatingData!None	2.0	1.0%	97.0%	97.0%	97.0%	97.0%	97.0%
TRICK field lens, surf 1	CoatingData!FSS99_500_0	2.0	1.0%	97.6%	97.6%	97.6%	97.6%	97.6%
TRICK field lens, surf 2	CoatingData!FSS99_500_0	2.0	1.0%	97.6%	97.6%	97.6%	97.6%	97.6%
TRICK mirror	CoatingData!FSS99_500_0	2.0	1.0%	97.6%	97.6%	97.6%	97.6%	97.6%
TRICK window, surf 1	CoatingData!None	2.0	1.0%	99.0%	99.0%	99.0%	99.0%	99.0%
TRICK window, surf 2	CoatingData!None	-40.0	0.5%	99.0%	99.0%	99.0%	99.0%	99.0%
TRICK dewar optics	CoatingData!None	-40.0	0.5%	90.0%	90.0%	90.0%	90.0%	90.0%
AO System				80.5%	79.9%	79.2%	78.7%	78.4%
AO System, Degraded				69.6%	69.2%	**68.6%**	68.1%	67.8%
TRICK Optics				79.5%	79.5%	79.5%	79.5%	79.5%
TRICK Optics, Degraded				74.7%	74.7%	**74.7%**	74.7%	74.7%
AO System + TRICK, Degraded				52.0%	51.7%	**51.2%**	50.9%	50.7%
AO + TRICK, Degraded + Sky + Telescope				4.6%	30.3%	**46.9%**	43.9%	43.7%

Table 6: Emissivity

Optic	Coating	Temp C	1.9	2	2.1	2.2	2.3
Kmirror, surf 1	CoatingData!Keck_Al	2.0	3.05E-02	9.68E-02	2.74E-01	7.02E-01	1.65E+00
Kmirror, surf 2	CoatingData!FSS99_106_45	2.0	2.03E-02	6.91E-02	2.09E-01	5.62E-01	1.35E+00
Kmirror, surf 3	CoatingData!Keck_Al	2.0	2.57E-02	8.15E-02	2.31E-01	5.93E-01	1.39E+00
TT mirror	CoatingData!FSS99_106_45	2.0	2.92E-02	9.82E-02	2.93E-01	7.81E-01	1.87E+00
OAP1	CoatingData!FSS99_106_45	2.0	3.04E-02	1.03E-01	3.07E-01	8.19E-01	1.96E+00
DM1	CoatingData!FSS99_500_0	2.0	3.48E-02	1.12E-01	3.20E-01	8.24E-01	1.94E+00
OAP2	CoatingData!FSS99_106_45	2.0	3.32E-02	1.12E-01	3.36E-01	8.98E-01	2.15E+00
IR/Vis Dichroic IR Path	CoatingData!None	2.0	5.25E-02	1.70E-01	4.85E-01	1.25E+00	2.94E+00
IR/Vis Dichroic IR Path	CoatingData!None	2.0	1.33E-02	4.30E-02	1.23E-01	3.17E-01	7.46E-01
TRICK Dichroic, surf 1	CoatingData!None	2.0	3.70E-02	1.20E-01	3.42E-01	8.80E-01	2.07E+00
TRICK field lens, surf 1	CoatingData!FSS99_500_0	2.0	3.27E-02	1.06E-01	3.02E-01	7.78E-01	1.83E+00
TRICK field lens, surf 2	CoatingData!FSS99_500_0	2.0	3.39E-02	1.09E-01	3.12E-01	8.05E-01	1.90E+00
TRICK mirror	CoatingData!FSS99_500_0	2.0	3.51E-02	1.13E-01	3.24E-01	8.33E-01	1.96E+00
TRICK window, surf 1	CoatingData!None	2.0	2.10E-02	6.77E-02	1.93E-01	4.98E-01	1.17E+00
TRICK window, surf 2	CoatingData!None	-40.0	1.12E-04	4.61E-04	1.65E-03	5.22E-03	1.48E-02
TRICK dewar optics	CoatingData!None	-40.0	7.81E-04	3.23E-03	1.16E-02	3.65E-02	1.04E-01
AO System, Degraded			0.27	0.88	2.58	6.74	15.99
TRICK Optics, Degraded			0.16	0.52	1.49	3.84	9.05
AO System + TRICK, Degraded			0.43	1.40	4.06	10.58	25.04
Sky + Telescope			2.02	2.99	2.40	8.96	9.01
Degraded AO System + TRICK + Sky + Telescope			2.45	4.39	6.47	19.54	34.05
AO System + TRICK as % of Sky + Telescope			21%	47%	169%	118%	278%

9.2 Signal-to-Noise Ratio

A spreadsheet tool has been developed to determine the signal-to-noise ratio (SNR) for the NIR TTS. The spreadsheet is shown in Table 7. The throughput numbers are from Table 5 and the Strehl numbers are from the performance of the current Keck II LGS AO system (these values will be improved with the Keck I laser and center launch system). The signal is then calculated for the indicated magnitude star at the indicated zenith angle and off-axis distance. The thermal background noise is calculated from the measured background for NIRC2 (which should be quite similar to those for the NIR TTS) and the read + dark noise is from Figure 34. A plot of SNR versus K-magnitude is shown in Figure 43 for a range of conditions; for the brightest stars (at left) the NIR TTS is run at 1 kHz using 4x4 pixels, while the rate is reduced to 50 Hz with 2x2 pixels for the faintest stars. This plot indicates a limiting magnitude of K ~ 16 for these conditions. The average star is redder than M0 (for a M0 star R-K = 2.4) so this limiting K magnitude corresponds to a limiting magnitude of R > 18.4 star. STRAP and the LBWFS are limited to R ~ 19 so the limiting magnitudes are comparable.

Table 7: SNR calculation spreadsheet

The case shown is 45° zenith angle, 45" off-axis, K=14 TT star with 100 Hz sampling using 4x4 pixels.

Quantity	Units	H-band	Ks-band	Notes
Telescope throughput		0.92	0.92	
AO system throughput to TRICK		0.50	0.51	
Detector QE		0.75	0.84	Measured H2RG median QE
Telescope + AO Throughput		***34.4%***	***39.7%***	
Strehl at zenith		0.12	0.30	LGS web page
Zenith angle		45	45	
Strehl at zenith angle		0.08	0.21	LGS web page: SR(K')=0.24 for R=17 & median seeing
Tip-Tilt star off-axis distance	arcsec	30	45	
Isokinetic angle	arcsec	55	70	LGS web page: 64, 73 & 95" measured
Tip-Tilt Star Strehl		***6%***	***13%***	
Wavelength	nm	1633	2124	NIRC2 Kp filter
Filter Bandwidth	nm	300	336	NIRC2 Kp filter
log f (in W/cm2/um) at zero mag		-13	-13.4	K-band (Allen, p. 202)
Telescope diameter	cm	1000	1000	
Flux (above atmosphere for 0 mag)	W	2.36E-08	1.05E-08	
Photon energy	J/photon	1.22E-19	9.35E-20	(Allen, p. 15)
Flux (above atmosphere for 0 mag)	photon/sec	1.94E+11	1.12E+11	
Magnitude		14.5	14.0	H-K = 0.5 assumed
Flux (above atmosphere for mag)	photon/sec	3.07E+05	2.82E+05	
Atmospheric Transmission		0.989	0.989	(Allen, p.126 - 0.6 air mass at zenith)
Photons on telescope	photon/sec	3.04E+05	2.79E+05	
Integration time	s	0.01	0.01	
Total signal in AO-corrected core	**electron**	***60***	***146***	
Background (sky + thermal)	mag/arcsec^2	13.6	12.56	K'-band background measured on NIRC2
Zero point magnitude		25.44	24.74	NIRC2 sensitivity manual
Number of pixels		16	16	
Arcsec/pixel		0.05	0.05	
Total background	***electron***	87	119	
Background noise	**electron**	**9**	**11**	
Seeing disk photon noise	**electron**	**12**	**12**	Assumes 15% of total seeing disk energy in 4x4 pixels
Readout + dark noise	**electron**	**5**	**5**	Lab noise measurements
Photon noise	**electron**	**8**	**12**	
Noise	**electrons**	**18**	**21**	
SNR		***3.4***	***7.0***	

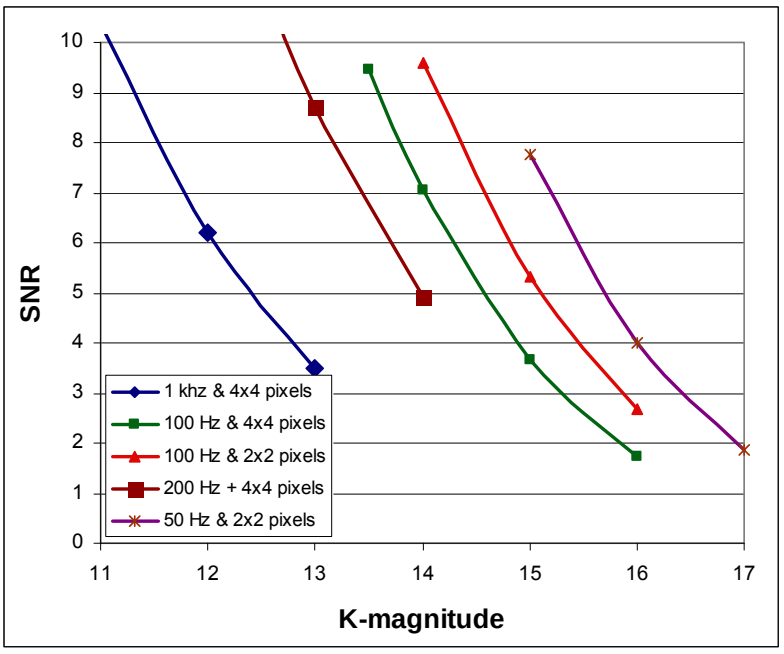

Figure 43: SNR versus K-magnitude (median seeing, 45° zenith angle, 45" off-axis and 5 electrons/pixel noise assumed in all cases).

9.3 Performance Trades

KAON 823 summarizes some performance trades studied during the system design, in particular analysis to support the choice of the pickoff optics options by evaluating the relative performance of H and Ks-band TT sensing. This analysis assumes the Keck I LGS AO system with a center launched 30W mode-locked CW laser. The NGAO galaxy assembly science case was evaluated which assumes median seeing conditions, 60° galactic latitude, 30° zenith angle and an integration time of 1800 seconds.

The residual 1-D RMS TT error for H and Ks-band tip-tilt sensing (TRICK), and for the existing STRAP sensor are shown in Figure 44. The advantage of Ks-band sensing for large sky fraction is very clear. H-band sensing has an advantage over STRAP for the low sky coverage case but the H-band Strehl is simply too low when moving far off-axis as required for high sky coverage.

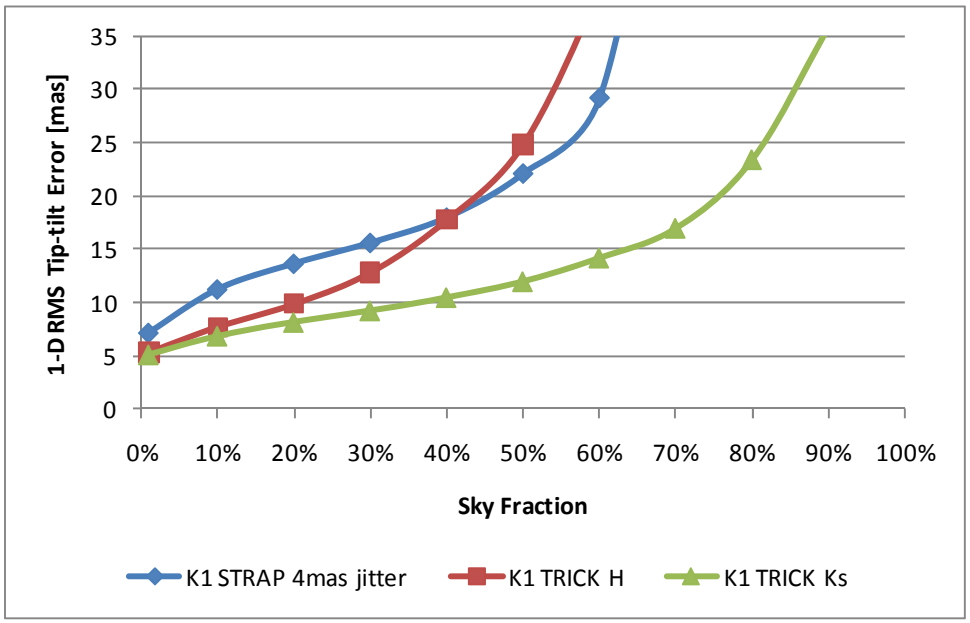

Figure 44: Residual 1-D RMS TT error for the NIR TTS at H and Ks, and for STRAP

The K-band science Strehl ratio and ensquared energy (EE) within a 50 mas spaxel, corresponding to the cases in Figure 44, are shown in Figure 45 and Figure 46, respectively. For 50% sky coverage Ks-band sensing results in a Strehl of 36% versus 18% for H-band sensing.

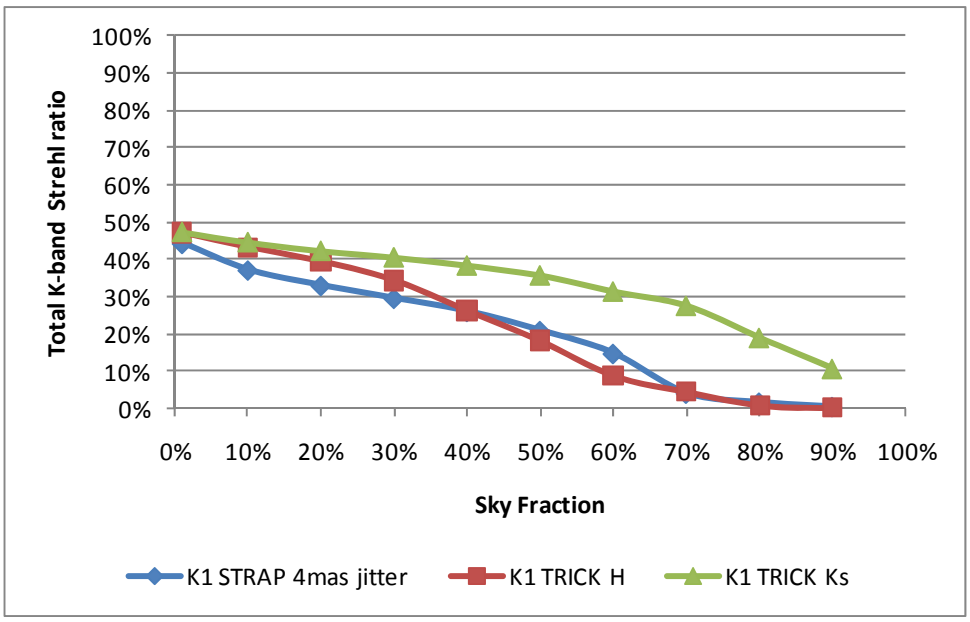

Figure 45: Strehl performance for the galaxy assembly science case

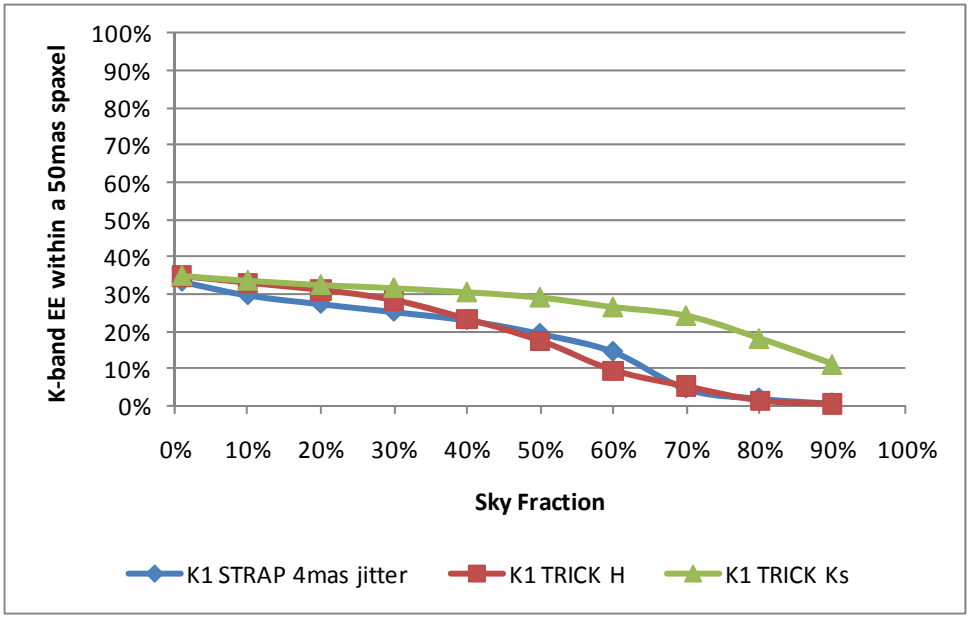

Figure 46: Ensquared energy performance for the galaxy assembly case

TT performance depends on TT star color as shown in Figure 47. STRAP outperforms NIR TT sensing for stars of G spectral type or earlier. The vast majority of main sequence stars are however M spectral class for which the NIR TTS performance, in Ks and H, significantly outperforms STRAP. As can be seen from this plot the performance predictions are very dependent on star color. During the preliminary design we intend to check our color and star frequency assumptions given this critical dependence.

The performance versus zenith angle is plotted in Figure 48. Both H and Ks-band performance degrades rapidly once a particular zenith angle is reached due to the breakdown of off-axis AO correction.

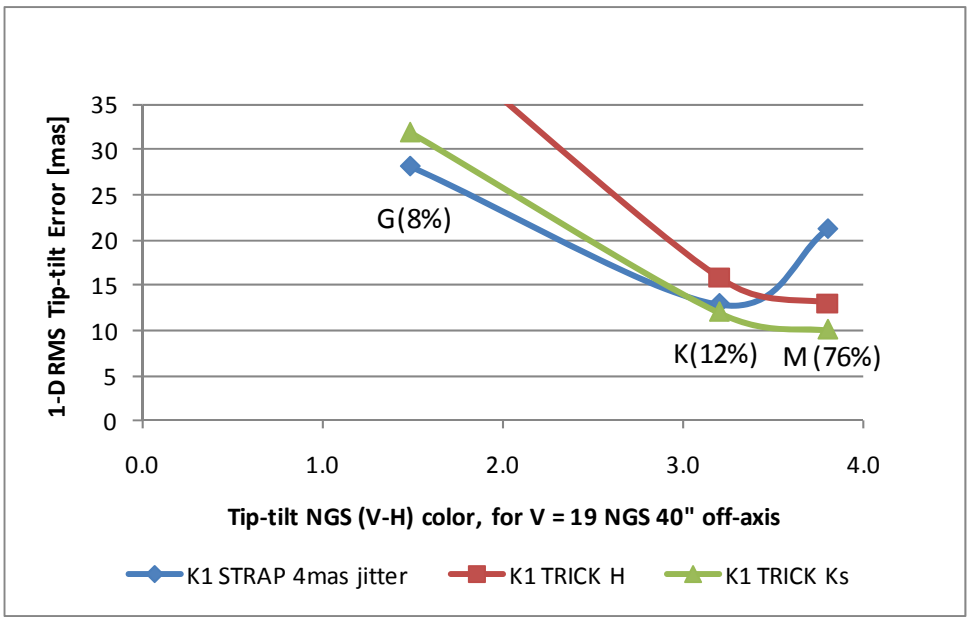

Figure 47: TT performance for a V = 19 NGS located 40" off-axis, assuming different spectral type stars. The number in parentheses is the fraction of all main sequence stars of that type (from LeDrew, 2001).

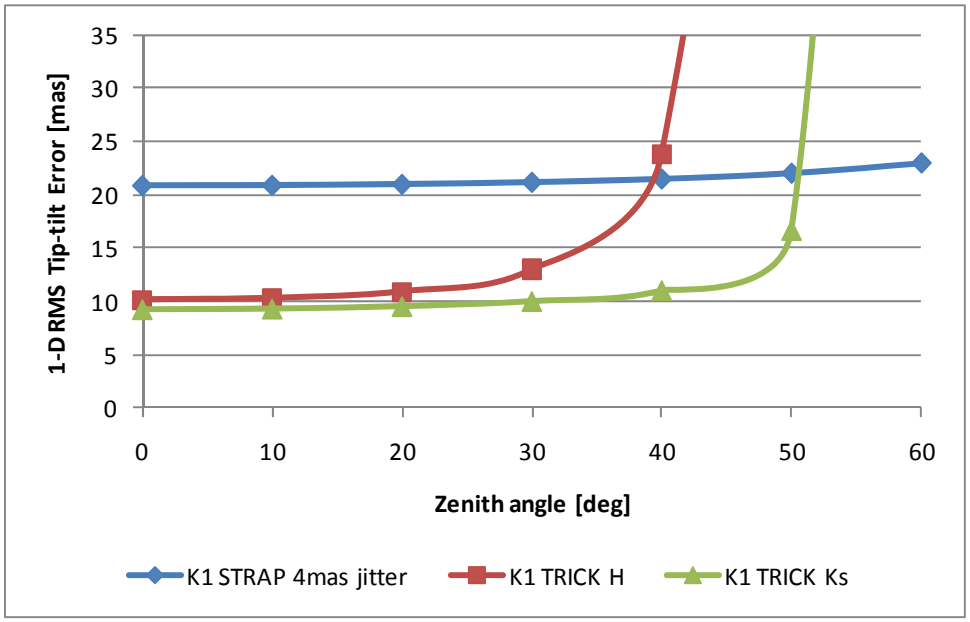

Figure 48: TT performance for the galaxy assembly science case as a function of zenith angle

These analyses influenced our optical pickoff choices. In addition to the originally planned K-band dichroic we concluded that it was worthwhile to have an H-band dichroic to allow us to do improved K-band science for the low sky coverage cases. The significantly higher Ks-band for the high sky coverage case also implied that an annular mirror, that passed the K-band science light while allowing us to use Ks-band sensing for off-axis TT stars, would also be valuable.

9.4 Error Budget

The analysis in this section was prepared for the proposal and has not been revisited during the system design. We will update this analysis during the preliminary design.

An extensive spreadsheet based error budget tool has been developed for WMKO and Palomar, with anchors to AO simulations and on-sky results. This tool has been used to generate the error budgets listed in Table 8 for observations of high redshifts galaxies at a zenith angle of 30° assuming a Spagna 2001 star density model. The predictions for the current Keck II LGS AO system are a K-band Strehl of 20% for imaging and an ensquared energy of 18% for 0.05" spaxel IFU observations. This is consistent with observations. For example, Wright et al. (2009) report Strehl ratios of between 22 and 30% for six z ~1.6 galaxy observations with OSIRIS using relatively bright TT stars (V-band 14.5 to 16.8); fainter TT stars are assumed for this higher sky coverage case. The Strehl is predicted to improve to 26% with a planned higher power laser on Keck I, and then to 41% with the implementation of the proposed TTS.

The predicted ensquared energies for Keck I as a function of the seeing parameter, r_0, is shown in Figure 49 for the case of high redshift galaxies. Three scenarios are shown, the existing STRAP TTS (green), a NIR TTS operating at J/H-band (blue) and a NIR TTS operating at K-band (red). For the proposed K-band NIR TTS, the reduction in the rms tilt error (dashed line) from 20 to 10 mas under median seeing conditions (r_0 =16 cm) results in an increase in the ensquared energy (solid line) from 23 to 32% in a 50 mas spaxel.

Error Term	High-Redshift Galaxies (r0 = 14.7 cm @ 30° zenith angle; wind 9.5 m/s)		
	K2 2009	K1 2010	K1 2013 (w/ new TTS)
Atmospheric Fitting	126	126	126
Telescope Fitting	66	66	66
Science Camera	30	30	30
DM Bandwidth	108	55	55
DM Measurement	146	71	71
Tip-tilt Bandwidth	145	145	89
Tip-tilt Measurement	191	192	95
Tip-tilt Anisoplanatism	190	190	111
LGS Focus Error	34	34	34
Focal Anisoplanatism	187	187	187
LGS High Order Error	50	50	50
Calibration Errors	29	29	29
Miscellaneous	90	36	101
Total Wavefront Error	442	405	329
Science Wavelength	2.2 μm		
Strehl Ratio	20%	26%	41%
Ensquared Energy (50 mas)	18%	23%	32%

Table 8: Keck LGS AO wavefront error budgets (in nm rms) for the high redshift galaxies science case at 30° zenith angle as performance is improved: current 2009 Keck II LGS AO system performance, predicted Keck I LGS AO system with the new laser in 2010, and the Keck I LGS AO system with the proposed TTS.

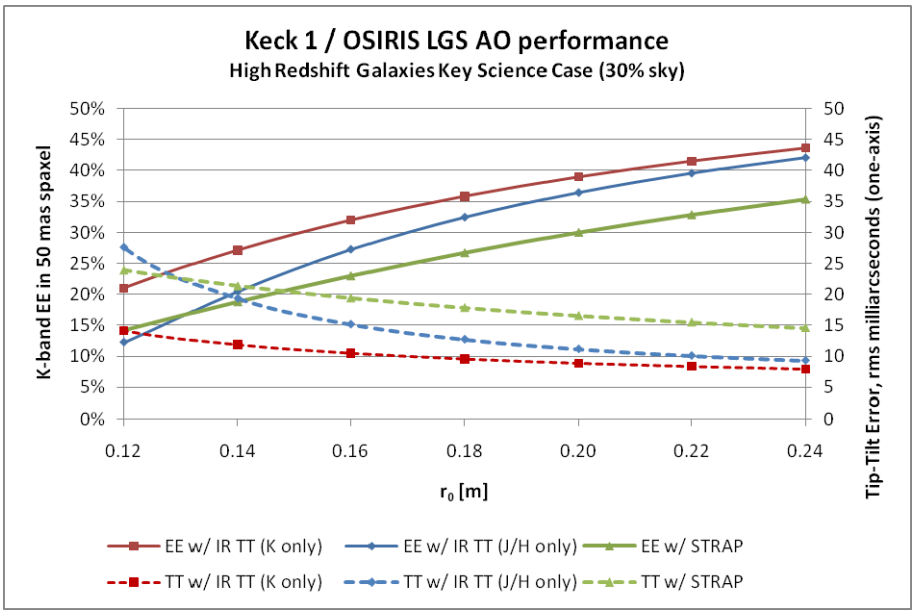

Figure 49: Predicted performance for the case of high redshift galaxies

A ~40% improvement in ensquared energy (~55% in Strehl) with the proposed NIR TTS would produce significant high-redshift galaxy science gains. A corresponding increase in signal-to-noise ratio (SNR) can be expected for AO observations of point sources for both photon-limited or background limited observations (or a Strehl-squared reduction in integration time to reach the same SNR). For LGS studies of extended sources or faint sources next to bright sources, the contrast is the key science metric and will be increased by Strehl/(1–Strehl).

10. Documentation

The documentation to be provided with the operational NIR TTS system will include the required documentation to support the astronomer, the operator and engineering personnel.

Observer/astronomer documentation will include the following items available from the public website:

- Performance data
- Observing preparation and observing guidelines/procedures

Operator documentation will include the following items available from the Keck intranet website:

- An operations guide
- Any maintenance procedures
- Any troubleshooting procedures

Engineering documentation will include the following items available from the AO folder in KeckShare:

- Design, implementation and performance documents (documented as KAONs)
- Vendor manuals & results

11. Acceptance, Integration and Test

11.1 Subsystem Acceptance

The system is considered to be made up of five subsystems:

- The camera subsystem. This system includes the optics internal to the camera dewar, the filter changer hardware and motion control, the camera control electronics and host computer, and the associated cryo and vacuum systems. This system will interface to the AO system mechanically via an interface plate, to the Microgate RTC via a fiber optic communication link and protocol

- The opto-mechanical subsystem. This system includes the dichroic changer and the camera focus stage with field lens and fold mirror, all mechanics needed to interface this system to the AO bench and the motion control hardware for the dichroic changer and focus stage. This system will be delivered by WMKO.
- The real-time control system modifications. Defined in KAON 824. This system will be delivered by Microgate and will be tested with the existing spare Microgate controller in the WMKO lab.
- The controls subsystem. This system provides the controls functionality at the level of the existing AO optics bench subsystem (OBS) and supervisory controller (SC). This system will include the motion control for the opto-mechanical subsystem, the device control for the camera and real-time control subsystems and the software that resides at the OBS and SC levels. The SC level software will include DAR compensation. This system will be delivered by WMKO.
- The observing software subsystem. This system provides the higher level control functionality needed for observing. This system, described in section 6, will be delivered by WMKO.

Each subsystem is expected to be fully assembled and tested to meet its functional requirements (see section 13) prior to subsystem acceptance. A subsystem acceptance mini-review will be held for each subsystem prior its movement to lab I&T.

In each to the subsystems the existing Keck I AO facility will need to be modified to accept these systems at the telescope. Mechanical modifications, including modifications to the AO bench or to support cryo or vacuum hardware, are the responsibility of the opto-mechanical subsystem. Electrical, cabling, computer, network or software infrastructure modifications are the responsibility of the controls subsystem.

11.2 Laboratory I&T

Laboratory I&T at WMKO headquarters involves the assembly, alignment, integration and test of the four subsystems. The integrated system must be demonstrated to meet the system requirements that can reasonably be demonstrated off of the telescope. A pre-telescope readiness review will be held prior to moving the integrated system to the telescope.

11.3 Telescope I&T

Telescope I&T will include system installation and alignment prior to both daytime and nighttime testing of system functionality. This will be followed by multiple nights of system performance characterization. We will also work with our science team to ensure that one or two science verification programs are performed to ensure that the system is working as an overall effective science facility.

All system requirements must be verified at the telescope to ensure that the system is ready for handover to operations. An operations handover review will be held.

12. System Requirements Compliance

The system requirements are defined in KAON 823 and managed in a spreadsheet, KAON 835, along with their compliance. The compliance choices are either: yes, no or PD (to be determined during the preliminary design). The system requirements and there compliance are provided in Table 9.

Table 9: System Requirements

#	Overall Requirements	Compliance
1	Provide a NIR TTS system for the Keck I LGS AO system and OSIRIS.	Yes
2	The NIR TTS system shall be capable of operating as an integrated part of the Keck I NGS AO control system.	Yes
3	3. When the NIR TTS system is not in use it shall allow the current science modes of the AO system and science instruments to be used with no reduction in performance.	Yes

4	Provide improved tip-tilt correction and improved sky coverage for LGS AO science operations. Specifically, the NIR TTS system shall achieve the performance improvements predicted in Table 1 under the conditions indicated. The performance is allowed to degrade with respect to Table 1 as the conditions worsen.	Yes
5	Goal: Provide TBD improved focus correction and reduce the overhead for focus measurements by TBD during LGS AO science operations.	No
6	The NIR TTS system shall be operable, with performance consistent with system requirement #4, over a range of seeing conditions up to the 80th percentile seeing. The goal is 90th percentile seeing.	Yes
7	The NIR TTS system shall be operable, with performance consistent with system requirement #4, over the telescope zenith angle range from 0.5° to 65°.	Yes
8	The NIR TTS system shall come equipped with a means of identifying the location of tip-tilt stars on the camera. For example, the NIR TTS could have its own acquisition mode or the existing acquisition camera should be capable of adequately positioning stars on the NIR TTS.	Yes
9	Goal: The NIR TTS system shall be capable of using up to three tip-tilt stars as input to the real-time controller tip-tilt determination.	Yes
10	The NIR TTS system shall be capable of using non-point sources ≤ 0.1" in diameter, with performance consistent with system requirement #4.	Yes
11	Goal: The NIR TTS system shall be capable of using non-point sources ≤ 1" in diameter, with performance consistent with system requirement #4.	0.8" max
12	The NIR TTS system shall be capable of operating in parallel with the existing visible TTS (STRAP) for improved tip-tilt correction. Both sets of data shall be capable of being used together by the real-time controller to calculate the tip-tilt to be applied to the tip-tilt mirror.	Yes
13	The NIR TTS system shall be capable of using stars as faint as K = 16 mag over its entire field of view.	Yes
14	The NIR TTS system shall be capable of using stars as faint as H = 16 mag over its entire field of view.	Yes
15	When the NIR TTS system is used the science field of view of interest shall be unvignetted. Depending on the science case the science field of view of interest may include just the OSIRIS IFU or both the IFU and imager. Options shall be provided to allow both the IFU and imager fields of view to be passed when the NIR TTS is operated in H or K-band.	Yes
16	The NIR TTS shall be positioned to be parfocal with the science instrument focal plane. This will require that the NIR TTS be able to refocus for different observing modes.	Yes
17	The time required for any routine daytime calibrations of the NIR TTS system shall not exceed 20 minutes.	PD
18	The time required for any routine nighttime start of night calibrations of the NIR TTS system shall not exceed 10 minutes.	PD
19	The time required to initialize the NIR TTS system shall not exceed 10 minutes. This initialization refers to the associated computer systems, software and motion control devices. The NIR TTS camera is assumed to be at operating temperature.	PD
20	The NIR TTS system shall not increase the typical LGS AO acquisition time by more than 15 seconds.	PD
21	Other than acquisition time, the NIR TTS system shall not reduce the observing efficiency of the current LGS AO system. Observing efficiency includes the time to perform such tasks as nodding, dithering and offsetting.	PD

22	The NIR TTS system shall support differential atmospheric refraction corrections between the TTS and the science instrument for a ≤ 20 minute science exposure for zenith angles ≤ 60°, with performance consistent with system requirement #4.	Yes
23	The NIR TTS system shall support normal science observing modes such as dithering, nodding and offsetting.	Yes
24	The NIR TTS system shall be able to position an object on the science instrument to an accuracy of ≤ 120 mas (3-sigma) for moves ≤ 60 arcsec and ≤ 70 mas for moves ≤ 5 arcsec, assuming the tip-tilt star stays within the NIR TTS field of view.	Yes
25	The NIR TTS system shall be able to reposition an object on the science instrument to a relative accuracy of ≤ 5 mas for moves ≤ 20 mas, assuming the NIR TTS system tip-tilt loop was already closed.	Yes
26	The stability of the NIR TTS with respect to the AO bench shall be ≤ 5 mas over a 1 hour exposure, assuming a temperature change of ≤ 1° C.	PD
27	The NIR TTS system shall be able to reposition an object on the science instrument to ≤ 10 mas after an intermediate move of ≤ 10 arcsec, in support of dithering.	PD
28	The NIR TTS system is not expected to support non-sidereal tracking; this mode will continue to be supported by STRAP. As a goal, the NIR TTS system shall be able to maintain the position of a non-sidereal object on the science instrument to ≤ 5 mas for a non-sidereal object with a deviation rate of 50 arcseconds per hour or less, assuming the tip-tilt star stays within the NIR TTS field of view.	Yes, but remains a goal
29	As a goal the NIR TTS should provide some measure of performance (for example, a Strehl measurement).	Yes
30	The NIR TTS system shall meet all of its performance requirements in the operating environment conditions given in Table 2.	PD
31	The NIR TTS system shall receive approval from the AO configuration control board prior to implementation into the Keck I LGS AO system.	Yes
#	**Optical Requirements**	**Compliance**
32	The unvignetted field of view of the NIR TTS shall be at least a 100" diameter circle with a goal of a 120" diameter circle.	Yes
33	The operational wavelengths of the NIR TTS shall be the short wavelength end of K-band (e.g. Ks or K') and H-band. Only one of these bands will be used at any given time.	Yes
34	When the NIR TTS system is used the transmission in the science wavelength shall not be reduced by more than 5%. The goal is 3%.	PD
35	When the NIR TTS system is used the emissivity in the science wavelength shall not be increased by more than 5% averaged over the science band. The goal is 3%.	PD
	Mechanical Requirements	
36	The NIR TTS system shall not introduce vibrations into the LGS AO system that would impact science performance. This requirement is already covered by requirement 4 but is included here to draw specific attention to the importance of minimizing vibrations.	PD
37	The NIR TTS system shall mount to the AO bench within a TBD envelope. The NIR TTS system shall not mechanically interfere with the components already on the AO bench, unless these components can be and are appropriately modified to support the integration of the NIR TTS system.	PD
38	The NIR TTS system mounted on the AO bench shall not exceed a total mass of 30 kg (TBC).	PD
39	The associated NIR TTS system equipment not on the AO bench shall not exceed a TBD envelope.	PD
	Electronic/Electrical Requirements	

40	The NIR TTS system shall use less than or equal to TBD of electrical power.	
41	The NIR TTS system on the AO bench shall not exceed a one-hour average heat dissipation of 5 Watts into the AO bench environment.	PD
42	The associated NIR TTS system equipment not on the AO bench shall not exceed a one-hour average heat dissipation of 10 Watts into the AO clean room.	PD
43	If practical the NIR TTS system electronics shall be located in a rack in the AO electronics room and cables must be of appropriate length to reach these locations. If cable lengths are required to be shorter, then the cables shall be at least long enough to allow placing this equipment outside of the enclosure directly around the AO bench.	PD
	Safety Requirements	
44	The NIR TTS system shall be able to withstand the acceleration profile (to be provided) without damage or severe misalignment. Restraints should be provided to prevent hardware from damaging itself or other hardware during an earthquake.	PD
	Software Requirements	
45	The NIR TTS system shall provide the needed operational tools to support its daytime calibration.	Yes
46	The NIR TTS system shall provide the needed tools to support science observation planning.	Yes
47	The NIR TTS system shall provide the needed operational tools to support nighttime science operations.	Yes
	Interface / Logging Requirements	
48	The NIR TTS system must support an interface to the Observatory standard KTL keywords. For example, command and status communications between the NIR TTS camera system and the optics bench, supervisory controller and operations software shall be via keywords.	Yes
49	All telemetry from the NIR TTS shall be provided to the existing telemetry server.	Yes
50	The NIR TTS system shall be capable of saving images in FITS format.	Yes
	Spares Requirements	
51	The spare NGWFC electronics hardware setup currently available in WMKO HQ shall be updated to match the final hardware configuration that will be designed for the NIR TTS project.	Yes
	Reliability Requirements	
52	The NIR TTS system shall meet all of its performance requirements without repair after shipment to Keck headquarters and to the telescope.	Yes
53	The NIR TTS system shall have a lifetime of ≥ 10 years.	Yes
54	The NIR TTS system shall be capable of operating on ≥ 200 nights per year.	PD
55	The NIR TTS system shall lose no more than 5% of its total observing time to faults.	PD
56	The NIR TTS system shall have a median time between faults that result in ≥ 10 minutes of lost observing time, of ≥ 10 nights of operation.	PD
57	The time to restart the NIR TTS system shall not exceed 10 minutes.	PD
58	The NIR TTS system shall meet all of its performance requirements without repair or realignment after being subjected to any number of cycles of any of the non-operating	PD

	environmental conditions shown in Table 3.	
59	The NIR TTS system shall be able to withstand a total and sudden loss of electrical power or a transient power event, without suffering damage.	PD
	Service and Maintenance Requirements	
60	AO system unavailability or downtime to install and integrate the NIR TTS system shall not exceed 2 weeks.	PD
61	Routine maintenance on the NIR TTS shall not require more than 1 technician for 4 hours every 4 months.	PD
	Documentation Requirements	
62	The NIR TTS system shall be provided with the documentation required to understand and document its as-built design, and to maintain and operate it.	Yes
63	The NIR TTS system shall be provided with the documentation required to support science operations planning. This should include at least 3 months of performance characterization data after the system has begun being used for shared-risk science.	Yes
64	Goal: The NIR TTS system shall be provided with a performance estimation tool for both pre-observing planning and observing. This would be even more useful with a PSF simulator attached to it.	PD
65	The NIR TTS system shall successfully complete a handover review, with TBD success criteria, before being transferred to the responsibility of the AO operations group.	Yes
	Configuration Management Requirements	
66	All code changes and documentation updates shall be managed according to existing WMKO configuration management practices.	Yes
67	All software releases on the operational system shall be revertible to an on-sky demonstrated software release within 15 (TBC) minutes.	PD

13. Functional Requirements Compliance

An initial set of functional requirements, which are flowed down from the system requirements to subsystems, have been developed for four subsystems: camera system, opto-mechanics, controls and observing software. The RTC functional requirements have been defined and are included in the Microgate SOW (KAON 824). The non-RTC functional requirements are maintained in the KAON 835 requirements spreadsheet. All subsystems must meet the system requirements, although in some cases the system requirements are not applicable to a particular subsystem. A summary of which system requirements are applicable to each subsystem can be found in KAON 835. The subsystem functional requirements, excluding the RTC requirements, are shown in Table 10, Table 11, Table 12 and Table 13, along with their compliance status. The flowdown column references the system requirements (SR) number from which a particular functional requirement flows.

Table 10: Camera system functional requirements

#	Overall Requirements	Flowdown	Compliance
1	The camera system shall include a cryogenic dewar containing reimaging optics, a filter changer mechanism with H and K' filters and motion control, and an H2RG detector; the camera control electronics and host computer, and the associated cryo and vacuum systems.	SR-1	Yes
2	The camera system shall interface to the opto-mechanical system as defined in KAON 836.	SR-1,2,37	Yes
3	The camera system shall interface to the controls and observing software systems as defined in KAON 836.	SR-1,2	Yes
4	The camera system shall interface to the Microgate RTC system as defined in KAON 824.	SR-1,2,9	Yes

5	The camera system shall deliver a read + dark noise of < 5 electrons total for up to 4x4 sampling at 1 kHz.	SR-4	Yes
6	The camera shall have a full frame readout mode that writes images in FITS format. As a goal the images should also be available in binary format via API.	SR-8	Yes
7	The camera shall provide H and Ks filters and a remote means of switching between these two filters.	SR-13,14	Yes
8	The time to read out a full frame image shall be ≤ 5 sec.	SR-8,20	PD
9	The time required to initialize the camera system shall not exceed 5 minutes.	SR-19	PD
	Optical Requirements		
10	The camera shall have a plate scale of 50 mas/pixel.	SR-4	Yes
11	The camera system shall have a wavefront quality ≤ TBD nm rms.	SR-4	PD
12	The camera system shall have a throughput of ≥ TBD % including the detector QE at Ks.	SR-13	PD
13	The camera system shall have a throughput of ≥ TBD % including the detector QE at H.	SR-14	PD
14	Optical distortions within the camera system shall be ≤ 10 mas for any two points separated by ≤ 60".	SR-24,25	PD
	Mechanical Requirements		
15	The stability of the camera system with respect to its mounting surface shall be ≤ 3 mas over a 1 hour exposure, assuming a temperature change of ≤ 1° C.	SR-26	PD
16	The camera system shall mount to the AO bench within a TBD envelope. The camera system shall not mechanically interfere with the components already on the AO bench, unless these components can be and are appropriately modified to support the integration of the NIR TTS system.	SR-37	PD
17	The camera system mounted on the AO bench shall not exceed a total mass of 10 kg (TBC).	SR-38	PD
18	The associated camera system equipment not on the AO bench shall not exceed a TBD envelope.	SR-39	PD
	Electronic/Electrical Requirements		
19	Each opto-mechanical stage shall be provided with an appropriate servo motor and encoder to ensure that the positioning requirements can be met. The filter exchanger positioning requirement is ≤ 1 mm.	SR-1,2,4	PD
20	The camera system shall use less than or equal to TBD of electrical power, in excess of the current system.	SR-40	PD
21	The camera system on the AO bench shall not exceed a heat dissipation of 3 Watts into the AO bench environment.	SR-41	PD
22	The associated camera system equipment not on the AO bench shall not exceed a heat dissipation of 7 Watts into the AO clean room.	SR-42	PD
23	The associated camera system equipment not on the AO bench shall be capable of being placed at least TBD m from the NIR TTS system location on the AO bench.	SR-43	PD
	Reliability Requirements		
24	The camera system shall lose no more than 3% of its total observing time to faults.	SR-55	PD
25	The camera system shall have a median time between faults of ≥ 20 nights of operation.	SR-56	PD

26	The time to restart the camera system in the event of a fault shall not exceed 5 minutes.	SR-57	PD
	Service and Maintenance Requirements		
27	Routine maintenance on the camera system shall not require more than 1 technician for 2 hours every 4 months.	SR-61	PD
28	The camera shall be operable in a stand-alone mode to support both development and diagnostics once installed	SR-61	PD
	Documentation Requirements		
29	Procedures must be provided for any required calibrations.	SR-17,18	PD

Table 11: Opto-mechanical system functional requirements

#	Overall Requirements	Flowdown	Compliance
1	The opto-mechanical system shall include a the opto-mechanics to fold the beam to the NIR TTS camera, the opto-mechanics for the NIR TTS that are outside of the camera dewar and any associated motors and encoders, as well as any required modifications to the AO bench to support this hardware.	SR-1	Yes
2	The opto-mechanical system shall provide an interface plate to mount the camera as defined in KAON 836.	SR-1,2	Yes
3	Each opto-mechanical stage shall interface to the controls via a TBD connector.	SR-1,2	Yes
4	The opto-mechanical system shall provide a means of sending H or K'-band light to the camera system while transmitting the other science bands to OSIRIS. Two options are required: an H-band reflective dichroic and a K-band reflective dichroic. A goal is to leave a position for a future annular mirror that will transmit the IFU science field.	SR-15	Yes
5	The opto-mechanical system shall provide a focus stage.	SR-16	Yes
6	The time to re-position a stage via the control system shall not exceed 10 seconds.	SR-17,18,20,21	PD
7	The time required to initialize the opto-mechanical system via the control system shall not exceed 5 minutes.	SR-19	PD
	Optical Requirements		
8	The opto-mechanical system shall have a wavefront quality ≤ TBD nm rms to the camera system.	SR-4	PD
9	The opto-mechanical system shall have a wavefront quality ≤ TBD nm rms to OSIRIS.	SR-4	PD
10	The opto-mechanical system shall have a throughput of ≥ TBD % at K' to the camera system.	SR-13	PD
11	The opto-mechanical system shall have a throughput of ≥ TBD % at H to the camera system.	SR-14	PD
12	Optical distortions within the opto-mechanical system shall be ≤ 10 mas for any two points separated by ≤ 60".	SR-24,25	PD
	Mechanical Requirements		
13	The reflected beam off each fold optic must be co-linear and repeatable to the following tolerances: the image shift shall be ≤ 0.1" and the pupil shift shall be ≤ 5% of the full pupil. The goal is ¼ of these numbers.	SR-21	PD
14	The stability of the output optical beam shall be ≤ 3 mas over a 1 hour exposure.	SR-26	PD

15	The opto-mechanical system shall mount to the AO bench within a TBD envelope. The opto-mechanical system shall not mechanically interfere with the components already on the AO bench, unless these components can be and are appropriately modified to support the integration of the NIR TTS system. Any required modifications are the responsibility of the opto-mechanical system.	SR-37	PD
16	The opto-mechanical system mounted on the AO bench shall not exceed a total mass of 10 kg (TBC).	SR-38	PD
	Electronic/Electrical Requirements		
16	Each opto-mechanical stage shall be provided with an appropriate servo motor and encoder to ensure that the positioning requirements can be met. The dichroic exchanger positioning requirement is ≤ 1 mm. The focus stage positioning requirement is ≤ 0.05 mm.	SR-1,2,4	Yes
17	The opto-mechanical system shall use less than or equal to TBD of electrical power, in excess of the current system.	SR-40	PD
18	The opto-mechanical system on the AO bench shall not exceed a heat dissipation of 2 Watts into the AO bench environment.	SR-41	PD
	Reliability Requirements		
19	The opto-mechanical system shall lose no more than 1% of its total observing time to faults.	SR-55	PD
20	The opto-mechanical system shall have a median time between faults of ≥ 100 nights of operation.	SR-56	PD
21	The time to restart the opto-mechanical system in the event of a fault shall not exceed 5 minutes.	SR-57	PD
	Service and Maintenance Requirements		
22	Routine maintenance on the opto-mechanical system shall not require more than 1 technician for 2 hours every 12 months.	SR-61	Yes

Table 12: Controls system functional requirements

#	Overall Requirements	Flowdown	Compliance
1	The controls system shall include the motion control required for the opto-mechanical system, the device control required for the camera system and real-time control system, and any other software residing at the optics bench (OBS) or supervisory control (SC) level. This subsystem shall include any required modifications to the AO electronics to support this functionality.	SR-1	Yes
2	The opto-mechanical system stages shall interface to the controls via a TBD connector.	SR-1,2	Yes
3	The controls shall interface to the camera system as defined in KAON 836.	SR-1,2	Yes
4	The controls system shall position the opto-mechanical focus stage to be conjugate to the science instrument focal plane.	SR-16	Yes
5	The time to re-position a camera system or opto-mechanical system stage via the control system shall not exceed 10 seconds.	SR-17,18,20,21	Yes
6	The time required to initialize the opto-mechanical or camera systems via the control system shall not exceed 5 minutes.	SR-19	PD
7	The controls shall support differential atmospheric refraction corrections between the TTS and the science instrument.	SR-22	Yes
8	The controls shall support normal science observing modes such as dithering, nodding and offsetting.	SR-23	Yes

9	Potential goal only: the controls system shall support non-sidereal tracking.	SR-28	Goal
	Software Requirements		
10	The controls system shall provide the needed operational tools to support its daytime calibration.	SR-45	Yes
11	The controls system shall provide the needed operational tools to support nighttime science operations.	SR-46	Yes
	Reliability Requirements		
12	The controls system shall lose no more than 2% of its total observing time to faults.	SR-55	PD
13	The NIR TTS shall have a median time between faults of ≥ 30 nights of operation.	SR-56	PD
14	The time to restart the controls system in the event of a fault shall not exceed 5 minutes.	SR-57	PD
	Service and Maintenance Requirements		
15	Routine maintenance on the controls system shall not require more than 1 technician for 4 hours every 8 months.	SR-61	PD

Table 13: Operations software system functional requirements

#	Overall Requirements	Flowdown	Compliance
1	The observing software system shall provide the high-level software to plan science observations, prepare the system for observations and to carry out the observations.	SR-1	Yes
2	The observing software system shall interface to the camera, real-time control and controls systems via ethernet using keywords.	SR-1,2,48	Yes
3	The observing software system shall identify the location of tip-tilt stars on the camera.	SR-8	Yes
4	The NIR TTS system shall coordinate operating in parallel with the existing visible TTS (STRAP) for improved tip-tilt correction.	SR-12	Yes
5	The time required to initialize the observing software system shall not exceed 3 minutes.	SR-19	PD
6	The observing software system shall support normal science observing modes such as dithering, nodding and offsetting.	SR-23	Yes
7	As a goal the observing software should provide some measure of performance (for example, a Strehl measurement).	SR-29	Yes
	Software Requirements		
8	The observing software system shall provide the needed operational tools to support its daytime calibration.	SR-45	Yes
9	The observing software system shall provide the needed tools to support science observation planning.	SR-46	Yes
10	The observing software system shall provide the needed operational tools to support nighttime science operations.	SR-47	Yes
	Interface / Logging Requirements		
11	The observing software system shall be capable of retrieving telemetry from the telemetry server.	SR-29,49	Yes
12	The NIR TTS system shall be capable of saving images in FITS format.	SR-8,50	Yes
	Reliability Requirements		
13	The observing software system shall lose no more than 2% of its total observing time to faults.	SR-55	PD

14	The observing software system shall have a median time between faults of ≥ 30 nights of operation.	SR-56	PD
15	The time to restart the observing software system in the event of a fault shall not exceed 5 minutes.	SR-57	PD
	Service and Maintenance Requirements		
16	Routine maintenance on the observing software system shall not require more than 1 software engineer for 4 hours every 12 months.	SR-61	PD
	Documentation Requirements		
17	Goal: The observing software system shall provided a performance estimation tool. This would be even more useful with a PSF simulator attached to it.	SR-64	Goal